CROSS-SCALE BIOPHYSICS MODELLING OF F-ACTIN CYTOSKELETON IN CELL

Tong Li

B.Eng. (Dalian University of Technology)

M.Sci. (Utah State University)

Submitted in fulfilment of the requirements for the degree of

Doctor of Philosophy

School of Chemistry, Physics and Mechanical Engineering

Faculty of Science and Engineering

Queensland University of Technology

February 2015

Keywords

Actin; Adhesion; Biomechanics; Biophysics; Coarse-Grained; Energy dissipation; Compressive response; Crosslinker unbinding; F-actin; F-actin crosslinker; F-actin cytoskeleton; Flexural rigidity; Filopodial protrusion; G-actin; Graphene, Graphene oxide; Numerical modelling; Mechanics; Mechanical stability; Mechanical vibration; Microfilament networks; Molecular Dynamics; Multiscale; Muscular contraction; Myosin; Sarcomere; Thermomechanical; Young's modulus.

Abstract

The cytoskeleton (CSK) is the structural basis of eukaryotic cells, and resists deformation that is induced by external loadings. The microfilament, intermediate filament and microtubule are the three principal elements of the cytoskeleton. Among these three cytoskeleton components, microfilament is also found in non-muscle cells, indicating that the mechanical behaviour of microfilaments can regulate cellular changes and force generation in cell migration and division. Therefore, the physical responses of F-actin CSK to external forces or stimuli are significant to the understanding of actin-related cellular processes.

In order to explain physical mechanisms of biophysical responses of F-actin CSK under external mechanical inputs, we have validated the suitability of using continuum mechanics modelling in representing the physical behaviours of F-actin CSK. Molecular characterisation of vibration properties of single filamentous actin (F-actin) was performed to obtain the mechanical vibration properties of single F-actin filaments up to 300nm. It has been found that, only when the length of F-actin filament is larger than 100nm, a beam model can be used to represent the behaviour of F-actin filament.

In order to overcome the difficulties of using continuum mechanics model for F-actin CSK, a highly coarse-grained (CG) model has been developed based on the hierarchical structures of F-actin. The physical interactions between adjacent globular actin (G-actin) monomers were obtained from the molecular dynamics simulations. The accuracy of this CG model in the prediction of F-actin deformation was validated by previous experimental results of the tensile behaviour of single F-actin filaments and vibrational theories.

In addition to the mechanical deformation prediction, this multiscale model underestimates the thermodynamic vibration of G-actins, which can weaken the ability of materials to overcome local energy traps in granular modelling. We have further developed a new stochastic thermostat algorithm for this highly coarse-grained (CG) model to fully represent the thermodynamic properties of microfilaments.

Based on the multiscale model of F-actin CSK developed in this research, we have investigated the mechanical responses in F-actin CSK with respect to external loadings and studied the interaction between actin and carbon materials.

This thesis reveals that the stability of filopodial protrusions is dependent on the density of F-actin crosslinkers. This cross-linkage strategy is a requirement for the optimisation of cell structures, resulting in the provision and maintenance of adequate bending stiffness and buckling resistance while mediating any vibration.

This multiscale modelling approach has been employed to study the mechanisms of compressive responses of F-actin CSK. It was found that the compressive response of F-actin CSK depends on the loading velocity. This research also theoretically validates the crucial role that transient crosslinker unbinding plays in the rheological properties of F-actin CSK. Coupled with F-actin elasticity, the energy dissipation was found to be more significant in bundled F-actin CSK.

Another application of this multiscale method is to study the mechanisms of muscular contraction. It was found that the number of myosin II motors can sensitively mediate the contraction force during muscular contraction. However, this force cannot be infinitely increased with the number of motor elements, which matches the self-protective properties of living cells.

Besides the mechanical deformation modelling of F-actin CSK, this thesis also conducted atomic modelling to investigate the interaction between actin and a newly developed single layer carbon material (graphene). The charge properties of graphene can dramatically change its adhesive properties on G-actin, thereby explaining the previous findings on graphene localising on F-actin.

In this project, a CG model was developed for F-actin CSK based on the multiscale concept, to overcome the difficulties of physical modelling of F-actin CSK in conventional continuum mechanics modelling and the computational challenges in all-atom molecular dynamics simulation. The thermostat algorithm was modified in this method to better predict the thermodynamic properties of F-actin CSK. This multiscale method framework has been applied to explain the physical mechanisms of F-actin CSK responses to external load and materials.

List of Publication

Paper 1 **Li, T.**, Gu, Y.T., Oloyede, A., Yarlagadda, P.K.D.V., 2014. Molecular investigation of the mechanical properties of single actin filaments based on vibration analyses. **Computer Methods in Biomechanics and Biomedical Engineering** 17, 616-622.

Paper 2 **Li, T.**, Gu, Y.T., Feng, X.-Q., Yarlagadda, P.K.D.V., Oloyede, A., 2013. Hierarchical multiscale model for biomechanics analysis of microfilament networks. **Journal of Applied Physics** 113, 194701-194707.

Paper 3 **Li, T.**, Gu, Y.T., 2014. A stochastic thermostat algorithm for coarse-grained thermomechanical modelling of large-scale soft matters: Theory and application to microfilaments. **Journal of Computational Physics** 263, 177-184.

Paper 4 **Li, T.**, Oloyede, A., Gu, Y.T., 2013. F-actin crosslinker: A key player for the mechanical stability of filopodial protrusion. **Journal of Applied Physics** 114, 214701-214705.

Paper 5 **Li, T.**, Hu, D., Yarlagadda, P.K.D.V. and Gu, Y. (2014). Physical mechanism of the compressive response of F-actin networks: significance of crosslinker unbinding events. Theoretical and Applied Mechanics Letters 4, 051006.

Paper 6 **Li, T.,** Liu, L., Hu, D., Oloyedea, A., Xiao, Y., Yarlagadda, P., and Gu, Y.T. Mechanobiological Energy Dissipation in F-actin Networks by Transient Crosslinker Unbinding. (accepted by **Cellular and Molecular Bioengineering,** DOI :10.1007/s12195-015-0382-y)

Paper 7 **Li, T.**, Gu, Y.T., Oloyede, A., 2014. Molecular Sliding Filament Model for Muscular Contraction based on Multiscale Investigation. **Science of Advanced Material** 6, 1346-1350(1345).

Paper 8 **Li, T.**, Oloyede, A., Gu, Y., 2014. Adhesive characteristics of low dimensional carbon nanomaterial on actin. **Applled Physics Letters** 104, 023702.

The following is a list of publications in refereed conference proceedings throughout the candidature.

Li, T., Gu, Y., Yarlagadda, P.K., Oloyede, A., 2013. Multiscale investigation of microfilament networks disruption in living cells. In International Conference on Fracture 2013 (ICF2013).

Li, T., Gu, Y.T., Yarlagadda, P.K.D.V., Oloyede, A., 2012. Continuum mechanics modelling of microfilament networks with different architectures based on molecular investigation of single F-actin. In 4th International Conference on Computational Methods (ICCM2012).

Thibbotuwawa, N., **Li, T.**, Gu, Y.T, 2014. Porohyperelastic finite element model for the kangaroo humeral head cartilage based on experimental study and the consolidation theory. In Proceedings of 5th International Conference on Computational Methods (ICCM 2014).

Thibbotuwawa, N., Gu, Y.T., Oloyede, A., Senadeera, W., **Li, T.**, 2012. Finite element shoulder models. In Proceedings of 4th International Conference on Computational Methods (ICCM 2012).

Table of Contents

List of Figures

List of Tables

List of Abbreviations

MD	Molecular Dynamics
CG	Coarse-Grained
CG-MD	Coarse-Grained Molecular Dynamics
FEM	Finite Element Method
F-actin	Filamentous Actin
G-actin	Globular Actin
CSK	Cytoskeleton
IFs	Intermediate Filaments
FFT	Fast Fourier Transform
NMS	Normal Mode Solution
RMSD	Root Mean Square Deviation
VMD	Visual Molecular Dynamics
WLC	Worm-Like Chain
NVE	Canonical Ensemble
NPT	Isothermal-Isobaric Ensemble
SGR	Soft Glass Rheology
QM	Quantum Mechanics
DPD	Dissipative Particle Dynamics

Statement of Original Authorship

The work contained in this thesis has not been previously submitted to meet requirements for an award at this or any other higher education institution. To the best of my knowledge and belief, the thesis contains no material previously published or written by another person except where due reference is made.

Signature:

Date: 27/02/2015

To my father, ChengLin Li

Acknowledgements

I thank my principal supervisor, Prof. YuanTong Gu, for his insightful guidance and encouragements on my research since inception. I also thank my associate supervisors, Prof. Kunle Oloyede and Prof. Prasad Yarlagadda, for their thoughtful advices and solid supports.

I acknowledge all members in the LAMSES group for helpful discussions during my candidature. My appreciation also goes to the staffs of CARF and HPC group at QUT, who facilitate the course of my study.

Finally, I thank my family Huashu Liu, Qing Liu and Nan Li for their essential supports.

This research is sponsored by the post graduate award of QUT.

Chapter 1: Introduction

Mechanical deformation is one of the most primitive signalling activities, that is fundamental to life and multicellular systems [1]. In biological systems, cells are the functional units in various dynamic physiological behaviours. It is critical to understand the behaviours of living cells with respects to the primary mechanical stimuli. In living cells, F-actin network is one of the principal components of cytoskeleton (CSK) which plays significant role in the remodelling of cellular structures in response to external mechanical stimuli. In this thesis, because of the difficulties of in vitro experimental characterization of F-actin CSK and the massive computational cost of full atom molecular simulation at nanoscale, a framework for the multiscale granular modelling of F-actin CSK has been developed. This enables the capturing of the mechanical events occurring in living cells when exposed to mechanical stimuli. The model was validated with the experiment results from the literature and applied to understand various static and dynamical characteristics of F-actin CSK under various mechanical constrains.

1.1 BACKGROUND

Cells are the functional units of living organs in various dynamic physiological behaviours. The difference between cell performance and behaviours of non-biological materials lies in their biological activities [2]. Normally, the size of eukaryotic cells is microscopic, such as osteoblasts, preosteoblasts, chondrocytes and fibroblast [3], rendering it difficult to create a universal mechanical constitutive models for living cell structures [4, 5]. A living cell is not a continuum material, but a mysterious system that consist of tremendous elaborated organelles [6]. These non-contiguous cell structures and biological fluids surrounding them make the continuum mechanical model inadequate to capture complete mechanical properties of living cells. Several biphasic mechanics models were proposed to understand the mechanics of cells based on cell aspiration experiments [7]. However, the mechanisms underlying such complex biphasic model is still partly unknown as the cell structures and components are dynamically changing in physiological activities. It is crucial to understand the mechanical behaviour of living cells based on the cellular structures at the microscale level. The cytoskeleton(CSK) is the material foundation of living cells that experiences mechanical inputs from its surrounding living environments and which in response induces the cellular dynamics underlying biological activities [8, 9]. The CSK consists of three principal components:

intermediate filaments (IFs), microtubule and microfilaments networks. These three biological filaments collaborate in living cells to provide the mechanical strength and material foundation of various cellular activities. Among these three components, microfilament network consists of abundant F-actin and actin-related proteins, which perform as the structural foundation in cellular dynamics [10]. The F-actin CSK plays significant role in the dynamic responses of living cells and the remodelling of cellular morphology in mechanical environments. As a large number of proteins are involved in the biological behaviours of F-actin CSK, it is necessary to understand the mechanical response of F-actin CSK from interdisciplinary viewpoints, such as mechanics, biology, physics and chemistry. Moreover, the mechanical response of F-actin CSK is dominated by the dynamics of protein in living cells that is up to nanoscale level, cross-scales study is necessary to bridge the gap between microscale mechanics and nanoscale physics/chemistry.

1.2 AIMS

The aim of this thesis is to develop a framework for the biophysical modelling of F-actin CSK based on the physical behaviours of G-actin molecules and the structural characteristics of CSK in living cells. This framework covers a wide spatial scale, from atomic modelling of G-actin molecules at nanoscale to the biophysical modelling of CSK dynamics at microscale. With the multiscale framework developed, deformation properties of F-actin-related cellular structures can be investigated. Moreover, the mechanisms of dynamical responses in F-actin CSK can be explained from the viewpoints of mechanics.

1.3 OBJECTIVES

I. Evaluate whether continuum mechanics models are sufficient to describe the deformation properties of F-actin filaments at nanoscale level

II. Discrete the F-actin CSK into bead networks and develop a representative coarse-grained (CG) model to quantify the mechanical performances of F-actin CSK

III. Improve the predictive quality of this specifically designed CG model of F-actin CSK in the prediction of thermodynamical behaviours

IV. Investigate the mechanical stabilization of F-actin filament bundles, facilitated by the crosslinker proteins

V. Study the mechanisms of compressive response of three dimensional F-actin CSK

VI. Understand the mechanisms of energy dissipation in F-actin crosslinker, induced by the unbinding of crosslinkers

VII. Study the mechanisms of muscular contraction

VIII. Investigate the interaction between G-actin and in-organic material, which further serves the biosafety evaluation of nano-biomaterials

The objectives and scope of this research is illustrated in Fig. 1-1.

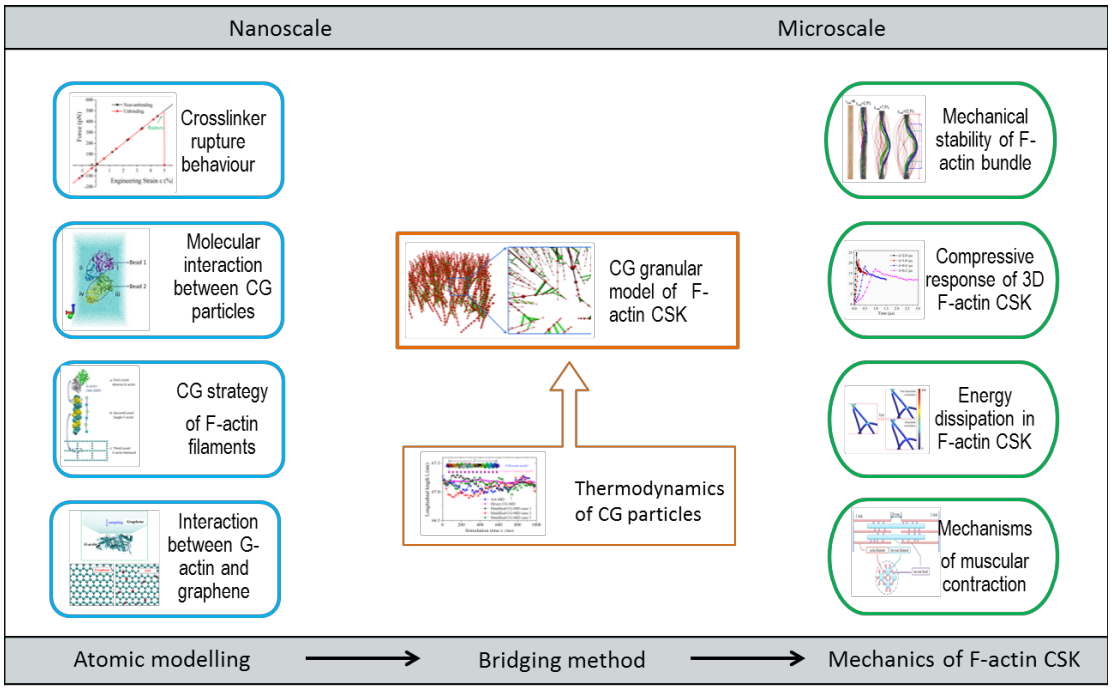

Fig. 1-1. Aims and scope of this research.

1.4 PROJECT OUTLINE

The project mainly consists of two subdomains, namely i) implementation of a novel multiscale method and ii) the application of such a model in the study of the mechanical response of F-actin CSK. The workflow and load distribution of different parts of this thesis are summarized in Fig. 1-2.

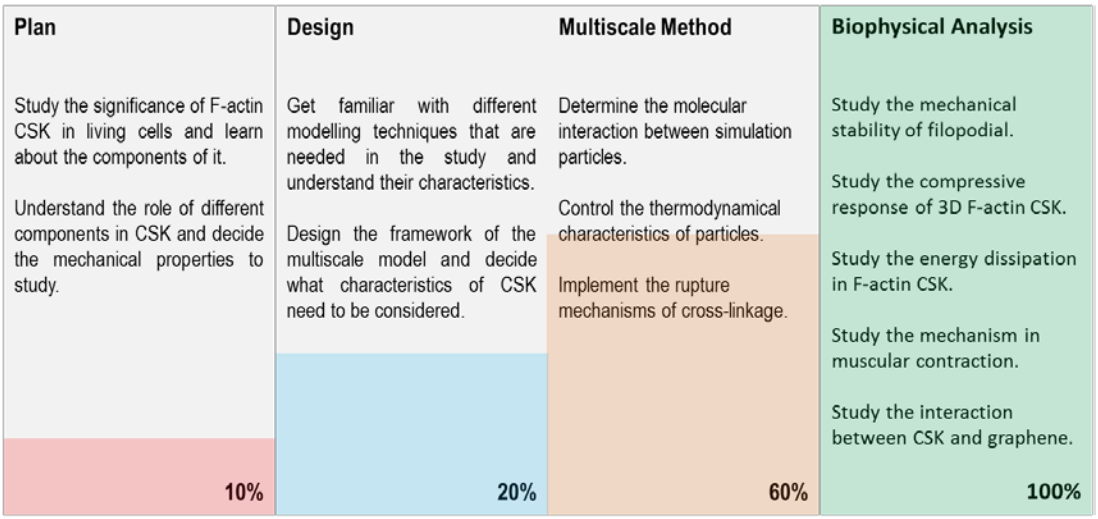

Fig. 1-2. Workflow and load distribution of this project.

The structure of this thesis is summarized in Fig. 1-3. The subdomain of multiscale method consists of three research papers and the subdomain of the application of this method is presented by another five research papers.

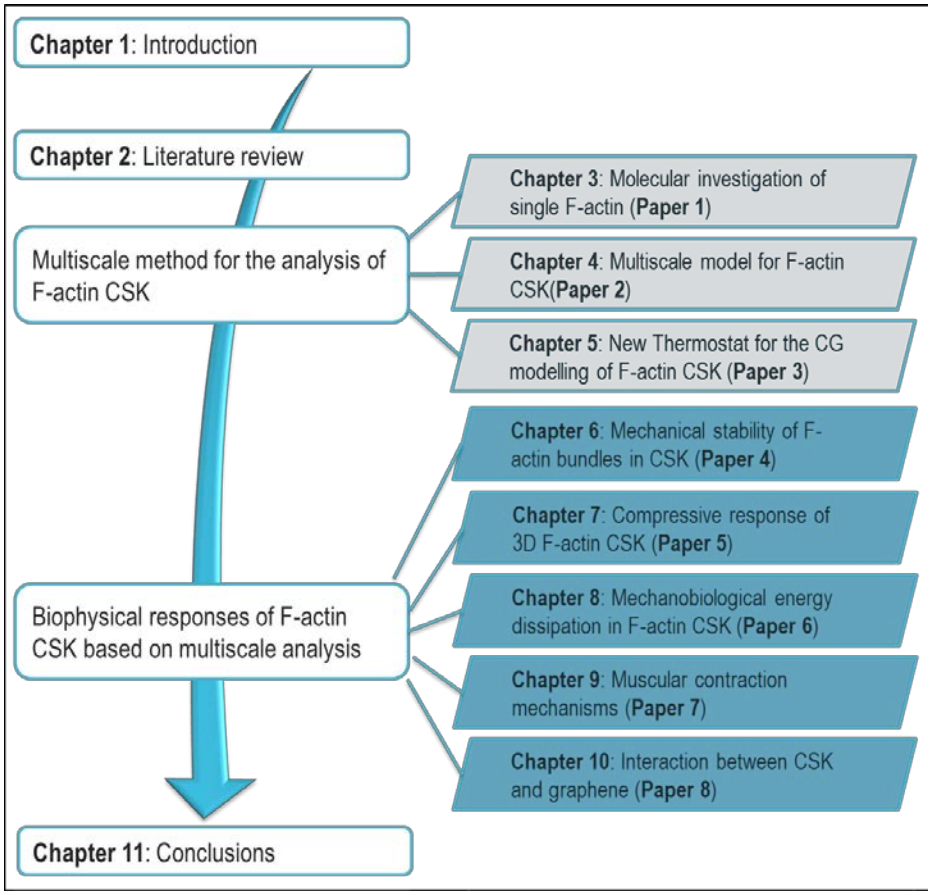

Fig. 1-3. Flowchart of the thesis.

1.4.1 Molecular dynamics modelling of single F-actin filament

It is questionable whether continuum mechanics model (such as beam model) can be applied in the studies of mechanical properties of F-actin filament. Herein, we have developed the atomic modelling of F-actin filament. Vibrational analysis was adopted to obtain the module of F-actin filament. The study verified that continuum mechanics model can be conditionally adopted in the modelling of F-actin filaments to predict their mechanical performances. This part was published in Computer Methods in Biomechanics and Biomedical Engineering [11] and is the Chapter 3 in this thesis.

1.4.2 Coarse-grained model of F-actin networks

As claimed in Chapter 3, continuum mechanics models only conditionally work in the modelling of single F-actin CSK. Moreover, the modelling of F-actin CSK consists of numerous single, flexible F-actin filaments, which is difficult for continuum mechanics model to handle. In chapter 4, we have designed a specific CG granular model for the F-actin filament with respects to the structural characteristics of F-actin. This explicit model also has the advantage of predicting the dynamical behaviours of F-actin CSK in the time domain. The model has been validated by the experimental results from the literature. This part was published in Journal of Applied Physics [12] and is the Chapter 4 in this thesis.

1.4.3 Stochastic thermostat designed for the CG model of F-actin CSK

The CG model developed in Chapter 4 has limitation in its ability in predicting thermodynamic motions of the F-actin fragments. Based on all-atom MD simulation, we have developed a new stochastic thermostat, which improves the predictive quality of the thermodynamical motions of F-actin and also reduce the computational cost of all-atom MD simulation was developed. This part was published in Journal of Computational Physics [13] and is the Chapter 5 in this thesis.

1.4.4 Mechanical stabilization of F-actin bundle

The F-actin crosslinkers is believed to be significant to the mechanical stabilization of F-actin bundles in cellular dynamics. Based on the CG granular model of F-actin CSK, it has been possible to quantify the mechanical performances of F-actin bundles and numerically understand the mechanism of mechanical stabilization of F-actin bundle which is facilitated by the crosslinker (such as fascin).

This part is published in Journal of Applied Physics [14] and is the Chapter 6 in this thesis.

1.4.5 Compressive response of three dimensional F-actin CSK

Besides the F-actin bundles mentioned in Chapter 6, three-dimensional F-actin networks are also commonly found structures in living cells. Based on the new CG model of F-actin CSK, the deformation mechanisms of the compressive response of three dimensional networks were investigated. The significance of crosslinkers to the mechanical performance of CSK was investigated. This part was published in Theoretical and Applied Mechanics Letters [15] and is the Chapter 7 in this thesis.

1.4.6 The energy dissipation in F-actin CSK induced by crosslinker unbinding

By applying a shear deformation to F-actin CSK, it is possible to capture the energy dissipation phenomenon in F-actin CSK. The mechanisms were summarized based on the long duration modelling of F-actin CSK with both thick and thin filaments. This part is accepted by Cellular and Molecular Bioengineering (DOI :10.1007/s12195-015-0382-y) and is the Chapter 8 in this thesis.

1.4.7 The mechanisms of muscular contraction

In order to investigate the contractile properties of skeletal muscle which is induced by the protein motor of myosin, a molecular model is proposed for predicting the dynamic behaviours of skeletal muscles based on classic sliding filament model. This molecular filament sliding model provides a theoretical way to evaluate the properties of skeletal muscles, and contributes to the understandings of the molecular mechanisms in the physiological phenomenon of muscular contraction. This part is published in Science of Advanced Material [16] and is the Chapter 9 in this thesis.

1.4.8 The interaction between F-actin CSK and graphene

The biosafety of carbon nanomaterial needs to be critically evaluated with both experimental and theoretical validations before extensive biomedical applications. An analysis of the binding ability of two-dimensional monolayer carbon nanomaterial on actin by molecular simulation to understand their adhesive characteristics on F-actin cytoskeleton is also presented as an application of the concepts developed in this thesis. This theoretical investigation provides insight into

the sensitivity of actin-related cellular activities on carbon nanomaterial. This part is published in Applied Physics Letters [17] and is the Chapter 10 in this thesis.

1.5 SUMMARY

In summary, the thesis systematically investigated the biophysical properties of F-actin CSK from the viewpoints of both mechanical deformation and interfacial problems. The feasibility of continuum mechanics modelling in the prediction of F-actin behaviours was first evaluated and a multiscale framework for the explicit modelling of F-actin CSK was developed based on the technique of granular modelling. The predictive quality of this new method is also improved by implementing a newly designed stochastic thermostat, while the efficiency and accuracy of this multiscale modelling framework was established in validation against existing experimental data in the literature. Based on the modelling incorporating different levels, it was possible to capture the mechanical stabilization of F-actin-related cellular structures during cell migration, the deformation mechanisms of F-actin CSK with respect to mechanical stimuli, the mechanisms in muscular contraction and also the interfacial relationship between F-actin CSK and inorganic nano-biomaterial. These modelling results can provide insight into the biophysical behaviours of living cells and associated the biosafety evaluation of newly-developed nano-biomaterials in biomedical applications.

Chapter 2: Literature Review

In this chapter, the history of cytoskeleton (CSK) mechanics is summarized and the recent developments of CSK modelling are also included. The content includes:

- Mechanics models of living cells.
- Mechanical characterization of F-actin CSK.
- Hierarchical multiscale modelling.
- Multiscale modelling of Ifs and microtubules.
- Structure and modelling of F-actin CSK.
- Interaction between protein and inorganic materials

2.1 MECHANICS OF LIVING CELLS

In animal body, living cells are subjected to various mechanical loadings throughout life [1, 7]. In response to the mechanical stimuli, living cells would convert these primary signals (strain and stress) to physiological behaviours in a variety of ways under both external and internal constrains, which depends on the characteristics of loadings. For example, in vitro fluid shear of endothelial cells can stiffen the cells by inducing rearrangement of the cytoskeleton [18, 19]. The mechanical compression of cells such as chondrocytes can modulate proteoglycan synthesis [20], which is physiologically significant to the behaviours of bone. Furthermore, the tensile stretching of cell substrate can alter both cell motility [21], orientation [22] and even differentiation [23]. Therefore, it is critical to understand the response of living cells to these above-mentioned mechanical stimuli, which is significant to the pathology study and physical therapy of cellular diseases at molecular level. Herein, we summarized the previously developed experimental techniques and mechanics models of the mechanical characterization of living cells.

2.1.1 Experimental techniques in cell mechanics

During last few decades, several experimental techniques have been developed to quantify the mechanical performances of living cells at different scales [24]. Back into 1950, Crick and Hughes adopted magnetic particle method to quantify the mechanical behaviours of cells [25]. Four years later, Mitchison and Swann designed the micropipette aspiration experiments and characterized the elasticity of sea urchin

eggs [26]. After this, as a standard characterization method, the micropipette aspiration method is widely adopted in the studies of various different types of cells for their mechanical characterizations [27].

With recent developments of experimental techniques at microscale, more microscale characterization methods for living cells have been developed, such as cell poker [28], particle tracking [29], magnetic twisting cytometry [19], oscillatory magnetic twisting cytometry [30], atomic force microscopy [31], microplate manipulation [32], cytoindenter electrical cell-substrate impedance sensing coupled with magnetic bead pulling [33], optical tweezers/laser trap [34, 35] and tensile tester [36].

With the abovementioned techniques at microscale, different kinds of loadings can be applied on cells, such as distributed loading (microplate manipulation) and concentrated loading (atomic force microscopy). These experimental techniques can provide insightful deformation properties of living cells with respects to different loading types. Based on the information from these deformation properties, different mechanics models of living cells have been developed.

2.1.2 Continuum models of living cells

Continuum mechanics models have been developed regarding the mechanical properties of cells under different loading types. This continuum mechanical approach can be generally divided into two subdomains: viscoelastic models and biphasic models, which is systematically summarized in literature [7]. The continuum mechanics model for living cells ignore the molecular events happening in living cells and treat the material as homogeneous material or composites of materials with different phases. However, these models provide more convenient ways to characterize the deformation properties as they only need constitutive parameters which can be obtained from experimental testings.

Solids models were first developed to study the mechanics of living cells by defining the whole cell as one homogeneous material. Under the solids model hypothesis, hyperelastic and viscoelastic theories are very straightforward mechanics models for living cells by defining the elasticity of the material. Back into 1960s, Fung talked about the solid mechanics model to study the mechanical behaviours of living cells. Later on, the solid mechanics model is upgraded to complex mechanics

models, including linear viscoelastic model [37], power law structural damping model [38], porohyperelastic model [39]. The typical expression of this kind of constitutive law of the whole cell can be summarized as Eq. (2-1).

$$\sigma = f(\varepsilon, \dot{\varepsilon}) \tag{2-1}$$

where, σ is the stress, ε is the strain and $\dot{\varepsilon}$ is the strain rate. They type of constitutive law characterized model is easy for modelling as all the deformation properties are summarized by a few mechanical properties. The mechanical events happening insides the living cells are neglected.

Besides the solids model, different solid models were also developed to study the complex mechanical behaviours of living cells. Another commonly used theoretical model for this is the shell-liquid simplification, in which the plasma membrane is simplified as flexible shell and the cytoplasma (complex components, such as cytosol, CSK and suspended organelles) is summarized as liquids. Comparing to solid model, this type of model has the advantages in handling the rheology of living cells which is mainly caused by the liquids state cytosol. Based on the treatment of liquid mechanics models, this domain can be divided into four categories: Newtonian liquid model [40], compound Newtonian liquid model [41], shear thinning liquid drop model [42] and Maxwell liquid mode [43]. The mechanics description of solid state plasma membrane is quite the same with solid mechanics theories. However, the liquid state cytoplasm follows complex hydrodynamics models, which can be typically written as:

$$\tau = f(\gamma, \dot{\gamma}) \tag{2-2}$$

where, τ is the shear stress, γ is the strain and $\dot{\gamma}$ is the shear strain rate.

Differently from the hypothesis in shell-liquid model, another type of continuum mechanics based model for cytoplasm is developed, in which the cytoplasm has two phases: solid polymeric contents and interstitial fluids. This biphasic model further describes the cytoplasm as a complex material with both solid and fluid state materials. This kind of model was first adopted in the studies of biomechanical tissues [44]. Later on, this biphasic model has been applied to model the indentation of a single chondrocyte [45].

With the help of these continuum mechanics of models, the deformation of cells can be predicted from the viewpoint of modelling. This would facilitate the understandings of the role of mechanics in cellular mechanotrasduction [7, 46]. As mechanical properties of living cells also play important roles in the diagnosis of cellular diseases [1], the deformation modelling is also significant to medical applications.

However, these continuum mechanics based models of living cells are insufficient in the prediction of dynamical cell behaviours in specific environments and when exposed external mechanical stimuli. These cryptic biological behaviours of living cells are governed by the mechanobiology of cell components and biochemistry events happening in the cells. One of the most typical players in the mechanobiological behaviours of living cells is F-actin CSK. Microfilament also mechanically drives the process of cellular motility by assembling and disassembling, which proves the essential role microfilament plays in cellular process including embryonic development, wound healing, immune response, and tissue development [47-49]. Therefore, besides the general deformation properties of the whole cell, detailed characterizations of the mechanobiological responses of F-actin CSK are also significant to the understandings dynamical responses of living cells. In following sections, the mechanical characterization and development in modelling for F-actin CSK will be detailed.

2.2 EXPERIMENTAL CHARACTERIZATION OF F-ACTIN CSK

Eukaryote cells are generally 1-100μm what contain complex structures and organics enclosed within membranes, as is shown in Fig. 2-1. Eukaryotic cells contain three main kinds of cytoskeletal filaments, which are microfilaments, intermediate filaments (IFs), and microtubules. The cytoskeleton provides the cell with structure and shape, and by excluding macromolecules from some of the cytosol it adds to the level of macromolecular crowding in this compartment. Cytoskeletal elements interact extensively and intimately with cellular membranes. A number of small molecule cytoskeletal drugs have been discovered that interact with actin and microtubules. These compounds have proven useful in studying the cytoskeleton and several have clinical applications.

Among these, microfilament is an important component of the cytoskeleton which plays a key role in cell's mechanical behaviour. Microfilaments range from 5 to 9 nanometres in diameter, designed to bear large amounts of tension which helps to generate forces used in cellular contraction and basic cell movements [48-52].

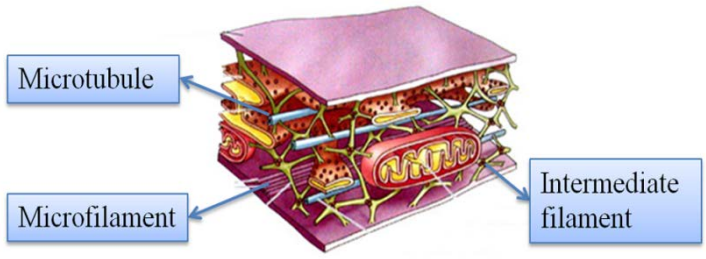

Fig. 2-1. Illustration of the components and structure of cell and cytoskeleton.

Different from cell mechanics testing, spatial scale for the characterization of CSK is at sub-microscale. More advanced characterization techniques are needed to provide full details about the mechanical events happening in the cytoskeleton. Several techniques have been developed for the mechanical characterization of F-actin behaviours. The microfilament network can be simplified to be an architecture which is constructed from basic building blocks; the elementary component is single microfilament fibre: F-actin filament. Therefore, the mechanical properties of F-actin filament plays important role and should be focused to find out the homogenized mechanical behaviour of the structure constructed from F-actin.

Back into 1990s, Micro-needle array technique and laser trap method were used in molecular level to measure mechanical properties of a single contractile protein, both tensile stiffness and torsion rigidity of single F-actin filament were measured [53, 54]. Dupuis, et al, tested the tensile stiffness of F-actin filament from chicken pectoral muscle cells, and estimated the bending rigidity based on continuum mechanics theory [55]. The tensile modulus and flexural rigidity of single F-actin has been obtained from experiments [55-58]. Complex mechanical performances, including viscosity, strain hardening, stress hardening and stress softening, were also discovered in the last few decades [59-63].

A novel silicon-nitride microfabricated levers were used to characterized the longitudinal elasticity of single actin filaments [64]. Single actin filaments were stretched from zero tension to maximal physiological tension. The obtained length-

tension relation was nonlinear in low-tension range (0–50 pN) with a resultant strain of 0.4–0.6% and then became linear at moderate to high tensions (50–230 pN). In this region, stretching stiffness of a single 1μm long F-actin is 34.5-3.5 pN/nm. Such a length-tension relation could be characterized by an entropic-enthalpy worm-like chain model, which ascribes most of the energy consumed in the nonlinear portion to overcoming thermal undulations arising from the filament's interaction with surrounding solution and the linear portion to the intrinsic stretching elasticity. By fitting the experimental data with such a worm-like chain model, an estimation of persistence length of 8.75μm was derived.

The stiffness evaluations of single F-actin by different techniques are summarized in Table 2-1.

Table 2-1 Stiffness characterization of F-actin from different literatures

Techniques	Young's Modulus (GPa)
Thermal fluctuation [56]	2.0
Micro-needle array [53]	1.8
X-ray diffraction [65]	2.5
Micro-fabricated cantilever [64]	1.5 (by comparison)

Besides the classic characterization of mechanical performances of F-actin filament, recently developed technique of atomic force microscopy (AFM) at nanoscale also facilitates the study of F-actin CSK behaviours. This technique has the advantage of a description with higher resolution of F-actin CSK under mechanical stimuli. Chaudhuri, et al. used AFM technique to detect the deformation of microfilament network under mechanical load; reversible elastic behaviour and large elastic modulus of dendritic actin networks are observed in the test, which indicates that the network has an architecture that is geared towards bearing high compressive loads [60]. Sharma, et al., used high resolution AFM to capture the morphology of F-actin at sub-nanometre scale, which provides insights into the F-actin responses to the environmental changes induced by mechanics and chemistry [66]. These highly developed techniques do not only provide the direct stiffness parameters of F-actin CSK, but also assist capturing instant responses of F-actin in complex environments, which is significant to the understandings of the dynamical

responses of CSK to external stimuli. For example, based on the morphology information of F-actin CSK, researchers found that the branching of F-actin CSK can be affected by the curvature of F-actin filament [67].

The rheological properties of actin gels is significant to maintain the flexibility of living cells at long timescales [68]. This adaptability of cells with respect to timescale is achieved by complex mechanosensing rearrangements of F-actin cytoskeleton, which is a composite network with constantly changing chemical components. Various functional and structural proteins work in conjunction to archive the phase change of cells under physical forces, which is significant to their self-protective properties in complex surviving environments.

The underlying structural rearrangements in living cells can be promptly accelerated once the cells are exposed to physical forces. Subsequent cell relaxation would result in a significant phase change [18] in which the local stress relaxation of cellular structure plays critical roles. This cryptic physiological phenomenon is known to depend on the remodelling properties of F-actin cytoskeleton. Dynamically synthesized by cytoplasm [69], the F-actin in living cells has multiple phases varying from single filaments to filament bundles [68]. Compared with single F-actin networks, the networks of F-actin bundle feature enhanced stiffness and strength, both favoured for living cells to resist transient mechanical deformation.

To sum up, the dynamical responses of F-actin CSK are significant to the behaviours of living cells. The mechanical performances of F-actin filaments are the material foundations of these biological performances. Different techniques have been developed and applied to measure the mechanical properties of F-actin filaments. The stiffness of F-actin filaments can be directly or indirectly evaluated. These mechanical behaviours of F-actin filaments can facilitate the understandings of dynamical responses of F-actin CSK, such as remodelling and rheology. However, it is still a challenge to directly couple the mechanics of single F-actin filament and the dynamics of F-actin CSK. Theoretical studies critically are needed to provide insights into the cryptic behaviours of CSK in living cells.

2.3 HIERARCHICAL MULTISCALE MODELLING

The significance of multiscale modelling in biological and material science has been firmly proved by the laureates of Nobel Prize in 2013. Molecular events up to

nanoscale in G-actin are involved in the dynamical responses of F-actin CSK, which makes it critical to consider the nanoscale effects of F-actin behaviours. Therefore, the analytical and computational modelling frameworks of F-actin CSK need to cover a wide range from the atomistic, through the microstructure or transitional, and up to the continuum [70, 71].

Different modelling techniques have been developed based on the physics and mechanics of materials, such as Quantum Mechanics (QM) at sub-nanoscale, Molecular Dynamics (MD) at nanoscale, Dissipative Particle Dynamics (DPD) at microscale and Continuum Mechanics at meso/macroscale. Fig. 2-2 provides the typical numerical techniques which are used in the multiscale computational frameworks.

In cells, F-actin is dynamically polymerized during biological processes and the functional unit is G-actin. Therefore, the smallest deformation unit in the CSK dynamics can be assumed to be atomic structures of G-actin. The molecular mechanisms of G-actin conformation change are significant to the biochemistry of actin dynamics. As our modelling research aims to investigate the mechanical response of the whole F-actin CSK under external stimuli, hence, the conformational changes of G-actin is not focused in this research. Therefore, the smallest modelling scale in this research starts from MD simulation, which can provide the insightful constitutive relationship of a single F-actin. However, the scale of F-actin CSK is up to micro, at which all-atom MD simulation is difficult to be carries out. Therefore, the 'Coarse-Grained' (CG) techniques, which is also known as 'zoom out', is developed to connect the nanoscale F-actin deformation and microscale F-actin CSK response.

In this section, the technical details of MD method and the strategy of CG technique are introduced.

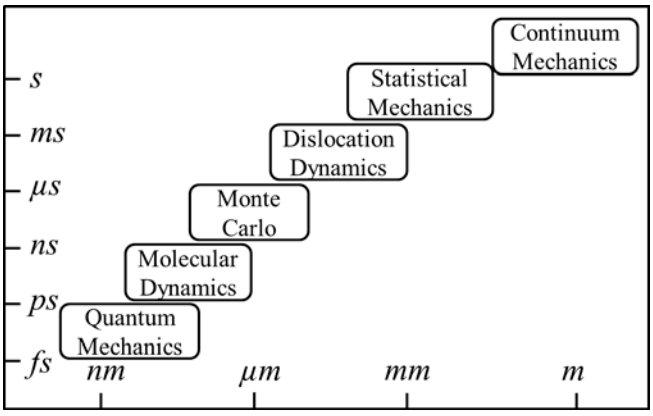

Fig. 2-2. Illustration of typical methods in the multiscale computational frameworks.

2.3.1 MD simulation

QM method is developed based on Schrödinger equation and can be applied to atomic systems to investigate related physical properties. With today's computer power, the system for QM method to model can only reach a few hundreds of atoms. Different from QM method, the MD method is developed to meet the modelling requirements of large systems, which contains millions of atoms. However, MD method is based on empirical potential functions, which are obtained from experiments or QM calculations [70]. The basic idea is to eliminate the electrons in the simulation and assume that they are conceptually included by single atoms (nuclei and electron), which are the smallest simulation units. By defining proper interaction (potential function) between different atoms, the forces applied on each atom can be obtained. According to classic Newtonian mechanics, the tracks of all atoms in the simulation system can be fully extracted by numerical integrations. There are two critical factors in the MD simulation: the interval of dynamic information update and the definition of potential functions.

The classical Hamiltonian for a system is defined as:

$$\mathrm{H} = \sum \frac{m_i v_i^2}{2} + \Phi \tag{2-3}$$

where, m_i and v_i respectively denotes the mass and velocity of atom i. Φ is the effective potential of other particles. Based on the Hamiltonian of an atom, the governing equation of its motion can be derived as:

$$m_i \frac{d^2 R_i}{dt^2} = F_i \tag{2-4}$$

where, R_i is the position of atom i, and t is the time. F_i denotes the force from other atoms with interaction, which is further derived from the predefined potential functions. The mass particle moves as a rigid particle with the velocity of v and the velocity is updated by a time interval based on the interaction from other atoms in the system.

Integration techniques are also important to the quality of MD calculation. We take the commonly used Verlet algorithm as an example to show hot the MD method process the motion of mass particles numerically. The Verlet algorithm is popular in MD method because it is stable and memory efficient for a large time step. In this integration method, the position of atom i after a temporal interval of δt can be calculated from the reference position as:

$$\begin{cases} R_i(t+\delta t) = R_i(t) + \delta t v_i(t+\frac{\delta t}{2}) \\ v_i(t+\frac{\delta t}{2}) = v_i(t-\frac{\delta t}{2}) + \delta t \frac{F_i}{m_i} \end{cases} \quad (2\text{-}5)$$

It is noteworthy that, the velocity of atoms at human body temperature is thousands times of the velocity of a bullet, which means that the size of time step should not be very large to avoid system exploration. This is very critical to the quality of MD prediction, as properly defined time step can guarantee the prediction quality and reduce the computational cost at the same time. By using the above-mentioned calculation principles, the full details of the evolution of atoms in a system can be properly obtained. This obtained dynamical information can be used to quantify the mechanical properties of molecular systems and track its dynamical responses in the temporal domain.

2.3.2 CG strategy

Even though the scale of molecular system can be extended to millions of atoms by MD, which is much improved comparing to QM method, the spatial scale of MD is still limited for a full application to materials at microscale. Take F-actin as an example, F-actin is assembled from G-actin (375 residues) and a molecular system for F-actin with one million atoms can only cover a single F-actin filament which is less than 100nm [72]. However, F-actin CSK contains thousands of F-actin filaments and some filaments are far more than 100nm, which indicates that all-atom

MD method cannot be directly applied to study the mechanics of F-actin CSK at microscale. CG techniques are needed to upgrade the modelling scale to meet the spatial requirements in the study of nano or micromechanics of materials.

In CG strategies, a certain group of atomic clusters are simplified as one simulation bead which performs equally as the mass particle in all-atom (AA) MD methods. Empirical potential functions between these simulation beads (atom clusters) need to be characterized by either experimental or higher level theoretical calculations. Therefore, the design of CG particle is significant to the quality of prediction in the material modelling. Different CG strategies have been proposed to study the mechanics and physics of materials in different disciplines, such as solid state condensed material [73] and proteins [74]. Detailed explanation of the CG strategies of F-actin modelling will be specifically discussed in the section of F-actin multiscale modelling.

2.4 MULTISCALE MODELLING OF IFS AND MICROTUBULES

As introduced in last sections, hierarchical multiscale has been recently applied to model naturally designed hierarchical materials [75]. This modelling method starts from the biophysical simulations of nanostructure of materials and aims to model their macroscale mechanical behaviours. Fig. 2-3 shows the logics of this multiscale modelling strategy and different methods that are usually adopted at different simulation levels. Up to angstrom scale, quantum mechanics calculation is needed for the analysis of interactions of the atomic configurations on the living filaments, as micro/nano scale filaments consist of various peptides. Full atom molecular dynamics (MD) method is adopted at nanoscale to understand the mechanical behaviours of single filaments [11, 17]. However, due to the computational expense of full atom simulation, coarse-grained (CG) strategies are needed to characterize the mechanical behaviours of complex networks that are built from the aforementioned nano/micro scale filaments. Based on systematic studies at all scales, the mechanics of CSK can be studied to understand the mechanical behaviours of a single living cell at microscale based on above-mentioned molecular level simulations.

In this section, multiscale modelling details of different CSK components are independently introduced. These components include IFs, microtubule and microfilament network.

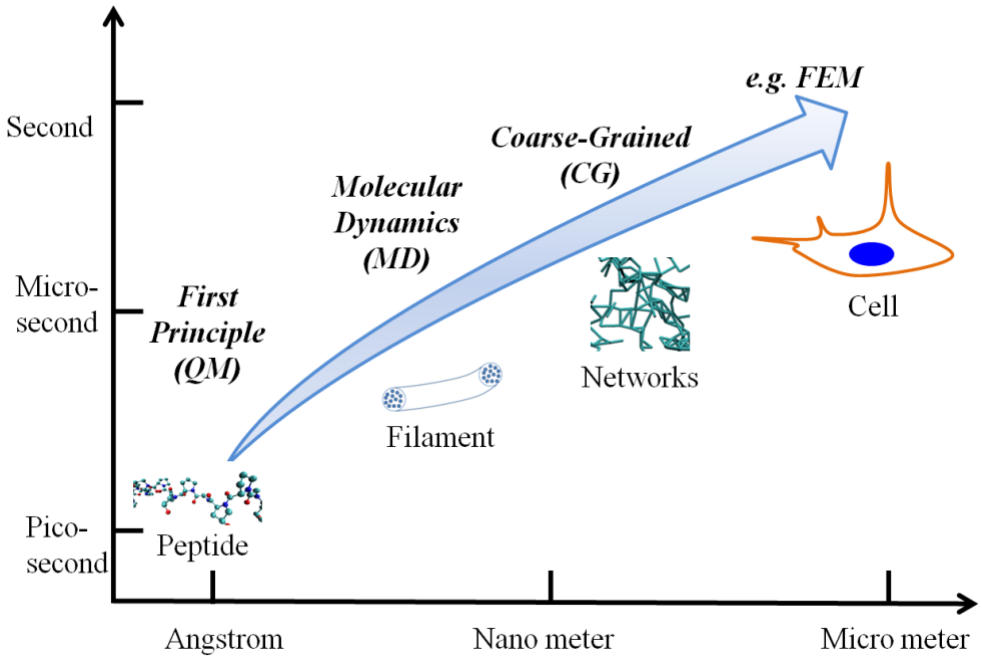

Fig. 2-3. Hierarchical multiscale methods for cell modelling.

2.4.1 IFs modelling

The name of IFs comes from its geometric properties. It is thicker than the microfilaments and thinner than the myosin filaments. The component is evolved related to the mechanical resistance and adhesion of cells [76]. Due to its critical role in the mechanics of cytoskeleton, the mechanical behaviours of IFs were focused for decades to understand the mechanical performance of cells [8, 77-80]. The mechanical significance of IFs to the living cells has been approved already. However, a mature mechanics model for this gel like material is difficult to be obtained due to the physical properties. Efforts have been applied to understand the mechanical contribution of IFs from the view point of numerical modelling [81].

Ackbarow et al. proposed a hierarchical multiscale model for the mechanical modelling of IFs and studied the rupture properties of IFs networks [82, 83]. In this modelling strategy, this alpha helix is simplified to be a string of virtual beads. The physical interaction between beads is obtained from mechanical testing. Fig. 2-4 provides the schematic of this multiscale method. And the simulation parameters are listed in Table 2-2, which are obtained from literature [83]. The interaction between different beads are simplified as multiple linear curves, whose stress transitions respectively sit at 5.3,11.5 and 13.0 angstrom. Between 5.3 and 11.5 angstrom, strain softening happens after the hydrogen bond has broken before 5.3 angstrom. The

main energy is absorbed by the flattening of the alpha helix. After 11.5 angstrom, strain hardening happens because more energy is needed to break the peptides on the single filaments.

Table 2-2 Simulation parameters in the IFs multiscale modelling

Parameters and unit	
Equilibrium distance ($\dot{A}$)	5.00
Stress transition points ($\dot{A}$)	5.3,11.5, 13.0
Stiffness (kcal/mol $\dot{A}^2$)	9.7, 0.56, 32.20, 54.60
Bond breaking distance ($\dot{A}$)	13.30
Equilibrium angle (degree)	180
Bending stiffness (kcal/mol/rad^2)	3.44
Bead mass (amu)	400

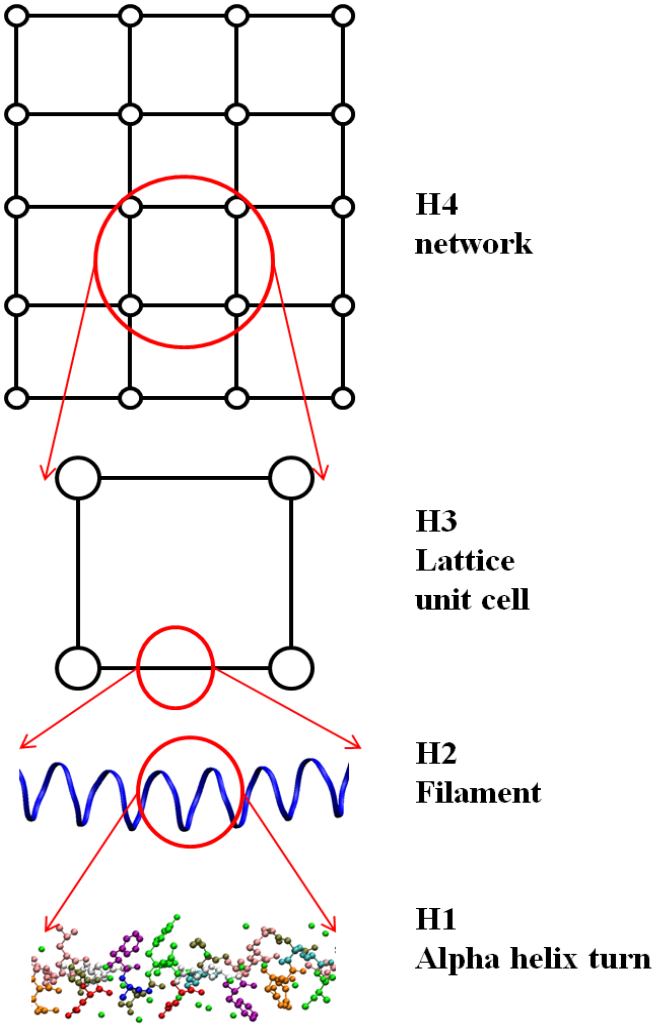

Fig. 2-4. Multiscale model for the IFs modelling.

With assistance from this multiscale model, the mechanical properties can be quantified. Ackbarow et al., have analysed the self-protective properties of IFs networks [83]. Comparing to continuum materials, the rupture strain needed for the same flaw size on the IFs network is larger. The flaw size has negative effects on mechanical strength of IFs networks, however, the toughness properties is better than linear fracture mechanical evaluation based on continuum mechanics theory, which explains the high mechanical strength of nature designed IFs networks in living cells.

2.4.2 Microtubules modelling

As the most rigid component of CSK, microtubule plays important role in the mechanical performance of living cells, such as maintaining the cell morphology and adjusting subcellular structures [84-87]. Due to the mechanical significance of microtubules, enormous efforts have been devoted to study its mechanical contribution to the physiological performances of living cells. Similar to IFs, the mechanical testing on single microtubule is hard to be carried out, and cannot fully consider the *in vivo* environments. In order to overcome these disadvantages, multiscale numerical models of microtubules have been proposed [86-88].

In most microtubule multiscale models, tubulin dimmers are simplified as individual simulation beads. The interaction between different beads is extracted from both full atom simulation or by assumptions [89]. Fig. 2-5 shows the logics in a typical microtubule model.

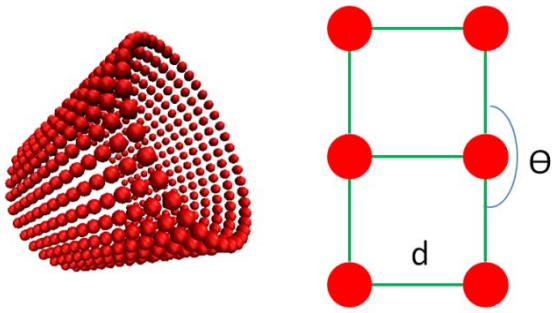

Fig. 2-5. Coarse-grained model for microtubules.

The potential energy between simulation particles in the multiscale model can be summarized as Eq. (2-6). Table 2-3 provides the keynote parameters for Ji and Feng's model [89].

$$U = U_{long} + U_{lat} + U_{diag} + U_{b,long} + U_{b,lat} + U_{d,long} + U_{d,lat} \quad (2\text{-}6)$$

Table 2-3 Simulation parameters in the microtubule multiscale modelling

Interaction	Stiffness Parameter
Longitudinal tension or compression	3 nN/nm
Lateral tension or compression	14 nN/nm
Diagonal tension or compression	3 nN/nm
Longitudinal bending	2 nN•nm
Lateral bending	8.5 nN•nm
Longitudinal dihedral bending	0.04 nN•nm
Lateral dihedral bending	0.17 nN•nm

By adopting these simulation parameters, Ji and Feng have deeply studied the deformation mechanisms of microtubules under external loadings. These mechanical properties study provides insights which can contribute to the understandings of deformation properties of a whole living cell.

Based on the single microtubule modelling, a long microtubule can be simplified as slender beams. By adopting beam assumption, Peter and Mofrad have developed continuum mechanics modelling of a microtubules bundle that consists aligned microtubule filaments [87]. Their study about the mechanical deformation of microtubules bundles can help explain the elongation, undulation, and delayed elasticity of axons following traumatic stretch loading.

2.5 STRUCTURE AND MODELLING OF F-ACTIN CSK

In this section, the crystallography and developments in the modelling of F-actin CSK mechanics are summarized.

2.5.1 Crystallography of the filamentous actin

F-actin is assembled from one of the most highly conserved structure protein: Actin. Straub originally isolated globular actin (G-actin) from muscle [90]. The monomer binds one molecule of ATP which is hydrolysed to ADP on polymerization. Holmes proposed an atomic model of the actin [91]. The detection of the atomic structure of globular actin (G-actin) using X-ray fibber diffraction technique has been focused for decades; Holmes and Oda separately developed atomic structures of G-actin monomer [92, 93]. Based on information of G-actin

atomic structure and F-actin filament assembling mechanisms, the nature of the translation of single G-actin to F-actin were also proposed [91-95].

The monomer, G-actin has unique orientations with respect to the helix. The atomic crystal structure of G-actin is firstly studied in 1990 [91]. High resolution G-actin atomic configuration has been studied after this, and can be found in the protein data bank (PDB) database. According to experiment results, G-actin is a rather flat molecular built from two similar major domains, as is shown in Fig. 2-6. The atomic configuration of G-actin and the high resolution F-actin configuration was separately well developed by Holmes and Oda [92, 93]. The nature of globular to fibrous actin transition was well studied. Fujii also proposed a way to visualize the secondary structures of F-actin by electron cryomicroscopy [96]. There are also many different kinds of G-actin and F-actin atomic configurations in the PDB [51, 97, 98] which were developed during different physiological phenomena. The proper selection of the atomic configuration in theoretical analysis is critical to the analysis results.

2.5.2 Numerical characterization of mechanical properties of F-actin

However, experimental tests of single F-actin filament's stiffness are limited by the operating cost. It is hard to apply testing under all kinds of physics and chemistry environments down at nanoscale. Analytical characterization is needed to assist all conditional stiffness evaluation of F-actin from the atomic microscopy point of view, which can also reduce the huge cost of experimental tests. Molecular ways to describe living systems in terms of physics and chemistry were studied for decades, with many successful application accomplished [99-101].

In nanoscale biotechnology, the performances of structural proteins are dominated by the atomic configurations, which are an already well-established database. MD simulations of living protein organisms provide the ultimate details of motional phenomena in principle. Kolahi and Mofrad performed an MD simulation of bending the rod filamin (actin binding protein), and the simulation results successfully illustrated the coupling between the mechanical and chemical properties governing activity within the cell [102]. With the high resolution atomic configuration of F-actin, MD simulation is executed on an F-actin protein fibber, and the structural properties are estimated from the MD simulations [103-105]. However, due to the challenge in reaching a fully equilibrated atomic configuration of F-actin filaments in MD simulation on a system with more than 40, 000 atoms using today's

computational power, it is hard to get mechanical properties directly from an unstable atomic configuration of a single F-actin filament. There are limited literatures about F-actin's mechanical property study using MD simulation. Matsushita, et al, studied the effect of tensile force on the mechanical behaviour of actin filaments using MD simulation [106]. Recently, mechanical properties of actin filaments were studied by analysing the thermal dynamics behaviours of the molecular system [107].

The MARTINI force field for the molecular simulations of biological systems was proposed by Marrink and Mark [108], and has been validated by the results of all-atom MD simulation [109]. With the MARTINI CG-MD technique, the overall particle number can be reduced to only 25% of the original atom number, which will significantly save the computational cost.

2.5.3 Continuum mechanics models for microfilament networks

The networks of cross-linked and bundled actin filaments are ubiquitous in the cytoskeleton. It is a kind of structure which is built from numerous F-actins which help a living cell to resist external mechanical load. The structure should be an optimisation reflecting a living cell's physical functions. The structures are very complex to summarize that the networks observed in living cells and vitro are totally different [110]. The biphasic model based on continuum mechanics theory has been proposed to investigate the mechanical behaviours of actin gel in solution based by homogenizing the actin cortex in living cells [111, 112]. However, later studies proved that the mechanical behaviours of microfilament networks are complex physiological processes which are related to architectures and the chemical components of microfilament networks. Wachsstock et al. proved that the dynamics of the networks cross linkers determines mechanical properties of microfilament networks [113], and Gardel et al. discovered that the density of cross-linkers is also quite crucial to the stiffness of microfilament networks [61]. All these fascinating physiology features of microfilament networks lead to the self-protective properties and the functional features of biological tissues.

By employing mechanical properties from experiments, continuum beam model has been used to predict the mechanical and thermal dynamics performances of the single F-actin and microfilament networks. Based on the continuum beam assumption, You et al. presented a mathematical model for the strain amplification in

the cytoskeleton of osteocytes [114], Mogilner and Oster proposed a model to explain the force generation by actin polymerization [115], Chen and Shenoy explained the myosin II induced strain stiffening of actin filament networks [116].

2.5.4 Multiscale approach for microfilament networks

Recent advances in analytical and computational modelling frameworks to describe the mechanics of materials on scales ranging from the atomistic, through the microstructure or transitional, and up to the continuum are reviewed. It was shown that multiscale modelling of materials approaches relies on a systematic reduction in the degrees of freedom on the natural length scales that can be identified in the material. Connections between such scales were achieved either by a parameterization or by a 'zoom-out' or 'coarse-grained' procedure [117].

Multiscale approaches can provide essential physical basis from atomic level biophysics analysis of protein molecules to understand the biomechanics and the mechanobiology of microfilament networks [10, 118]. The concepts of bottom-up approaches have been proposed to understand mechanical behaviours of the single F-actin and microfilament networks [119, 120]. At molecular level, the MD method can describe the ultimate motion phenomena of living systems in terms of chemistry and physics [101]. However, due to the limitation of the computer power, the CG level investigation abstracted from all-atom MD simulations is needed to unravel the biological complexity from physical basis. Chu et al. and Deriu et al. independently proposed CG models for single F-actin based on structural features of G-actin by thermal dynamics matching methods [121, 122]. Shimada et al. introduced a serial linear spring model based on Brownian dynamics method [123]. As introduced, Ji and Feng proposed a CG model for the dynamics simulation of microtubules which is another important mechanical component of cytoskeleton in living cells [89]. However, as these CG models were primarily designed to predict dynamics behaviours, the potential functions in these models were typical harmonic potential or Lennard-Jones (LJ) potential, which are hard to describe the special constitutive relation between the adjacent G-actin monomers.

2.6 INTERACTION BETWEEN PROTEIN AND INORGANIC MATERIALS

With the recent developments of advanced nano-technology, biomedical applications are facing a revolution that subjects to these functional materials, especially in the science of drug delivery, surgical replacement and bio-scaffolds. Many cellular toxicity experiments have been done to evaluate the direct effects of these materials. However, strict biosafety evaluation is still necessary for any kind of new material to be used in biomedical applications.

Experimental techniques have been adopted to investigate the micro/nanoscale interactions between living organisms and inorganic materials. Atomic force microscopy has been used to characterize the adhesion between living cells and an inorganic substrate [124]. However, the inorganic particles to which in cells attach are often nanoscopic in size, thereby rendering it difficult to perform physical or experimental characterization involving the micromanipulation of proteins to gain quantitative insight. In combination with experimental characterization, modelling provides a powerful tool for probing the mechanism of the interaction between organic macromolecules and inorganic materials. Despite these numerical explorations of the mechanical behaviours of carbon nanomaterials, their adhesive characteristics on biomolecules need further theoretical studies. *ab initio* and MD modelling strategies have been applied to characterize the interaction between biomolecules (e.g. protein, amino acids and nuclei acids) and inorganic materials (i.e. graphene, metal particles and hydroxyapatite) [125-127].

There is limited study on the interaction between actin and inorganic material as actin mainly performs as a structural protein in cells. Comparing to other functional proteins, the dynamics of protein is of ‘less’ significance’ in directly explaining the biological performances of living cells. However, the biophysical behaviours of F-actin can regulate the mechanical performance of living cells. All of the factors that are adhesive to F-actin CSK and change its mechanical performances can potentially mediate the behaviour of living cells. Therefore, we suggest that the interaction between actin and nanomaterials need to be strictly evaluated to exclude the potential risk of these new biomedical materials in clinical applications. In this thesis, as an example, we have studied the interaction between actin and graphene, which is one of the most popular 2D single layer functional materials.

2.7 SUMMARY AND IMPLICATIONS

As the essential component of the cytoskeleton, the actin plays critical roles in many cellular processes of eukaryotic cells such as wound healing [128], cellular motility [47, 129] and cytokinesis of eukaryotic cells [130]. The mechanisms of force generating and transferring via microfilament networks were focused for decades to understand the mechanobiology of cellular processes in living eukaryotic cells. Microfilament networks can be simplified as an architecture which is built from the basic building blocks: F-actin. Therefore, mechanical properties of F-actin play an important role and should be focused to find out homogenized mechanical behaviours of microfilament networks.

Back into 1990s, both tensile Young's modulus and torsion rigidity of single actin filament were measured at molecular level. However, experimental tests of single actin filament's stiffness are limited by its operating cost. Analytical characterization is needed to assist all conditional Young's modulus evaluation of single F-actin from the atomic configuration's viewpoint, which can also reduce the huge cost of experimental testing. The MD simulations were mostly designed for the thermal dynamics response of the actin molecules. To the best of our knowledge, few discoveries about the mechanical performance by MD simulation can be found. Specific molecular simulations about the mechanical performances of F-actin and microfilament networks should be designed to investigate mechanical properties of the single F-actin from microscopy point of view.

The molecular modelling method, as a theoretical tool for microfilament networks mechanical performance analysis, still faces the challenge from the computation power. The biggest all-atom MD simulation of a single F-actin is less than hundred nano meters, which is far less than the real size of the eukaryotic cells. In order to explore mechanical properties of microfilament networks, a new multiscale approach, is needed to bridge bottom physics basis of actin molecules and continuum mechanics modelling of microfilament networks.

The biphasic model based on continuum mechanics theory had been proposed to investigate mechanical behaviours of actin gel in solution by homogenizing the actin cortex in living cells. However, later studies proved mechanical behaviours of microfilament networks are complex physiological processes which are related to

architectures and the chemical components of microfilament networks. Due to the difficulties in abstracting all these dynamics features into a pure mathematical presentation on continuum mechanics level, the multiscale approach from microscopy point of view are needed to predict dynamics behaviours of microfilament networks.

In addition to the deformation properties of CSK, the adhesive characteristics of inorganic material from biomedical applications are also significant to the safety of living cells. The interaction between actin and inorganic materials should also be strictly evaluation from both experimental and numerical modelling ways.

To sum up, a new multiscale framework is critically needed to understand the biomechanics and mechanobiology of microfilament networks. This method is designed under the bottom-up philosophy: from atomic physics basis to continuum mechanics description. This framework ranges from nanoscale to microscale, can provide a bridge to explain the biological performances of cells from the fundamental understandings of the molecular events happening at atomic scale. This framework can be applied in the analysis of the mechanical performances of microfilament networks which is significant to the cellular responses under external stimuli. This multiscale framework provides a powerful numerical tool to understand the mechanobiology of F-actin CSK in cells and design artificial biomaterials which have interaction with F-actin CSK in biomedical engineering.

Chapter 3: Molecular Investigation of Single F-actin (Paper 1)

Research paper one:

Li, T., Gu, Y.T., Oloyede, A., Yarlagadda, P.K.D.V., 2014. Molecular investigation of the mechanical properties of single actin filaments based on vibration analyses. ***Computer Methods in Biomechanics and Biomedical Engineering*** 17, 616-622.

Computer Methods in Biomechanics and Biomedical Engineering, 2014
Vol. 17, No. 6, 616–622, http://dx.doi.org/10.1080/10255842.2012.706279

Molecular investigation of the mechanical properties of single actin filaments based on vibration analyses

Tong Li, Y.T. Gu*, Adekunle Oloyede and Prasad K.D.V. Yarlagadda

School of Chemistry, Physics and Mechanical Engineering, Queensland University of Technology, 2 George St, GPO Box 2434, Brisbane, QLD 4001, Australia

(*Received 9 May 2012; final version received 21 June 2012*)

The mechanical vibration properties of single actin filaments from 50 to 288 nm are investigated by the molecular dynamics simulation in this study. The natural frequencies obtained from the molecular simulations agree with those obtained from the analytical solution of the equivalent Euler–Bernoulli beam model. Through the convergence study of the mechanical properties with respect to the filament length, it was found that the Euler–Bernoulli beam model can only be reliably used when the single actin filament is of the order of hundreds of nanometre scale. This molecular investigation not only provides the evidence for the use of the continuum beam model in characterising the mechanical properties of single actin filaments, but also clarifies the criteria for the effective use of the Euler–Bernoulli beam model.

Keywords: actin filament; mechanical vibration; flexural rigidity; Young's modulus; coarse-grained molecular dynamics

Statement of Contribution of Co-Authors for Thesis by Published Paper

The following is the format for the required declaration provided at the start of any thesis chapter which includes a co-authored publication.

The authors listed below have certified* that:

1. they meet the criteria for authorship in that they have participated in the conception, execution, or interpretation, of at least that part of the publication in their field of expertise;
2. they take public responsibility for their part of the publication, except for the responsible author who accepts overall responsibility for the publication;
3. there are no other authors of the publication according to these criteria;
4. potential conflicts of interest have been disclosed to (a) granting bodies, (b) the editor or publisher of journals or other publications, and (c) the head of the responsible academic unit, and
5. they agree to the use of the publication in the student's thesis and its publication on the QUT ePrints database consistent with any limitations set by publisher requirements.

In the case of this chapter:

Li, T., Gu, Y.T., Oloyede, A., Yarlagadda, P.K.D.V., 2014. Molecular investigation of the mechanical properties of single actin filaments based on vibration analyses. Computer Methods in Biomechanics and Biomedical Engineering 17, 616-622.

Contributor	Statement of contribution*
Tong Li Signature 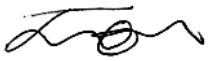 Date 24/11/2014	Designed and conducted numerical model. Conducted data analysis. Wrote the manuscript.
YuanTong Gu*	Designed and conducted numerical model. Involved in the conception and design of the project. Assisted data analysis. Provided feedback on manuscript.
Kunle Oloyede	Involved in the conception and design of the project. Provided feedback on manuscript.
Prasad Yarlagadda	Involved in the conception and design of the project. Provided feedback on manuscript.

Principal Supervisor Confirmation

I have sighted email or other correspondence from all Co-authors confirming their certifying authorship.

YuanTong Gu	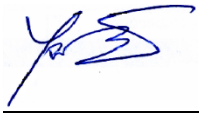	24/11/2014
Name	Signature	Date

3.1 ABSTRACT AND KEYWORDS

The continuum beam model had been used to predict the mechanical properties of single actin filaments on continuum mechanics level. However, this continuum model clearly has limitations to represent the nanoscale single actin filaments. In this paper, the mechanical vibration properties of single actin filaments with lengths from 50 to 288nm are numerically investigated by the molecular simulation, i.e., the Coarse Grain Molecular Dynamics (CG-MD) simulations. The Fast Fourier Transform (FFT) power spectrum analysis is then applied to the periodic motion information from the molecular simulations to extract the natural frequencies of the simulated single actin filaments. The natural frequencies obtained from the molecular simulations are compared with the Normal Mode Solution (NMS) of the equivalent Euler-Bernoulli beams, and the mechanical properties including the flexural rigidity and the Young's modulus are then evaluated. Based on the convergence study of the mechanical properties with respect to the filament length, it has found that the Euler-Bernoulli beam model can only be reliably used when the aspect ratio of the single actin filament is larger than 17. Hence, this molecular investigation not only provides the evidence for the use of the continuum beam model in characterizing the mechanical properties of single actin filaments, but also clarifies the criteria for the effective use of the Euler-Bernoulli beam model.

Keywords: Actin filament; Mechanical vibration; Flexural rigidity; Young's modulus; Coarse-Grained Molecular Dynamics

3.2 INTRODUCTION

The cytoskeleton is the structural fundament for an eukaryotic cell to resist deformations due to external loads [8]. Microfilament, intermediate filament and microtubule are three principal cytoskeleton elements [131]. Among these three cytoskeleton components, microfilament is discovered in non-muscle cells, which indicates that the mechanical behaviours of the microfilament networks may regulate the cellular change and the force generation in cell migration and division [129, 132-134]. As the principal component of microfilaments, mechanical properties of single actin filaments should be focused to understand the mechanical performances of the microfilament.

As the development of experiment techniques in last few decades, scholars experimentally studied the flexural rigidity and the Young's modulus of single actin filament by either directly stretching tests [53, 55, 64, 135], or thermal fluctuation analysis [56, 58, 65]. By employing the mechanical properties from experiments, the continuum beam model has been used to predict the mechanical and thermal dynamics performances of single actin filaments and microfilament networks. Based on the continuum beam assumption, You et al. presented a mathematical model for the strain amplification in the actin cytoskeleton of osteocytes [114], Mogilner and Oster proposed a model to explain the force generation by actin polymerization [115], Chen and Shenoy explained the myosin II induced strain stiffening of actin filament networks [116]. However, the reliability of continuum beam model being employed in the predictions on nanoscale is still unclear, and this calls for further studies.

The molecular characterization of the mechanical performances provides a way to unravel the physical basis of biological phenomena in living cells [101]. In the nanoscale biotechnology, the performance of a structural protein is decided by the atomic configuration. With the high resolution atomic configuration of actin filament [92, 93], molecular dynamics (MD) simulations are executed on single actin filaments, and the structural properties are estimated [103, 105]. Deriu et al. and Matsushita et al. independently studied the thermal dynamics behaviours of single actin filaments by molecular dynamics and elastic networks model simulation, and estimated the mechanical properties of the single actin filaments [106, 107].

However, to the best of our knowledge, the study of direct MD simulations of mechanical performances of single actin filaments is limited.

In this paper, the molecular simulations of mechanical vibrations of single actin filaments are conducted to validate the reliability of continuum beam model in the nanoscale single actin filaments modelling. Due to the challenge in reaching a fully equilibrated atomic configuration of single actin filaments in all-atom MD simulation using today's computational power, it is hard to evaluate the mechanical properties directly by MD simulations of the quasi static stretching or bending tests of single actin filaments. However, the mechanical vibration, as the dynamics motion, can also reflect the mechanical constitutive information of the system. Therefore, in this paper, the free vibrations of single actin filaments after direct mechanical excitations are investigated by the molecular simulations.

The MARTINI force field for the molecular simulations of biological systems is proposed by Marrink and Mark [108], and has been validated by the results of all-atom MD simulation [109]. With the MARTINI Coarse Grain Molecular Dynamics (CG-MD) technique, the overall particle number can be reduced to only 25% of the original atom number, which will significantly save the computational cost. The Fast Fourier Transform (FFT) is subsequently applied to the periodic motion information from the CG-MD simulations to find out the natural frequencies of the single actin filaments. The natural frequencies obtained from the molecular technique are compared with the Normal Mode Solution (NMS) of the equivalent Euler-Bernoulli beams, and the flexural rigidity and the Young's modulus can be then evaluated. Based on the mechanical properties evaluations from the molecular technique, the reliability of continuum beam model can be studied correspondingly.

3.3 METHODS

In order to investigate the mechanical performances of single actin filaments, the molecular simulation technique is employed in this paper. Numerical simulations are conducted to study the mechanical vibration properties of the actin filament molecular system by the CG-MD (MARTINI force field) method. The power spectrum analysis is used to extract the natural frequencies from the molecular simulations. The natural frequencies are compared with those obtained from the analytical solutions of the Euler-Bernoulli beam theory, and the flexural rigidity and

the Young's modulus of single actin filaments can be then evaluated. The CG-MD simulation technique, the power spectrum analysis and the analytical solutions of the natural frequencies based on the Euler-Bernoulli beam model will be detailed in this section.

3.3.1 Atomic structure of the single actin filaments

The atomic structure of a globular actin is obtained from Protein Data Base (PDB) under the ID 2ZWH which is classified in contractile protein family [93]. The 'Oda 2009' actin filament model is developed based on the nature of the globular actin to the filamentous actin transition [93] by an original code. There are 13 globular actin subunits in every actin filament repeat, the rotation for every monomer is 166.2o and the length of one actin filament repeat is 35.9nm [95]. The rotation mechanism makes the actin filament appear to be a turning right-hand double helix structure. Fig. 3-1 shows the detailed configuration of a single filamentous actin repeat.

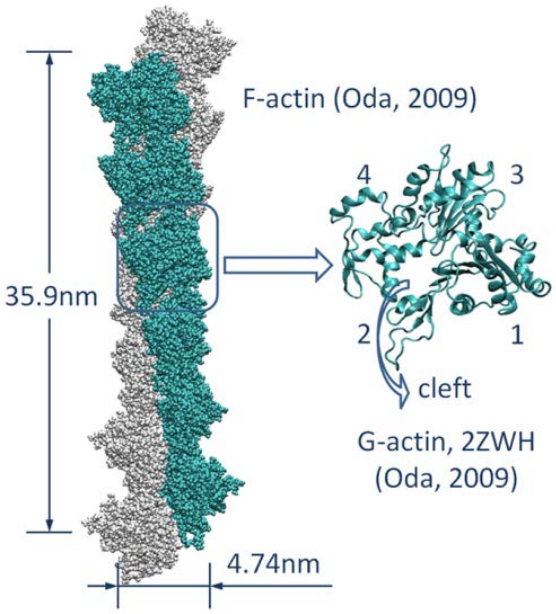

Fig. 3-1. Actin filament repeat built from globular actin ('Oda 2009'). 13 globular actin monomers build one actin filament repeat with the length of 35.9 nm.

3.4 THE CGMD SIMULATION OF FREE VIBRATION

The CG-MD simulations (MARTINI force field) are employed on the actin filaments with lengths from 50 to 288nm to investigate the mechanical properties of single actin filaments, and the molecular simulations are all performed on the platform of non-commercial package of GROMACS [136].

The CG-MD simulation is divided into two parts: the simulation of the mechanical excitation and the simulation of the free vibration. In the simulation of the mechanical excitation, 10 ns CG-MD simulation with a mechanical excitation is performed in an NPT ensemble (pressure 1 bar, temperature 303K), in which both pressure and temperature are controlled by the Berendsen method [137]. Both of the ends of the simulated actin filament are fixed, and a transverse step force (from 75 to 1500kJ/mol·nm, with respect to the filament length) is applied to excite an initial deformation for the free vibration of the filament. Langevin dynamics [138] is used in this part to mimic the friction from water. Subsequently, 20-40ns CG-MD simulations without external force besides the fixed-fixed boundary condition are performed in an NVE ensemble after the mechanical excitation simulation to mimic the free vibration of single actin filaments. Note that the free vibration simulations are performed in vacuum to avoid the damping effect from water molecules.

The Root Mean Square Deviation (RMSD) of certain atoms in a molecule with respect to a reference structure is defined by least-square fitting [139]:

$$RMSD(t_1, t_2) = [\frac{1}{M}\sum_{i=1}^{N} m_i (p_i(t_1) - p_i(t_2))^2]^{\frac{1}{2}}, M = \sum_{i=1}^{N} m_i \quad (3\text{-}1)$$

where $p_i(t_1)$ is the position of atom i at the time t, mi is the mass of atom *i*, *N* is the atom number and the reference structure in this paper is the initial structure (t_2=0). Because there are millions of freedoms in a complex biological molecular system, it is hard to summarize total energy or a single atom's motion as a vibration signal of the whole system's vibration. However, the system's homogenized motion information can be then evaluated from the value of RMSD.

The CG-MD simulation in the second part can be taken as the free vibration after an initial mechanical excitation has been applied and then withdrawn. With the help of the FFT power spectrum analysis, the discrete data with different vibration modes from the molecular simulations can be processed to distinguish the vibration modes from the complex system motions.

3.4.1 The NMS of the Euler-Bernoulli beam model

In the vibration theory, the NMS is the process to solve the frequencies of the normal modes of a system known as natural frequencies. To validate the reliability of the beam model in the mechanical behaviours prediction of single actin filaments,

equivalent beams with the same geometry and material constants of single actin filaments are analysed through the NMS of the classic beam model. To be comparable with the experimental studies, the radius of the single beam cross section is assumed to be 2.82nm, which is the same as literatures [53]. The actin filaments simulated in this paper are with lengths from 50 to 288 nm. It is noteworthy that, the length of the single actin filament is different from the beam length because the actin molecules on the ends of the filament are frozen as fixed boundary condition. Therefore, the beam length is shorter than the real filament length. The aspect ratios of the equivalent beam model are from 6.9 to 49.1, The Euler-Bernoulli beam model is employed to represent the single actin filaments [140]. Fig. 3-2(a) shows the equivalent beam model with the same geometry as the single actin filaments. Fig. 3-2(b) shows the deformed configuration of the beam under the transverse excitation.

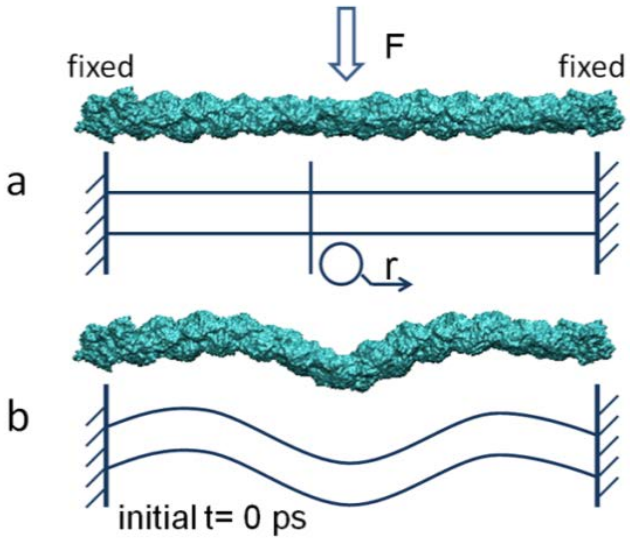

Fig. 3-2. Schematic of initial transverse excitation applied on the single actin filament. a: is the transverse step force loading on a both ends fixed actin filament. b: is the initial atomic configuration after the transverse excitation. The beam length is L and the cross section radius is r; there are 26 G-actin monomers in this case, and each end has two actins monomers being fixed.

The analytical NMS of a Euler-Bernoulli beam can be found in Rao's book [141]. For a uniform Euler-Bernoulli beam, the governing equation of free vibration is:

$$\frac{d^4 w}{dx^4} - \beta^2 w = 0 \tag{3-2}$$

where, w is the deflection, and β is a constant for frequency according to the boundary conditions. Therefore, the natural frequency f can be calculated for this equivalent beam based on its geometry and material constants:

$$f = \frac{\beta}{2\pi L^2}\sqrt{\frac{EI}{\rho A}} \tag{3-3}$$

where E is the Young's modulus, I is the moment of inertia of the cross section, ρ is the density of the material and A is the area of the beam cross section. L is the effective beam length, which is 11nm (the length of four actin molecules) smaller than the real filament length as the four actin molecules on the ends of the filament are fixed. Note that, EI is defined as the flexural rigidity of the beam. Under the circular cross section assumption, the moment of inertia I is supposed to be $\pi r^4/4$, where r is the radius of the cross section (2.82nm) [53]. The homogenized constant ρA can be estimated by dividing the mass of one filament repeat by the repeat length as $\rho A = Mn/N_A l$. Where n=13, which is the number of globular actin monomers in one repeat of the filamentous actin. N_A is the Avogadro's number, M is the molar mass of an globular actin which is 42kDa and l is the length of one actin filament repeat, which is 35.9nm. With these constants, ρA is estimated to be 2.53×10^{-14}kg/m. The flexural rigidity (EI) and the Young's modulus (E) of single actin filaments can be then evaluated from the NMS results by comparing the natural frequencies obtained from the molecular simulations and the corresponding NMS of the Euler-Bernoulli beam model.

3.5 RESULTS AND DISCUSSION

Herein, the molecular technique is employed to characterize the mechanical vibrations of single actin filaments. Based on the evaluations of the key mechanical properties, we studied the reliability of the Euler-Bernoulli beam model in the nanoscale single actin filaments modelling.

3.5.1 The free vibration of single actin filaments

The free vibration simulation of CG-MD (MARTINI force field) for the 144nm actin filament is specifically extended to 40 ns, which is 20 ns longer than the other filament length cases, to study the duration dependency of the characterization result from the molecular simulations. The FFT analyses are independently applied to the RMSD results within four different free vibration simulation stages, including 0-10 ns, 10-20ns, 20-30ns and 30-40ns. Fig. 3-3 shows the results of the power spectrum analyses obtained from different simulation stages.

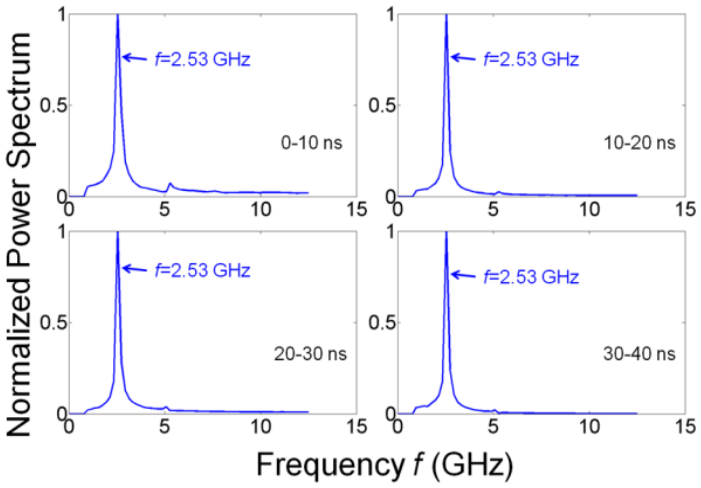

Fig. 3-3. Power spectrum analyses within different simulation stages of a 144 nm actin filament. The results in different simulation stages all present the same natural frequency of 2.53 GHz.

All the natural frequencies obtained have identical values of 2.53GHz in different simulation stages, indicating that the natural frequency is insensitive with the simulation time durations. Therefore, the vibration simulation technique developed in this paper is reliable during the whole simulation procedure. This is an attractive advantage of this technique because the reliable results can be extracted by employing a short free vibration simulation time duration (i.e., 10 ns for this case), which will significantly save the computational cost.

Fig. 3-4 shows the deformation configurations of a 144nm single filament at different time in the free vibration simulation. In the CG-MD simulation, the step force is applied in a short duration of 10ns in the first simulation part of the mechanical excitation. As a result of the dynamic excitation, the deformation of the single filament is not in the absolute bending status. Based on the deformation configurations obtained from the simulation as shown in Fig. 3-4, it can be concluded that the initial mechanical excitation has led to the third order free vibration mode, and the corresponding natural frequency constant β in Eq. (3.3) is 120.9 [141]. It should be mentioned here that the order of the free vibration mode to be excited depends on the boundary conditions at the two ends and the external excitation force. The third order free vibration mode obtained in this study is because we consider a fixed-fixed filament under a transverse step excitation force.

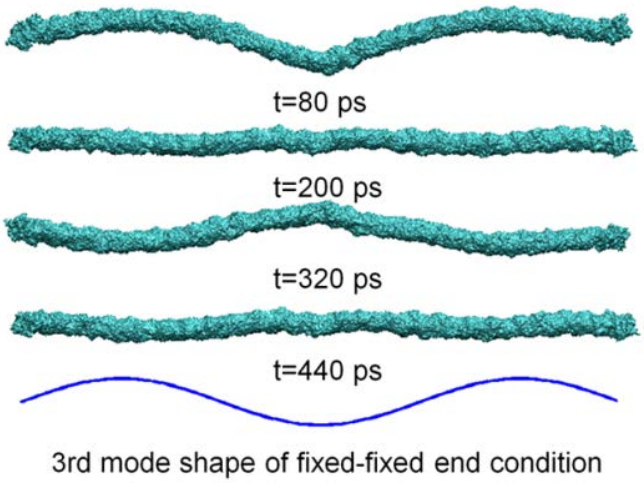

Fig. 3-4. The deformation of a both ends fixed single actin filament (144 nm) during free vibration. The deformations with respect to simulation time match the third mode shape of free vibration from analytical solution.

The free vibration investigations are performed on different actin filaments with lengths from 50 to 288nm. By employing a typical Young's modulus (2.5Gpa) of single actin filaments obtained from experiments [55-58], the analytical solution of the natural frequency of these actin filaments can be evaluated using Eq. (3-3), which is derived based on the Euler-Bernoulli beam model. Fig. 3-5 shows the frequencies evaluated theoretically by the beam model and obtained numerically by the CG-MD simulation, respectively. The frequencies obtained by these two approaches agree with each other. These identical results indicate that the Euler-Bernoulli beam model can be a reasonable candidate to describe the mechanical vibration properties of single actin filaments. From Fig. 3-5, it can be also found that the natural frequencies decrease while the length of the single actin filament increases.

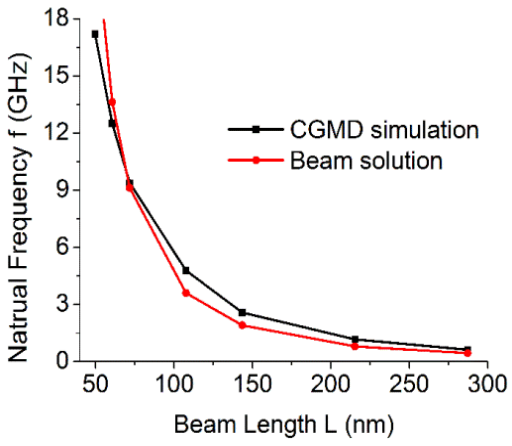

Fig. 3-5. Frequency from CGMD simulation compared with the theoretical beam solution derived from the NMS of the Euler-Bernoulli beam model. The frequencies are obtained from the first 10 ns CGMD simulations of the free vibration of single actin filaments.

3.5.2 The reliability of the Euler-Bernoulli beam model

The numerical characterization technique can also be employed as an effective approach for the estimation of the key material properties of single actin filaments. Take the flexural rigidity as example, the flexural rigidity of single actin filaments can be derived from Eq. (3-3), i.e.,

$$EI = 4\pi^2 \rho A L^4 \frac{f^2}{\beta^2} \tag{3-4}$$

With the provided geometry and material constants of the single actin filament, for a 144nm filament, the natural frequency obtained by the CG-MD and the FFT is 2.53GHz, as shown in Fig. 3-3 and Fig. 3-5. Therefore, the flexural rigidity can be calculated using Eq. (3-4), i.e., EI= 13.3×10^{-26} Nm^2. According to literatures, the flexural rigidity evaluated from the experimental studies varied between 3 to 10×10^{-26} Nm^2 [55, 56, 58, 107]. The characterization result obtained in this study by the molecular investigation of the free vibration is on the same order with the experimental results.

It is noteworthy that, the solution environment is important to the experiment results and theoretical evaluations [58]. To avoid the damping effect from water molecules in the vibration analysis, in the studies of this paper, the molecular simulation of the free vibration is performed in vacuum, while previous experiments and thermal dynamics evaluation were taken in solution environment. In other words, the undamped free vibration is studied in this paper while previous experiments and thermal dynamics evaluation considered an underdamped system. Based on the mechanical vibration theory [141], the undamped natural frequency will be larger than the underdamped natural frequency, which explains why the flexural rigidity obtained from our studies is in the upper limit for the range of the flexural rigidity obtained from the experimental studies.

Single actin filaments were assumed to be Euler-Bernoulli beams on the continuum mechanics level to understand the biomechanics of the microfilament networks in living cells including strain amplification [114], force generation [115] and strain hardening [116]. In order to validate the reliability of the Euler-Bernoulli beam model in predicting the mechanical vibration behaviours of single actin filaments on nanoscale, mechanical properties of single actin filaments with different

lengths are evaluated to investigate the size dependency of the beam model. Fig. 3-6 shows the flexural rigidity and the Young's modulus evaluated from the NMS of Euler-Bernoulli beam model by using the natural frequencies from the molecular simulations with respect to the actin filament lengths. The flexural rigidity, which is evaluated based on the Eq. (3-4), increases with the length of the filament and converges to 13.3×10^{-26} N·m2 when the length of the single actin filament is on the order of hundreds nano meter scale. The Young's modulus presents a same trend which converges to 2.6GPa.

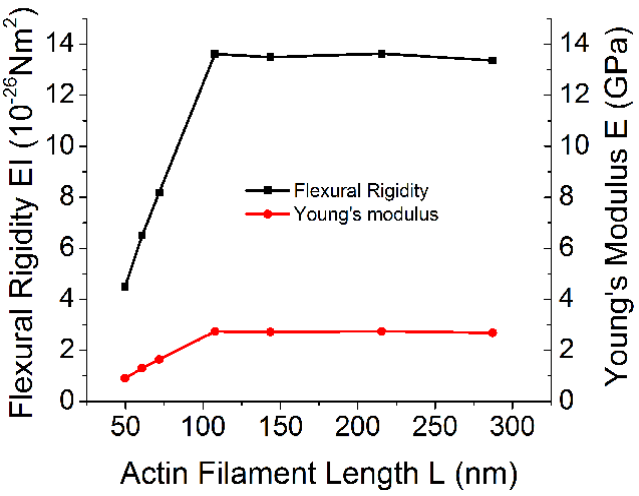

Fig. 3-6. The flexural rigidity and the Young's modulus evaluations of filaments based on beam model. The flexural rigidity converges to 13.3×10-26 N·m2, and the Young's modulus converges to 2.6 GPa when the length is on the order of hundreds nano meter scale.

According to the mechanics of materials, for the continuum material, the flexural rigidity and Young's modulus should not be related to the length of beam. However, the mechanical properties of the filaments evaluated from the classic beam model do not converge until the beam aspect ratio of the equivalent beam exceeds 17, which means the Euler-Bernoulli beam model is not applicable when the aspect ratio of the single actin filament is less than 17. This is an important finding because complex single actin filaments exist with a wide range of lengths in living cells[142], and the beam models should be carefully selected to accurately characterize the mechanical properties of the single actin filaments whose lengths vary from nanoscale to microscale.

3.6 CONCLUSION

The mechanical vibration properties of single actin filaments are studied by a comprehensive numerical technique based on the Coarse-Grained Molecular

Dynamics simulations, the Fast Fourier Transform power spectrum analysis and the Normal Mode Solution of the Euler-Bernoulli beam. The frequency results are found to have no dependence on the duration of the simulations, which can significantly save the computational cost by conducting only short duration molecular simulations. For single actin filaments with lengths from 50 to 288 nm, the natural frequencies obtained by the numerical simulations match the analytical solutions of the Euler-Bernoulli beam model, which proves that the continuum beam model can be a good candidate in the nanoscale single actin filaments modelling. The evaluations of the flexural rigidity and the Young's modulus agree with those obtained by the experiments, Through the study on the convergences of the evaluations with respect to the filament length, it can be found that the Euler-Bernoulli beam model can be only reliably used for continuum mechanics analyses of single actin filaments when the aspect ratio is larger than 17, which is different from the mechanics of traditional materials [140].

In summary, the investigation of the mechanical vibration provides the evidence for the use of continuum beam model in nanoscale single actin filaments modelling from the microscopy point of view. The molecular simulation of the mechanical behaviours of single actin filaments provides a way to evaluate the mechanical properties of single actin filaments which are needed in the continuum mechanics level study to predict the performances of the cytoskeleton. It has also clarified the criteria of the aspect ratio of the single actin filaments for the effective use of the Euler-Bernoulli beam model. This will eventually contribute to understand the biomechanics and mechanobiology of the microfilament networks in living cells.

3.7 ACKNOWLEDGEMENT

Support from the ARC Future Fellowship grant (FT100100172) is gratefully acknowledged. The authors thank Dr. T. Oda for the help in the atomic structure modelling of actin filament.

Chapter 4: Multiscale Model for F-actin CSK (Paper 2)

Research paper two:

Li, T., Gu, Y.T., Feng, X.-Q., Yarlagadda, P.K.D.V., Oloyede, A., 2013. Hierarchical multiscale model for biomechanics analysis of microfilament networks. ***Journal of Applied Physics*** 113, 194701-194707.

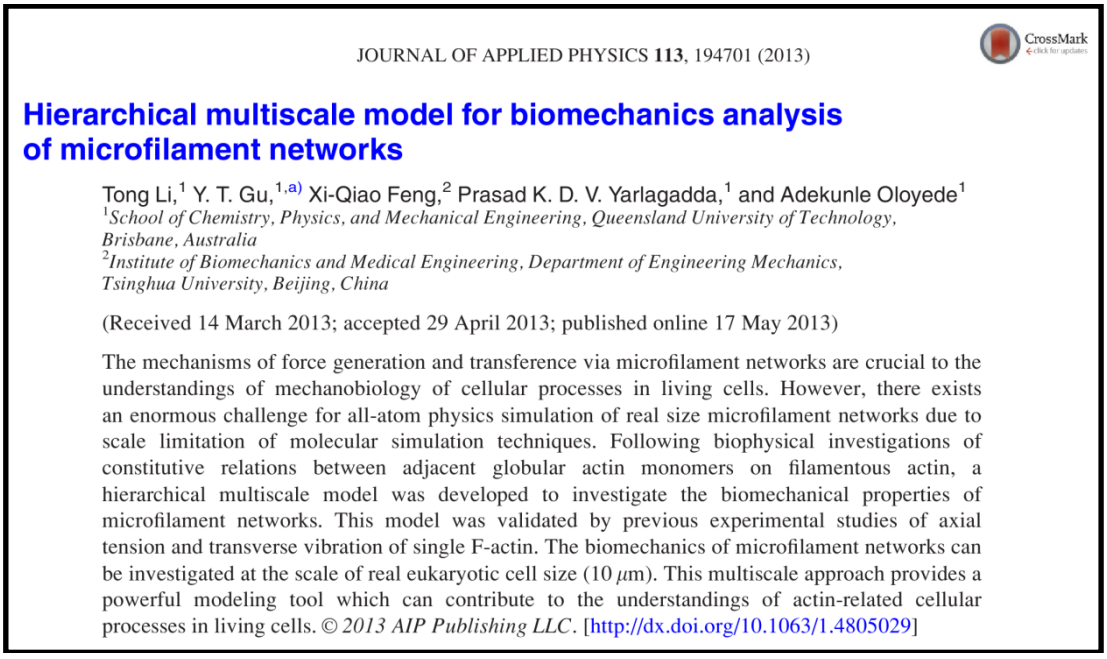

JOURNAL OF APPLIED PHYSICS **113**, 194701 (2013)

Hierarchical multiscale model for biomechanics analysis of microfilament networks

Tong Li,[1] Y. T. Gu,[1,a)] Xi-Qiao Feng,[2] Prasad K. D. V. Yarlagadda,[1] and Adekunle Oloyede[1]
[1]*School of Chemistry, Physics, and Mechanical Engineering, Queensland University of Technology, Brisbane, Australia*
[2]*Institute of Biomechanics and Medical Engineering, Department of Engineering Mechanics, Tsinghua University, Beijing, China*

(Received 14 March 2013; accepted 29 April 2013; published online 17 May 2013)

The mechanisms of force generation and transference via microfilament networks are crucial to the understandings of mechanobiology of cellular processes in living cells. However, there exists an enormous challenge for all-atom physics simulation of real size microfilament networks due to scale limitation of molecular simulation techniques. Following biophysical investigations of constitutive relations between adjacent globular actin monomers on filamentous actin, a hierarchical multiscale model was developed to investigate the biomechanical properties of microfilament networks. This model was validated by previous experimental studies of axial tension and transverse vibration of single F-actin. The biomechanics of microfilament networks can be investigated at the scale of real eukaryotic cell size (10 μm). This multiscale approach provides a powerful modeling tool which can contribute to the understandings of actin-related cellular processes in living cells. © *2013 AIP Publishing LLC*. [http://dx.doi.org/10.1063/1.4805029]

Statement of Contribution of Co-Authors for Thesis by Published Paper

The following is the format for the required declaration provided at the start of any thesis chapter which includes a co-authored publication.

The authors listed below have certified* that:

1. they meet the criteria for authorship in that they have participated in the conception, execution, or interpretation, of at least that part of the publication in their field of expertise;
2. they take public responsibility for their part of the publication, except for the responsible author who accepts overall responsibility for the publication;
3. there are no other authors of the publication according to these criteria;
4. potential conflicts of interest have been disclosed to (a) granting bodies, (b) the editor or publisher of journals or other publications, and (c) the head of the responsible academic unit, and
5. they agree to the use of the publication in the student's thesis and its publication on the QUT ePrints database consistent with any limitations set by publisher requirements.

In the case of this chapter:

Li, T., Gu, Y.T., Feng, X.-Q., Yarlagadda, P.K.D.V., Oloyede, A., 2013. Hierarchical multiscale model for biomechanics analysis of microfilament networks. Journal of Applied Physics 113, 194701-194707.

Contributor	Statement of contribution*
Tong Li Signature 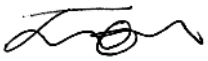 Date 24/11/2014	Designed and conducted numerical model. Conducted data analysis. Wrote the manuscript.
YuanTong Gu*	Designed and conducted numerical model. Involved in the conception and design of the project. Assisted data analysis. Provided feedback on manuscript.
Xi-Qiao Feng	Involved in the conception and design of the project. Provided feedback on manuscript.
Kunle Oloyede	Involved in the conception and design of the project. Provided feedback on manuscript.
Prasad Yarlagadda	Involved in the conception and design of the project. Provided feedback on manuscript.

Principal Supervisor Confirmation

I have sighted email or other correspondence from all Co-authors confirming their certifying authorship.

YuanTong Gu 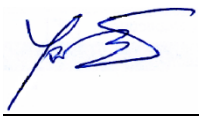 24/11/2014

Name Signature Date

4.1 ABSTRACT AND KEYWORDS

The mechanisms of force generation and transference via microfilament networks are crucial to the understandings of mechanobiology of cellular processes in living cells. However, there exists an enormous challenge for all-atom physics simulation of real size microfilament networks due to scale limitation of molecular simulation techniques. Following biophysical investigations of constitutive relations between adjacent globular actin monomers on filamentous actin, a hierarchical multiscale model was developed to investigate the biomechanical properties of microfilament networks. This model was validated by previous experimental studies of axial tension and transverse vibration of single F-actin. The biomechanics of microfilament networks can be investigated at the scale of real eukaryotic cell size (10 μm). This multiscale approach provides a powerful modelling tool which can contribute to the understandings of actin-related cellular processes in living cells.

Keywords: Multiscale; Biomechanics; Microfilament networks; Coarse-Grained

4.2 INTRODUCTION

As an essential component of a cytoskeleton, actin plays critical roles in many cellular processes of eukaryotic cells, such as wound healing [128], cellular motility [47, 129], and cytokinesis of eukaryotic cells [130]. The mechanisms of force generation and transference via microfilament networks was focused on for decades in order to understand the mechanobiology of cellular processes in living eukaryotic cells. Complex mechanical performances including viscosity, strain hardening, stress hardening, and stress softening were discovered in the last few decades [60, 62]. Various actin-binding proteins working in concert to regulate the kinetics of filamentous actin (F-actin) assembly [110], which significantly affects the mechanical performances of microfilament networks. All these discoveries indicate that absolute mathematical model is hard to achieve by homogenizing microfilament networks as continuous materials without losing biological features of these soft tissues.

Multiscale approaches provide a view of the essential physical basis to allow an understanding of biomechanics and mechanobiology of microfilament networks from atomic level biophysics analysis [118, 143, 144]. The concepts of bottom-up approaches have been proposed to understand mechanical behaviours of single F-actin and microfilament networks [120]. On molecular level, the molecular dynamics (MD) method can describe ultimate motion phenomena of living systems in terms of chemistry and physics [101]. However, due to the limitation of computer power, Coarse-Grained (CG) level investigation abstracted from all-atom MD simulations is necessary to unravel the biological complexity from the physical basis [145]. Chu et al. and Deriu et al. independently proposed CG models of single F-actin based on structural features of globular actin (G-actin) by thermal dynamics matching methods [121, 122]. Shimada et al. introduced a serial linear spring model for F-actin dynamics based on the Brownian dynamics method [123]. Ji and Feng proposed a CG model for dynamics simulation of microtubules which is another important mechanical component of the cytoskeleton in living cells [89]. However, the potential functions in these models were simplified to be harmonic potential or Lennard-Jones (LJ) potential, which are hard to describe the special nonlinear constitutive relations between adjacent G-actin monomers.

In order to meet the requirements of the complex constitutive laws of soft matter, such as protein fibers, Buehler proposed a multiscale method to investigate the biomechanics of alpha-helical intermediate filament networks based on constitutive relations that are extracted from all-atom MD simulation and experiments [146]. By employing this method, Ackbarow et al. explained self-protective features of alpha-helical protein networks [83], and Cranford et al. successfully explained the superior performances of spider silk webs [147]. However, single F-actin presents a right-handed double-helical structure and the mechanical behaviours are different from those alpha-helical protein filaments.

In this paper, a hierarchical multiscale strategy is specifically designed to investigate the biomechanical behaviours of microfilament networks based on nanoscale biophysics investigations of G-actin clusters. Molecular simulations were conducted to extract the constitutive relation between adjacent G-actin clusters. A multiscale bead model for F-actin was then developed as a bridge between nanoscale biophysics and microscale biomechanics, which follows the constitutive relations from molecular simulations. This model was first validated by tensile experiment results of single F-actin from literatures and was then employed to investigate the stretching of a single layer microfilament networks at microscale.

4.3 MULTISCALE BEAD MODEL

Fig. 4-1(a) shows the Oda 2009 F-actin model [94], which was used in this research to extract the constitutive relations between adjacent G-actin clusters in molecular simulations. A new multiscale bead model for F-actin is proposed based on the interaction between neighbouring actin molecules from Martini level molecular dynamics (MD) simulations, as shown in Fig. 4-1(b). Finally, this model was applied to a two-dimensional microfilament network to explore biomechanics properties of microfilament networks, as shown in Fig. 4-1(c).

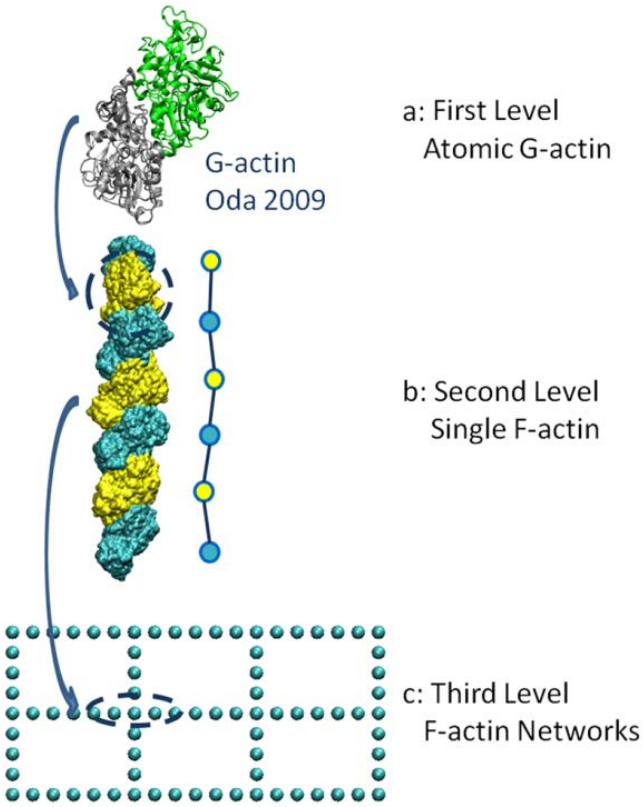

Fig. 4-1. The multiscale approach for microfilament networks. a: Crystallography of Oda 2009 G-actin model, there are two G-actin monomers in an elementary bead. b: A single F-actin constructed from Oda 2009 G-actin model following the nature from G-actin to F-actin [93]. c: Part of an idealized two-dimensional microfilament network in rectangular shape.

4.3.1 Coarse-grained (CG) serial bead model

A coarse-grained (CG) serial bead model for biomechanics analysis was proposed, in which detailed chemistry information inside G-actin monomers was neglected, and only the mechanical interactions between different monomers were focused on.

By observing the double helix atomic structure of single F-actin, as shown in Figs. 4-1(a) and 1(b), every G-actin monomer was found to be related to its neighbouring G-actin monomers on both helix chains. The F-actin is simplified to be a string of mass beads with longitude and rotation freedoms. Every two neighbouring G-actin monomers from different helix chains were simplified as one mass bead. This simplification strategy can avoid losing double helix structural features of F-actin. The molecular sliding between the neighbouring G-actin monomers is included in the general deformation between the virtual mass beads. From a common-sense observation of all-atom MD simulation, cut-off distance for non-bonded interactions between atoms is usually under 2nm [148]. However, distances between non-

neighbouring G-actin monomers are more than 5nm, which is much larger than the typical cut-off distance in MD simulations. Therefore, the long range interactions between non-neighbouring G-actin monomers are negligible during molecular simulations.

Fig. 4-2 shows the mechanisms of this CG serial bead model. The equilibrium distance between adjacent beads is 5.529nm according to crystallography of F-actin from X-ray diffraction experiments [93]. The balance angle for angular potential in the crystallography of single F-actin is not absolutely 180^{o} according to the X-ray diffraction characterization. However, in order to simplify the simulation model, 180^{o} was employed as the average balance angle on the long right-handed double helix structure.

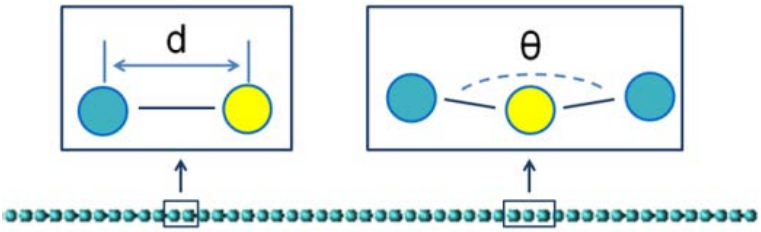

Fig. 4-2. Schematic of the CG serial bead model. Every bead in the lattice has two adjacent beads in longitudinal direction, between which tensile relation is applied. Rotational constraint is defined within three adjacent monomers on the same filament.

4.3.2 Biophysics investigation of the constitutive relations

In order to employ the CG serial bead model to represent microfilament networks, relative constitutive relations between neighbouring beads need to be extracted. MD simulation technique at Martini [109] level was employed in this paper to extract constitutive relations between adjacent beads in this model. As the detailed conformation changes inside G-actin monomers were not focused on in this study, Martini level MD simulation presents more efficiency comparing to all atom MD simulation.

Molecular simulations were performed with Gromacs [136]. Four G-actin monomers were divided into two groups in the MD simulation model, and the CG water model [109] was employed in a 6nm×6nm×20nm simulation box with periodic boundary conditions, as shown in Fig. 4-3. Firstly, 10ns relaxation was performed in an NPT ensemble (pressure 1 bar, temperature 303K), in which both pressure and temperature were controlled by the Berendsen method [137]. In the steered MD simulations, different couples of constant pulling forces with opposite directions

were then applied on the two G-actin groups for 20ns to mimic tension, compression, and rotation processes. The time steps are all 4fs to stabilize the molecular simulations. The physiological limit of single F-actin for living cells is under 300pN [64], however, the loads in our simulations were up to 1000pN to expand the scope of this theoretical model. The bead distances in different loading cases were averaged on the simulation results in the last 10ns, during which the thermal fluctuation of the mass bead is stable.

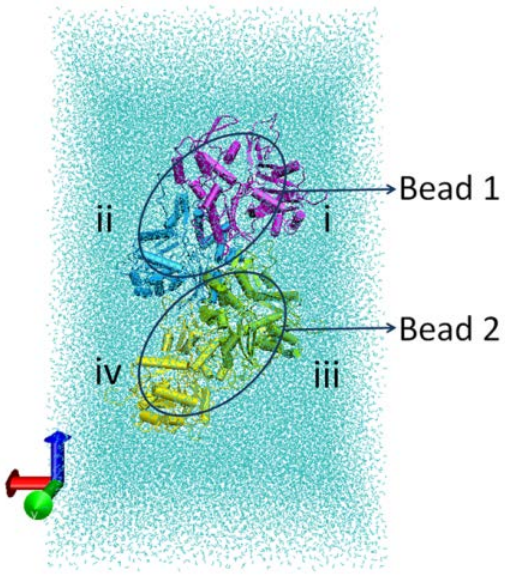

Fig. 4-3. The model box in molecular simulations. Points in cyan are water molecules. The four G-actin monomers, numbered from i to iv in different colors, are divided into two groups (i & ii and iii & iv), which are correspondingly abstracted as two beads in the multiscale bead model.

The illustration of the longitude loading process and constitutive relation results are shown in Fig. 4-4. It was found that the force-deformation curve between these two beads can be divided into five linear proportional regions. In the compression region, where the applied force F was negative, there was only one stiffening transition (point A) when the distance between neighboring beads is 5.51nm. The balance distance is 5.529nm (point B), which makes the length of one F-actin repeat 35.94nm. However, in tension region, there were both stiffening and softening transitions (point C and D). The stiffness between these two individual beads increased from the preliminary 9.59×10^{3}pN/nm to 5.52×10^{4}pN/nm when the distance between them became 5.546nm (point C). However, the stiffness will decrease to 4.16×10^{3}pN/nm when the distance increases to 5.556nm (point D). Rotation tests present a similar force-deformation trend. However, there was no

significant stiffening or softening transition in the rotation process. Rotational stiffness is characterized as 1.06×10^5pN·nm/rad, according to the simulation results.

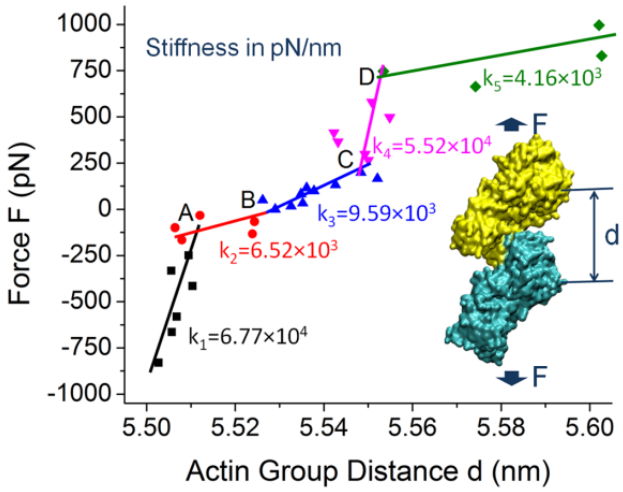

Fig. 4-4. The constitutive relation in tensile and compression numerical simulations. In compression region, there is a stiffness transition at 5.512nm. The balance distance between different beads is 5.529nm. In tension region, there are two stiffness transitions respectively at 5.546nm and 5.556nm. Transitions points are correspondingly marked as A, B, C and D.

The interactions between adjacent beads follow these constitutive relations, which are extracted from molecular simulations under different loading conditions. Detailed force field parameters with respect to relative positions of adjacent beads can be characterized from the constitutive relations, (in Supplementary Material).

As a multiscale strategy, the CG model proposed in this paper only reveals the mechanical behaviour of actin filaments. The freedoms for every CG bead are simplified to be only longitudinal and rotational. The sliding between opposite strands on F-actin occurs when the F-actin is under torsion, whose effects to the tension and bending of single actin filament is phenomenologically included in the longitudinal and rotational deformation.

4.4 VALIDATION AND APPLICATION

This multiscale model was employed initially to investigate tension and vibration behaviours of a 1.1μm single F-actin, and the results can be validated by experimental studies of tensile and bending vibration properties of single F-actin from the literature. After validation, this newly developed model will be employed to investigate the stretching of a single layer microfilament network with dimensions of 4.43μm × 9.93μm.

4.4.1 Tensile test on single F-actin

The tensile stiffness of single F-actin under physiological limits was directly tested using the micro-needle array technique [53], micro-fabricated cantilever technique [64] and optical trap technique [55]. In order to validate the multiscale model proposed in this paper, a single F-actin with a length of 1.1μm, which consists of 200 beads, was stretched with different engineering strain rates from 2^{-10}/fs to 5^{-10}/fs based on the multiscale bead model. The simulations were performed with the package of Lammps [149] with the aforementioned force field table whose crucial parameters can be found in Supplementary Material. The simulations were performed in NVT ensemble at 303K. Langevin dynamics [150] are adopted in the CG simulation to consider the friction from putative solvent.

Fig. 4-5 provides force-deformation relations during these numerical stimulations. While pulling force was under the physiological limit, the stiffness extracted from simulations for a 1.1μm F-actin was from 39.81 to 60.04pN/nm. The stiffness per unit length (1μm) of F-actin under different loading strain rates corresponded between 43.79pN/nm and 66.04pN/nm. The stiffness of a single F-actin has dependence on loading strain rate according to simulation results. A higher loading strain rate leads to a higher stiffness, which is similar to traditional materials. According to mechanics of materials, a lower loading strain rate is close to quasi-static loading cases [151]. The lower limit of the stiffness from these simulation cases was 43.79pN/nm, which is under small loading strain rate condition. This stiffness result is close to experimental explorations. The detailed comparison can be found in Table I. The simulation result is identical with experimental results in tensile tests, indicating that this multiscale model is accurate and effective for the analysis of axial stretching of single F-actin when the mechanical deformation is small.

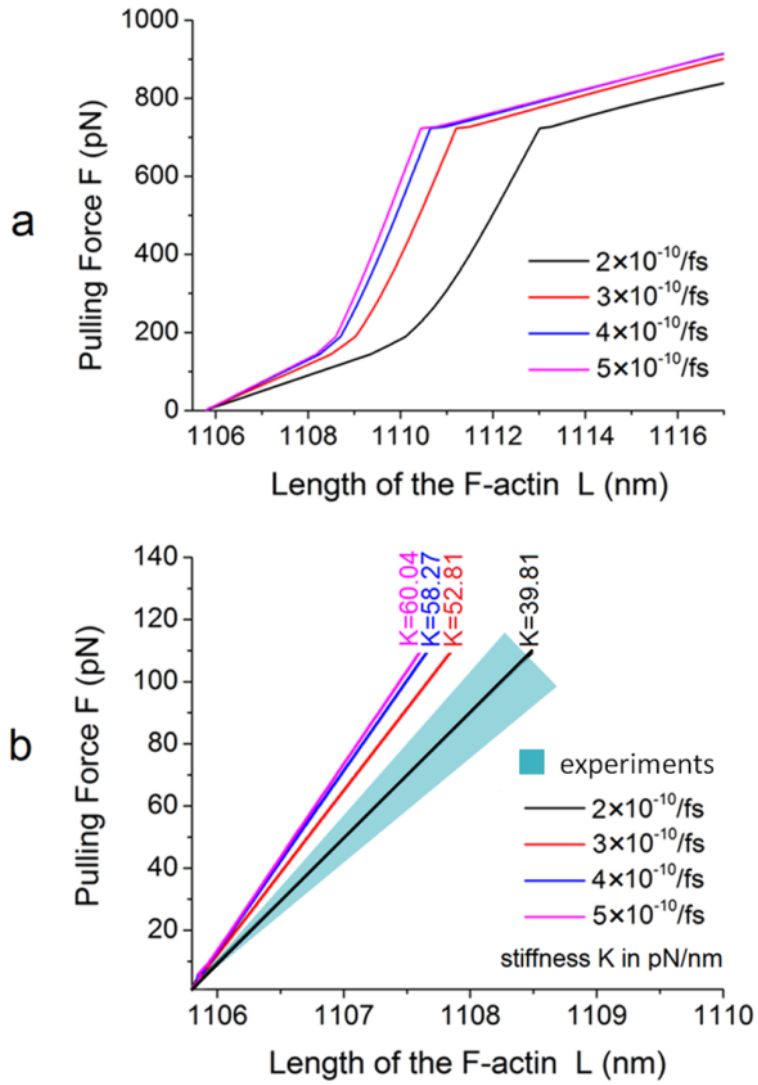

Fig. 4-5. Force-deformation relation during simulations of the tension of a 1.1μm single F-actin. a: Stiffening and softening strains all have dependence on loading strain rate. b: When loading strain is under the physiological limit (the linear region at the beginning of the tensile tests), the stiffness evaluation agrees with experimental results. The blue area represents the stiffness region of single F-actin (1.1μm) based on experimental results [53, 64].

Table 4-1 The stiffness evaluation by experiments and the multiscale model in this paper.

Method	Stiffness (pN/nm)
Mechanical measurements [57]	45~67
Micro-needle array [53]	43±4.6
Micro-fabricated cantilever [64]	34.5±3.5
Multiscale model	43.79~66.04

4.4.2 Bending vibration of single F-actin

The bending performance of F-actin directly affects the transverse thermal fluctuation of microfilament networks. However, direct bending tests of F-actin is hard to be carried out. In order to validate the capability of this multiscale model in the prediction of F-actin bending behaviours, the natural frequency of F-actin bending vibration was studied by numerical simulation in this paper. We have previously explored the bending vibration properties of F-actin by Martini MD simulation to validate the capability of beam model in continuum mechanical modelling of F-actin [152]. Based on Euler-Bernoulli beam theory, the theoretical solution of the natural frequency f of a circular cross-sectional F-actin is:

$$f = \frac{(\beta L)^4}{4\pi}\sqrt{\frac{Er^2}{\rho L^4}} \tag{4-1}$$

where βL is the natural frequency constant regarding boundary conditions, E is the tensile modulus of F-actin, r is the radius of F-actin, ρ is the density of F-actin and L denotes the length of filament. It should be noted that the force field parameters were extracted by Martini MD simulations, in which explicit water molecules were employed to avoid the unrealistic G-actin morphology changes in vacuum. These force field parameters directly reflect the constitutive law of single actin that is not significantly affected by the water environment. However, the morphology for each bead is solid sphere in the multiscale model, and we were only aiming to validate this multiscale model by vibration tests of single actin filaments in vacuum. Hence, the water environment should not be included to avoid damping effects, and the effects of water molecular on the force field parameters were neglected. If this multiscale model is used to characterize the vibration of single actin filaments in water, Langevin dynamics is necessary to implicitly consider the friction from water.

By employing typical tensile modulus (E=2.5GPa) and radius (2.8nm) of F-actin [55, 56], the analytical solution of the natural frequency of these actin filaments can be evaluated using Eq. (4-1). More detailed material constants and beam solution of actin filament transverse vibration were described in literature [152]. The granular simulation strategy for the characterization of F-actin vibration properties is similar to metal nanowire [153]. Half sinusoidal profile velocity excitation was applied on the F-actin to obtain the first order vibration mode, which can be found in Fig. 4-6.

The natural frequency constant βL for the first order vibration of double clamped beam is 4.73 [141].

Fast Fourier transform (FFT) algorithm was employed to capture the lowest natural frequency f from the discrete potential energy output. The natural frequency results explored by the multiscale model proposed in this paper were compared with the Euler-Bernoulli beam solution in Fig. 4-6. The multiscale characterization is close to the theoretical solution based on Euler-Bernoulli beam model, which proves the capability of this method in obtaining the transverse deformation of single F-actin.

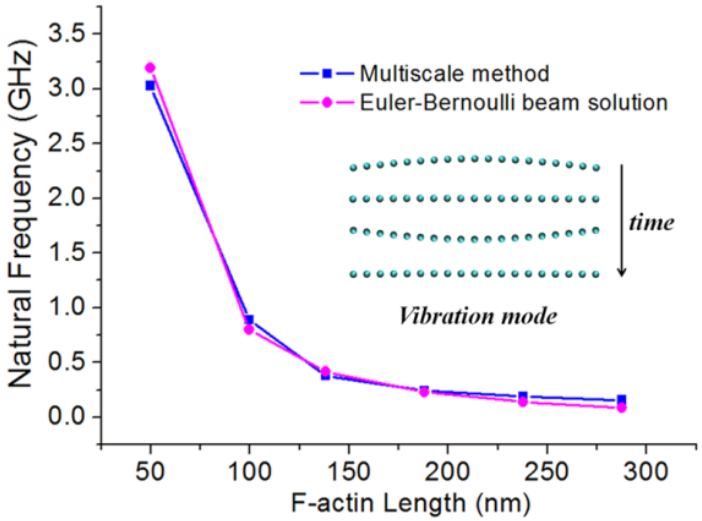

Fig. 4-6. The first order natural frequency of double clamped F-actin from 50 to 300nm, square dots represent the results from the multiscale method proposed in this paper and circular dots represent the theoretical solution of Euler-Bernoulli beam.

4.4.3 Stiffening and softening of rectangular microfilament networks

The mechanical properties of microfilament networks are difficult to describe by direct mathematical equations like macroscale continuum materials[154]. In order to predict the complex mechanical performances of microfilament networks from the crystallography of F-actin, this newly developed multiscale model was employed to study a microfilament network at microscale. For simplification, a two-dimensional rectangular network was adopted in this study. More complex three-dimensional, randomly distributed, wormlike F-actin can be built with the same force field parameters, which will be our future work. The microfilament network analysed in this paper was 4.43μm×9.93μm, which is at the scale of real eukaryote cell size. The thickness of this microfilament network was assumed to be the diameter of G-actin

monomer, which is 5.64 nm[53]. The loading strain rate was controlled at 2×10^{-10}/fs, which is small in molecular simulation to model the quasi-static loading. The tensile modulus can be derived from $E=\frac{Kl}{A}$, where $k=\frac{\partial F}{\partial l}$ is the stiffness of microfilament network, which is derived from the multiscale simulation directly. L (4.43μm) and A ($0.056\mu m^2$) respectively denotes the original length and cross section area of this two-dimensional network. There were 16,965 beads in the simulation box, and the simulation was performed on Lammps under the same simulation conditions as the stretching of single F-actin. Fig. 4-7(a) shows the geometry of this single layer microfilament network. Force-deformation relation of this microfilament network and the tensile modulus with respect to engineering strain/stress obtained from simulation are presented in Figs. 4-7(b) through 4-7(d), respectively. It is noteworthy that the crosslinkers on the network in this paper were conducted with the same mechanical properties of G-actin monomers. Further development should be made regarding the mechanical properties of these actin binding proteins, such as ARP2/3, α-actinin, Fascin, and et al [155].

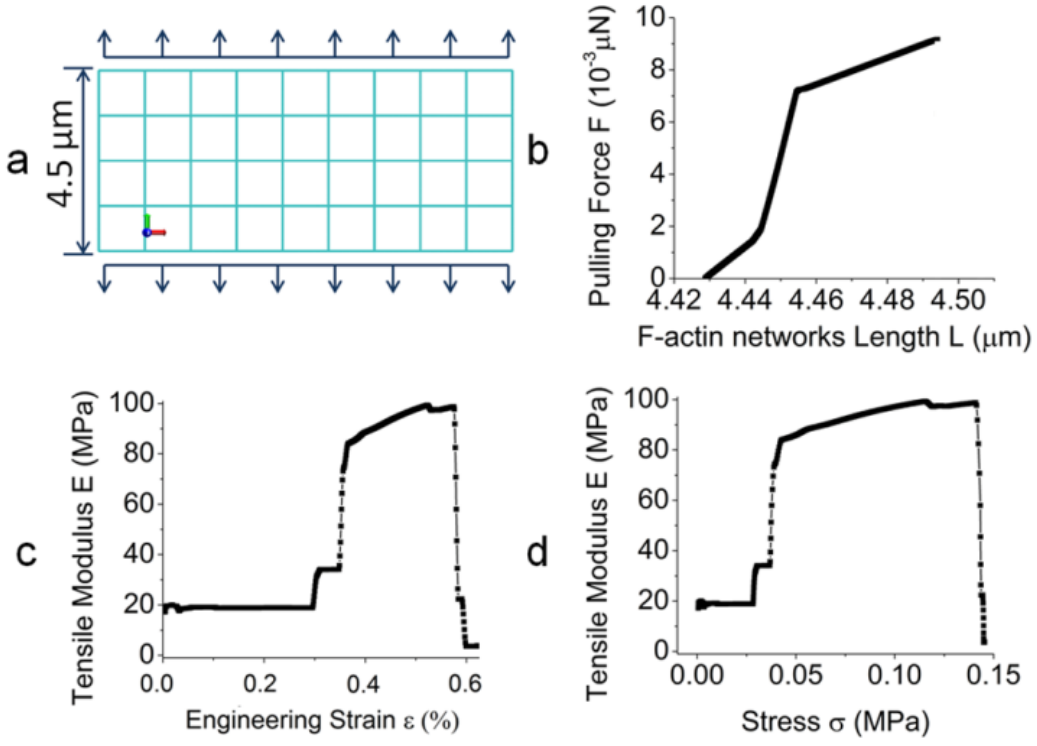

Fig. 4-7. The tensile performance of a 4.43μm×9.93μm microfilament networks. a: geometry of the networks and the loading illustration; b: force-deformation relation, which is similar to single F-actin simulation results; c: the strain stiffening and softening; d: the stress stiffening and softening.

Both stiffening and softening of microfilament networks in different loading stages were discovered recently by highly-developed experimental techniques [60, 62]. With the multiscale model proposed in this paper, stiffening and softening phenomena can be investigated and predicted theoretically, as shown in Figs. 4-7(c) and 7(d). In the stage of low loading strain, the tensile modulus of microfilament networks remains constant. The tensile modulus will increase correspondingly after the strain exceeds 0.3% or the stress exceeds 0.03MPa, which means strain stiffening takes place when the loading strain approaches a critical value. However, the increment of tensile modulus will decrease while loading strain increases. When loading strain reaches 0.6%, the stiffness drops to 5MPa. Softening of microfilament networks will happen after a stiffening stage, and the corresponding softening stress is 0.135MPa for this two-dimensional microfilament network. These theoretical evaluations of these nonlinear properties provide clues to understand the mechanical performances of microfilament networks in living cells.

To the best of our knowledge, the largest scale of all-atom molecular simulations for single F-actin is at the hundred-nanometre scale. With the multiscale bead model proposed in this paper, it is possible to conduct simulations to explore the mechanical properties of microfilament networks at the microscale, which still follows the intrinsic physics basis of G-actin molecules.

The engineering strain of single actin filaments is less than 1% in this multiscale model, which is close to experimental results[53, 65]. It should be noted that the external loading in MD simulation is extended to 1000pN in this paper, which is already higher than the physiological limit (approximately 300pN). This deformation of single actin filaments is smaller compared to microfilament networks deformation (more than 10%[62]) that is mainly caused by the reorganization of dendritic network structures. Further MD simulations and experiments should be investigated to study the large deformation and damage of single actin filaments under mechanical loadings, which can contribute to the understandings of the rupture mechanism of microfilament networks.

4.5 DISCUSSION

Biphasic models based on continuum mechanics theory were proposed to investigate the mechanical behaviours of actin gel in solution based by homogenizing

the actin cortex in living cells[111]. However, later studies proved that the mechanical behaviours of microfilament networks are complex physiological processes related to architecture and chemical components of microfilament networks. All these fascinating physiology features of microfilament networks lead to self-protective properties and functional features of microfilament networks. Due to the difficulties in abstracting all these complex features to pure mathematical presentations, we proposed this multiscale model from a molecular point of view to explain and predict the mechanical behaviours of microfilament networks in living cells. This multiscale model provides the fundamental constitutive mechanical relations between adjacent protein beads on F-actin to unravel physiological mystery from a physical basis.

Wachsstock et al. proved that dynamics of networks crosslinkers can affect the mechanical properties of microfilament networks[113], and Gardel et al. discovered that the density of crosslinkers is also quite crucial to the stiffness of microfilament networks[61]. The crosslinkers in the microfilament networks consist of many different proteins, whose mechanical performances are still unclear[155], thus they are assumed to have the same mechanical properties as G-actin monomers. Further investigations of the mechanical properties of crosslinkers should be conducted for more accurate prediction.

It should be noted that although the stretching simulations on a two-dimensional network can predict strain/stress hardening and softening phenomena of microfilament networks, there is still not a full understanding of the cryptic physiological phenomena of microfilament networks in living cells. The stiffening and softening phenomena of microfilament networks in living cells are not results of only material properties, but also complex physiological processes including dynamic F-actin binding by crosslinkers[156] and protein motors inducement, such as m

yosin II[157]. This proposed hierarchical multiscale model of actin filaments can represent the fundamental constitutive mechanical performances of microfilament networks, different crosslinker rupture mechanisms and biomechanical contribution from protein motors are needed in the future to understand more complex physiological performance of microfilament networks.

The mechanobiology of microfilament networks also has dependence on the architectures of microfilament networks and the functions of actin-binding proteins. Three dimensional randomly distributed microfilament networks model should be developed in future for better understandings of the biomechanical properties of microfilament networks. It should also be noted that special features with respect to the structural contributions of actin-binding proteins should be added to this fundamental multiscale approach to investigate the mechanobiology of microfilament networks.

4.6 CONCLUSION

Based on constitutive relations extracted from molecular simulations for a single F-actin, a hierarchical multiscale model is proposed as the bridge between nanoscale biophysics and microscale biomechanics to investigate the mechanical properties of microfilament networks at microscale.

This multiscale bead model was first validated by the results of single F-actin tensile experiments and transverse bending vibration properties. The tensile stiffness and the bending vibration properties of single F-actin evaluated by this hierarchical multiscale model agrees with experiment results and analytical models from literatures. According to multiscale simulations of the stretching of a single layer microfilament network (4.43μm×9.93μm), the microfilament networks present both strain stiffening and softening in different stretching stages. This means the stiffening and softening of actin structure are not only results of the dynamic binding of actin filament and the inducement of protein motors, but also a constitutive material behaviour of single actin filaments. This multiscale approach provides a numerical tool which can contribute to the investigation of the biomechanics of microfilament networks from a molecular point of view. Further models about actin crosslinker properties and thermal fluctuation of wormlike F-actin can be developed to predict the dynamic responses of dendritic microfilament networks under extracellular imposed forces.

4.7 ACKNOWLEDGEMENTS

Support from the Australian Research Council Future Fellowship grant (FT100100172) and National Nature Science Foundation of China (Grant Nr. 31270989) is gratefully acknowledged.

4.8 SUPPLEMENTARY MATERIAL

4.8.1 Part I: Biophysics investigation of the rotational stiffness

As described in the paper, following exactly the same molecular dynamics (MD) simulation conditions, pulling forces with opposite directions are applied in the rotational direction, as is shown in Fig. 4-8. There is a force of *2F* applied on the middle bead, and separately two single forces of *F* are applied on the beads at the ends. As the loading condition is symmetric, semi structural analysis is selected to save the computational cost. To simplify the model, the balance angle is abstracted as 180^o to present the overall averaging balance angle even though the balance angles are not absolute 180^o case by case due to the double helical structure.

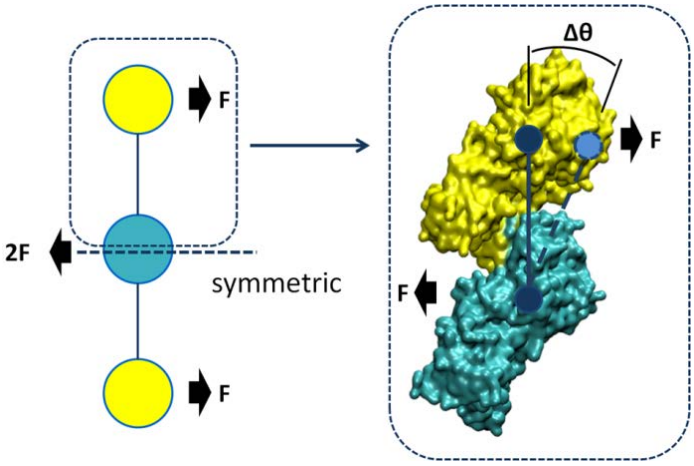

Fig. 4-8. The schematic of rotational tests for the characterization of the rotational stiffness.

The force-rotation relation is provided in Fig. 4-9. By fitting the results from the rotational simulations, a linear rotational force-deformation relation can be extracted. The rotational stiffness can be therefore evaluated. By using balance distance *d* in the tensile test, which is 5.529 nm, the moment caused by the rotational loading conditions can be expressed as:

$$M = F \times d \times \cos^2 \theta \qquad (4\text{-})$$

where F is the applied force, d (5.529 nm)is the balance distance between the different groups, and θ is the rotation.

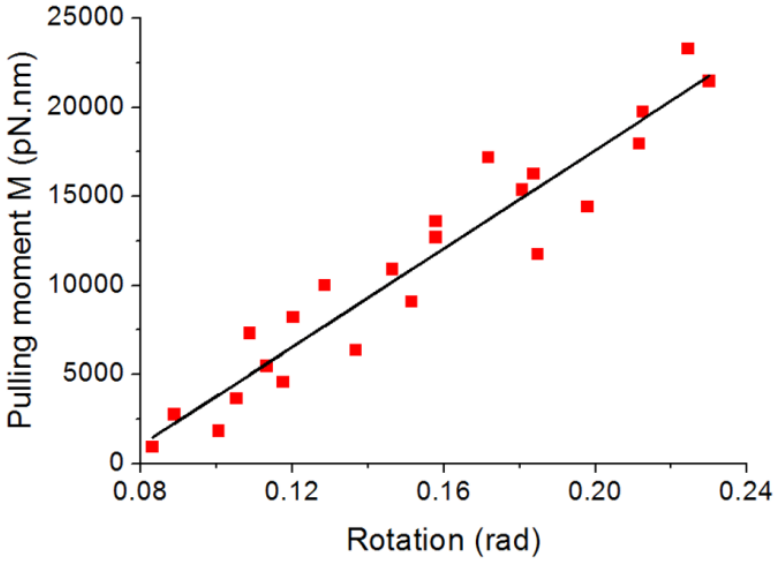

Fig. 4-9. The evaluation of the rotational stiffness with respect to the rotation. The rotational stiffness is characterized to be 1.06×10^5 pN·nm/rad.

4.8.2 Part II: Characterization of the force field table

As described in the paper, there are two freedoms which are considered in the force field selected for actin filament networks simulation: bond potential function and angular potential. In LAMMPS [149], the linear search potential table is employed to present the complex nonlinear bond force between different particles. However, for the rotational stiffness, the potential function is reasonable to be simplified as harmonic potential which is already illustrated in Fig. 4-9.

The bond potential between these two adjacent beads is divided into five regions, which is hard to be simplified as harmonic potential functions. The function of Table Potential with linear search method in LAMMPS [149] package is employed to present the complex nonlinear mechanical constitutive relations between different beads. The force and potential with respect to the bead distance are shown in Figs 4-10 and 4-11. There are different stiffening and softening transitions on these curves. The critical constants are shown in table 1.

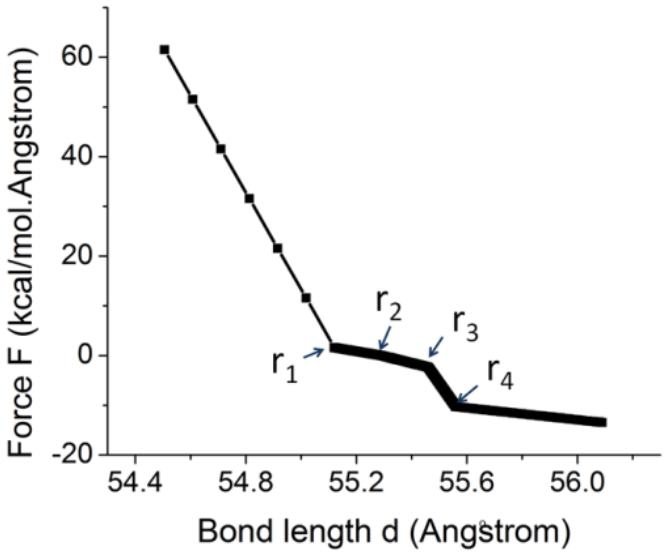

Fig. 4-10. The interaction force between the beads with respect to the bond length. There are several different transitions including both stiffening and softening transitions on this curve.

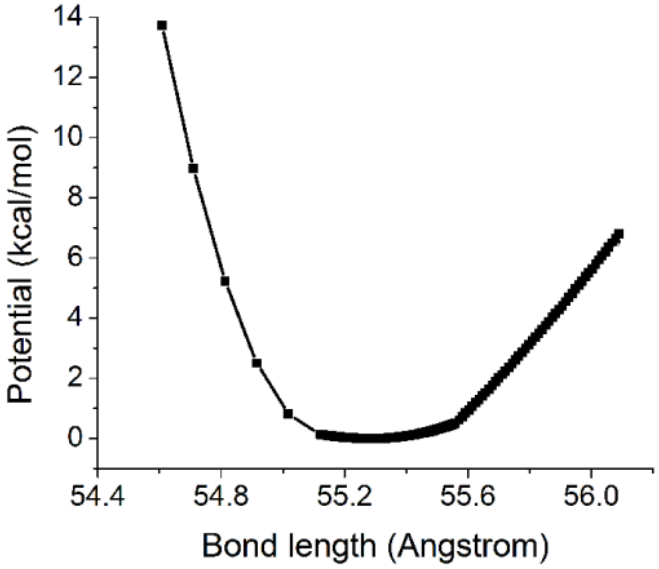

Fig. 4-11. The potential between the beads with respect to bond length between different beads. At the balance point, where the bond distance is 5.529 nm, the potential will become zero as the static equilibrated state.

Table 4-2 Critical force field constants for the multiscale bead model

Distance (Angstrom)	Stiffness (kcal/mol·Angstrom2)
r1=54.00	97.53
r2=55.12	9.39
r3=55.29	13.81
r4=55.56	79.50

It should be noted that the points of the simulation results to characterize the nonlinear force field are scattering due to the chaos from the thermal dynamics calculation in MD simulation. The fitted curve excluded these chaoses from the thermal dynamics loading (temperature). As this multiscale bead model is designed preliminary for mechanical behaviours prediction, the thermal dynamics properties with respect to this temperature, which is 300K in these simulations, are contained in the force field abstracted from the MD simulations. If the working temperature is changed, the force field constants should be changed correspondingly.

For the angular potential, because there are no significant nonlinear mechanical behaviours in the results from the simulations, the potential function is defined in the harmonic style. The balance angle is 180^o by averaging all the angles between beads on the same filament. The force field constant k_{ang} can be then evaluated from the rotational stiffness which is already introduced in the previous part:

$$\int M d\theta = k_{ang}(\theta - \theta_0)^2 \tag{4-3}$$

where M is the rotational moment, θ_0 is the balance angle which is assumed to be 180^o, and the k_{ang} can be characterized to be 7.63×10^3 kcal/mol·rad^2 according to the simulation results.

Chapter 5: New Thermostat for the CG Modelling of F-actin CSK (Paper 3)

Research paper three:

Li, T. and Gu, Y.T., 2014. A stochastic thermostat algorithm for coarse-grained thermomechanical modelling of large-scale soft matters: Theory and application to microfilaments. ***Journal of Computational Physics*** 263, 177-184.

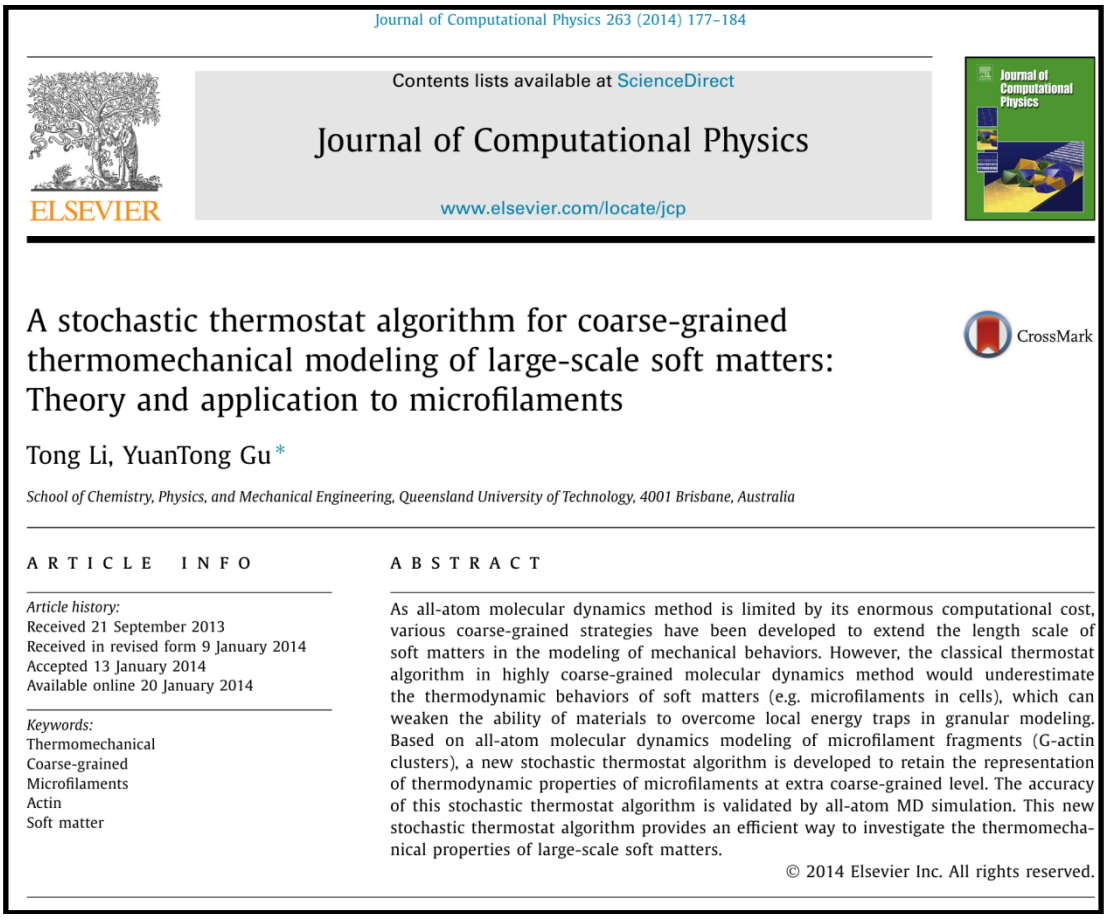

Journal of Computational Physics 263 (2014) 177–184

Contents lists available at ScienceDirect

Journal of Computational Physics

www.elsevier.com/locate/jcp

A stochastic thermostat algorithm for coarse-grained thermomechanical modeling of large-scale soft matters: Theory and application to microfilaments

Tong Li, YuanTong Gu *

School of Chemistry, Physics, and Mechanical Engineering, Queensland University of Technology, 4001 Brisbane, Australia

ARTICLE INFO

Article history:
Received 21 September 2013
Received in revised form 9 January 2014
Accepted 13 January 2014
Available online 20 January 2014

Keywords:
Thermomechanical
Coarse-grained
Microfilaments
Actin
Soft matter

ABSTRACT

As all-atom molecular dynamics method is limited by its enormous computational cost, various coarse-grained strategies have been developed to extend the length scale of soft matters in the modeling of mechanical behaviors. However, the classical thermostat algorithm in highly coarse-grained molecular dynamics method would underestimate the thermodynamic behaviors of soft matters (e.g. microfilaments in cells), which can weaken the ability of materials to overcome local energy traps in granular modeling. Based on all-atom molecular dynamics modeling of microfilament fragments (G-actin clusters), a new stochastic thermostat algorithm is developed to retain the representation of thermodynamic properties of microfilaments at extra coarse-grained level. The accuracy of this stochastic thermostat algorithm is validated by all-atom MD simulation. This new stochastic thermostat algorithm provides an efficient way to investigate the thermomechanical properties of large-scale soft matters.

Statement of Contribution of Co-Authors for Thesis by Published Paper

The following is the format for the required declaration provided at the start of any thesis chapter which includes a co-authored publication.

The authors listed below have certified* that:

1. they meet the criteria for authorship in that they have participated in the conception, execution, or interpretation, of at least that part of the publication in their field of expertise;
2. they take public responsibility for their part of the publication, except for the responsible author who accepts overall responsibility for the publication;
3. there are no other authors of the publication according to these criteria;
4. potential conflicts of interest have been disclosed to (a) granting bodies, (b) the editor or publisher of journals or other publications, and (c) the head of the responsible academic unit, and
5. they agree to the use of the publication in the student's thesis and its publication on the QUT ePrints database consistent with any limitations set by publisher requirements.

In the case of this chapter:

Li, T., Gu, Y., 2014. A stochastic thermostat algorithm for coarse-grained thermomechanical modelling of large-scale soft matters: Theory and application to microfilaments. Journal of Computational Physics 263, 177-184.

Contributor	Statement of contribution*
Tong Li	Designed and conducted numerical model. Conducted data analysis. Wrote the manuscript.
Signature 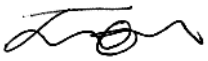	
Date 24/11/2014	
YuanTong Gu*	Designed and conducted numerical model. Involved in the conception and design of the project. Assisted data analysis. Provided feedback on manuscript.

Principal Supervisor Confirmation

I have sighted email or other correspondence from all Co-authors confirming their certifying authorship.

YuanTong Gu	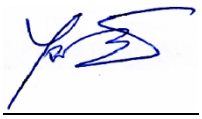	24/11/2014
Name	Signature	Date

ABSTRACT AND KEYWORDS

As all-atom molecular dynamics method is limited by its enormous computational cost, various coarse-grained strategies have been developed to extend the length scale of soft matters in the modelling of mechanical behaviours. However, the classical thermostat algorithm in highly coarse-grained molecular dynamics method would underestimate the thermodynamic behaviours of soft matters (e.g. microfilaments in cells), which can weaken the ability of materials to overcome local energy traps in granular modelling. Based on all-atom molecular dynamics modelling of microfilament fragments (G-actin clusters), a new stochastic thermostat algorithm is developed to retain the representation of thermodynamic properties of microfilaments at extra coarse-grained level. The accuracy of this stochastic thermostat algorithm is validated by all-atom MD simulation. This new stochastic thermostat algorithm provides an efficient way to investigate the thermomechanical properties of large-scale soft matters.

Keywords: Thermomechanical, Coarse-grained, Microfilaments, Actin, Soft matter

5.1 INTRODUCTION

Instead of relatively rigid materials that can be characterized in classic mechanics, soft matters consists of flexible material components whose mechanical performances can be significantly affected by its thermodynamic behaviours [158]. Molecular modelling approach provides a suitable way for the modelling of soft matters based on the truth that the internal entropic motion is benefiting the macroscale mechanical behaviours [159]. However, the length scale of soft matters in all-atom (AA) modelling is only hundreds of nanometres [160], which is limited to explore the overall performance of soft matters that consist of enormous randomly crosslinked chains/fibres at microscale. In order to enlarge the length scale of soft matters modelling, different coarse-grained (CG) strategies have been developed to describe the mechanical deformation of both organic and inorganic materials in terms of chemistry and physics [89, 161, 162].

Depending on the research objectives, there are two main strategies to develop corresponding CG modelling parameters: thermodynamic matching [121] and mechanical properties matching [12]. In order to guarantee the reliability of mechanical modelling of soft matters, we herein discuss the later strategy specifically. As a typical organic soft matter, microfilament is specifically investigated in this paper as a typical application. Microfilament network plays critical roles in eukaryotic cellular processes such as cell cytokinesis, spreading and migration [130], determining the fate of living cells [8, 14, 163]. *in-vivo* biomechanics experiments on single microfilaments are difficult to be carried out at molecular level due to the limits of experimental techniques and ethical constraints. Molecular dynamics (MD) simulation has been developed to reveal the conformational changes in actin monomers, which provides insights into the molecular mechanisms of the metabolism in association to microfilaments dynamics [104]. A large scale coarse-grained (CG) strategy for microfilaments modelling has been proposed to study the mechanical properties of microfilament networks at microscale [12]. Each simulation bead in this CG model is made up of two neighbouring G-actin monomers and the mechanical deformation of microfilament networks are evaluated based on the interaction between simulation beads. In this CG modelling strategy, there is no need to adjust the force constant with respect to the effective bond lengths, and the mechanical behaviours of microfilament are to uncomplicated be unified with AA-

MD characterization by defining proper force constants between simulation beads [12]. However, each bead in this CG strategy consists of more than 700 amino acids, which is far more than the typical 'one-bead' CG strategy whose simulation bead only represents one amino acids [74]. The thermal dynamic information of each physical atom in AA modelling is described by energy equipartition theorem [137], in which the mean kinetic energy of each harmonic solid can be directly derived as,

$$E_k = \frac{3}{2} k_B T \tag{5-1}$$

where k_B is the Boltzmann constant and T is the absolute temperature of thermal bath, E_k is the kinetic energy of the high frequency harmonic motion of simulation beads. These random motions of single atoms due to entropic energy can lead to both the structural disorder and the random movement of G-actin monomers, which are potentially obscured on the simulation beads in CG modelling strategy. Hence, it is arguable whether CG model can fully reveal the thermal dynamic motions of microfilaments by directly implementing the classical thermostat algorithm, i.e., Eq. (5-1). The thermodynamic motions of microfilaments, e.g. thermal fluctuations, can lead to wormlike configurations of microfilaments, which is significant to the biological activities and mechanical deformation of microfilaments [164]. An efficient thermostat algorithm in CG modelling of microfilaments is crucial to assist the theoretical exploration of the biophysical properties of cell structures (e.g. filopodia and lamellipodia) at microscale, where AA-MD characterization is difficult to be applied due to its computational cost.

In this paper, by analysing the thermodynamic behaviours of microfilaments, we investigate the ability of classical thermostat algorithm for the characterization of internal dynamic motions of microfilaments in association to the mechanical deformation modelling. A new stochastic thermostat algorithm is therefore proposed and implemented in a large-scale CG modelling strategy to estimate the thermomechanical properties of microfilaments with respects to its hierarchical structures.

5.2 THERMODYNAMIC CHARACTERIZATION OF MICROFILAMENT FRAGMENT

In order to investigate the difference of thermodynamic predictions between AA and CG molecular dynamics (MD) simulation of microfilament, a small fragment of microfilament that consists of only four G-actin monomers are at first studied. The F-actin crystallography 2ZWH [93] is adopted in the AA-MD characterization. The AA simulations are performed in Gromacs [165] with the force field of all-atom optimized potentials for liquid simulations (OPLS-AA) [166] in isothermal–isobaric (NPT) ensemble at the temperature of 303K (Berendsen method [137]) and the pressure of one bar (Parrinello-Rahman method [167]). Simple point-charge (SPC) water model [168] is used to explicitly consider the effects from solvent environment. The time step of AA-MD simulation is 2 femtoseconds and the simulation duration is 100 picoseconds. The longitudinal stiffness of a single microfilament is 43pN/nm [53] and the angular stiffness is 5.3×10^4pN·nm/rad^2 [12]. The equilibrium distance between simulation beads is 5.6nm and the equilibrium angle between adjacent bonds is 180^o. The CG-MD simulations are performed in Lampps [149] by utilizing the aforementioned harmonic potential energy equation. The temperature in CG-MD simulation is controlled at 303K by Langevin dynamics [150]. In the Langevin dynamics algorithm, two terms are added to the force calculation on each particle: viscous damping term due to solvent and a randomly bumping term due to temperature. The combination of these two terms is $F_d = -mv/C_d + \sqrt{mk_BT/dtC_d}$. Where, m is the mass of particle, v is the velocity of particle, dt is the time step. C_d is the damping factor with a time unit, which determines how rapidly the temperature is relaxed in the simulation. This C_d is the only flexible parameter that needs to be set up in the simulation. This parameter has dependency on the natures of both solvent and material particle. Based on the viscosity of water at 303K and the mass/diameter of G-actin clusters, C_d is estimated to be 1fs. The time step and modelling time in CG-MD simulation are all the same with AA-MD simulation. All the molecular visualization work are finished by using visual molecular dynamics (VMD) [169].

Fig. 5-1 provides the illustration of the aforementioned simulation models of microfilament fragment (both AA and CG level) and compared the longitudinal thermal fluctuation results from AA and CG level MD simulations. The

configuration of microfilaments is rapidly equilibrated by using the CG modelling strategy for microfilaments. The molecular simulation model is simplified from 163 thousands atoms (AA-MD simulation) to only two mass beads (CG-MD simulation, which saves enormous computational resources). However, the variation of filament length with regards to modelling time in CG-MD simulation is not significant compared to AA-MD simulation, which indicates that the thermodynamic motion of microfilament fragment is mostly missed in CG-MD simulation. This oversimplified CG-MD modelling technique with classical thermostat algorithm is sufficient to obtain stable conformation of microfilament fragment under mechanical boundary constrains [12], but inadequate in predicting the longitudinal thermal fluctuations. These results validated our concerns in the thermomechanical characterization of microfilaments by utilizing a highly CG modelling strategy.

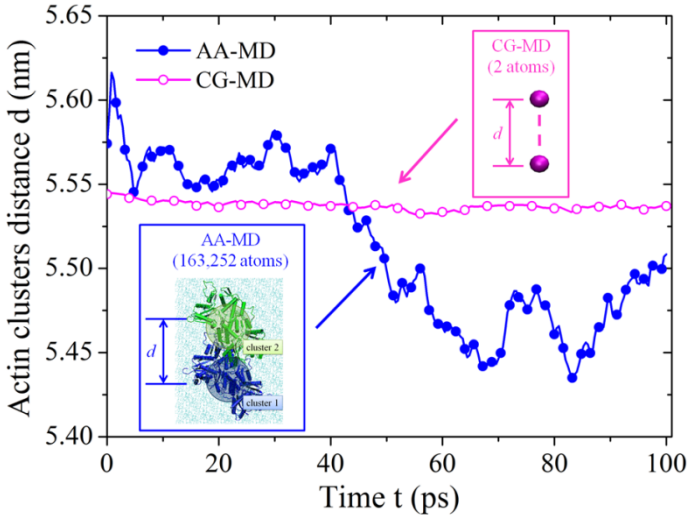

Fig. 5-1. The clusters distance in AA-MD (blue solid circle) and CG-MD (red hollow circle) simulations. The AA-MD simulation is finished by using 12 CPUs on HP Z600 workstation (Intel X5620, 2.67CHz) and the CG-MD simulation is finished by using single processor (Intel E8600, 3.3GHz). The calculation time for AA-MD simulation is 2 hours and four minutes, while the CG-MD simulation takes less than one second.

The force applied on each atom in the molecular system includes the interatomic action force, the damping effects from solvent and the random bumping due to temperature. Compared to the AA model of a molecular system, the interatomic forces and damping effects are similar to that in AA model based on the nature of these two terms. However, the temperature bumping effects present a different characteristic. All the atoms in one CG particle have their unique velocity vectors that are randomly distributed. Molecular resonance (violent oscillation of CG particles) will take place when the random velocity vectors of atoms present similar

patterns in the same CG particle. The molecular resonance can increase the intensity of thermal fluctuation of particles in the modelling of soft matters. This characteristic =results in the difference of fluctuation prediction in AA and CG models, but cannot be described directly by the classical theorem of energy equipartition (i.e. Eq. (5-1)). Specific thermostat algorithm for this CG modelling strategy is needed to accurately predict the thermodynamic behaviours of microfilaments related cell structures at microscale.

5.3 NEW STOCHASTIC THERMOSTAT ALGORITHM

The kinetic energy of G-actin clusters mass centre, which directly reflect the thermodynamic of G-actin clusters, is quantified by both CG-MD and AA-MD simulations to understand the law of G-actin clusters dynamics in MD simulations. Based on these molecular investigations, a new stochastic thermostat algorithm for large-scale CG-MD modelling of microfilament is proposed to improve the quality of thermomechanical characterizations.

5.3.1 G-actin clusters kinetic energy

The theatrical fundaments of actin clusters kinetic energy evaluation in both CG-MD and AA-MD simulations will be detailed in this section. In CG-MD simulation, the mean kinetic energy of each single G-actin cluster is defined as in Eq. (5-1). A dimensionless factor, k_t, can be calculated as a kinetic energy ratio to estimate the accuracy of thermostat algorithm, i.e.

$$k_t = \frac{2E_k}{3k_B T} \tag{5-2}$$

For direct CG-MD technique, this variable k_t is a constant of one, which is not changing during the whole simulation process. In AA-MD simulations, the Newtonian kinetic energy of G-actin cluster mass centre can be extracted from the co-momentum of all atoms that belong to this G-actin cluster:

$$\begin{cases} M\vec{V} = \sum_{i=1}^{n} m_i \vec{v}_i \\ E_k = \frac{1}{2} M(\vec{V} \cdot \vec{V}) \end{cases} \tag{5-3}$$

where M is the overall mass of a G-actin cluster (84 kDa) and $\vec{V}$ is the overall velocity vector of cluster mass centre. m_i and $\vec{v}_i$ respectively denotes the mass and velocity vector of atom i in the n atoms G-actin cluster.

Two simulation models, which respectively include one and four G-actin clusters, are adopted to track the thermodynamic motions of G-actin clusters in solvent. Fig. 5-2 provides the illustration of these two simulation models. The molecular simulations are of the same temperature and pressure parameters with aforementioned AA-MD simulations in last section.

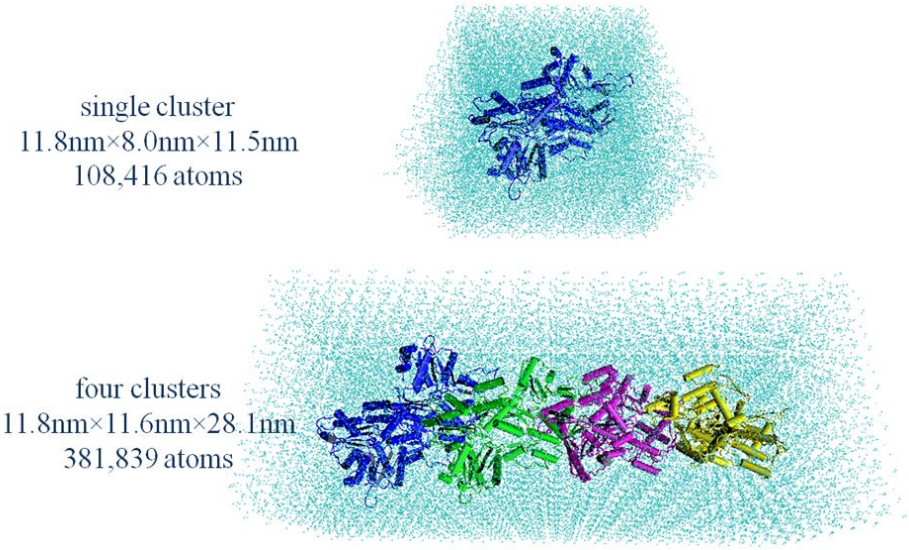

Fig. 5-2. The different simulation models of AA-MD microfilament thermal fluctuation simulations which respectively include one and four G-actin clusters. The cyan dots represent water molecules in the simulation.

5.3.2 Statistical property of k_t in AA-MD

The factor k_t is derived from AA-MD characterization results with respects to the modelling time. Fig. 5-3 provides the comparison of direct CG-MD technique and AA-MD simulation. It can be found that, the evaluations of G-actin clusters kinetic energy from AA-MD characterizations are more scattered than the constant value from direct CG-MD technique, indicating the insufficiency of direct CG-MD simulations in predicting the thermodynamic behaviours of microfilament. In order to understand the statistic rule to which the kinetic energy of G-actin cluster belongs, the k_t results of a single G-actin cluster in solvent at 303K are extracted by utilizing AA-MD simulation. The statistical results are shown in Fig. 5-3(b). Gamma distribution is used to fit the distribution rule of scattered k_t values, and corresponding parameters of the distribution are also provided in Fig. 5-3(b).

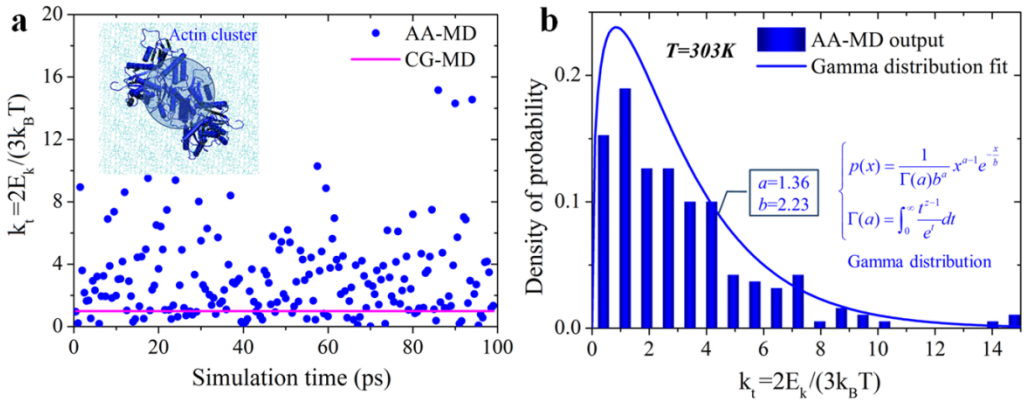

Fig. 5-3. The evaluation of k_t for a single G-actin cluster in water at 303K regarding modelling time. a: The scattered results of k_t with respect to simulation time; b: The Gamma distribution fitting of k_t results.

AA-MD simulations under different temperature from 50K to 303K are conducted to investigate the temperature dependency of k_t distribution. The Gamma distribution fitting results are given in Fig. 5-4. These distribution parameters, including shape parameter *a*, scale parameter *b* and expectation *E* of the distribution, are approximately constant in the temperature domain, which indicates the temperature dependency of the distribution parameters is not significant. In order to simplify the model, the average values of these three parameters are adopted in temperature domain to represent the overall distribution of k_t at different temperatures ranging from 50K to 303K.

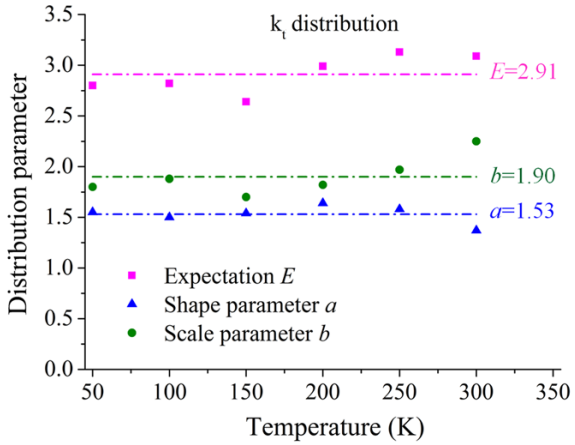

Fig. 5-4. The distribution parameters of k_t fitting at temperatures from 50K to 303K.

A larger model with 380 thousand atoms, which includes four G-actin clusters, is simulated to validate the reliability of the k_t distribution rule in multi-clusters system. Fig. 5-5 shows the Gamma distribution fitting of k_t for different G-actin clusters in the same simulation system. It can be found that different G-actin clusters

follow similar distribution rules, and the Gamma distribution fitting can be a good candidate to describe the distribution of scattered k_t in this multi-clusters simulation system.

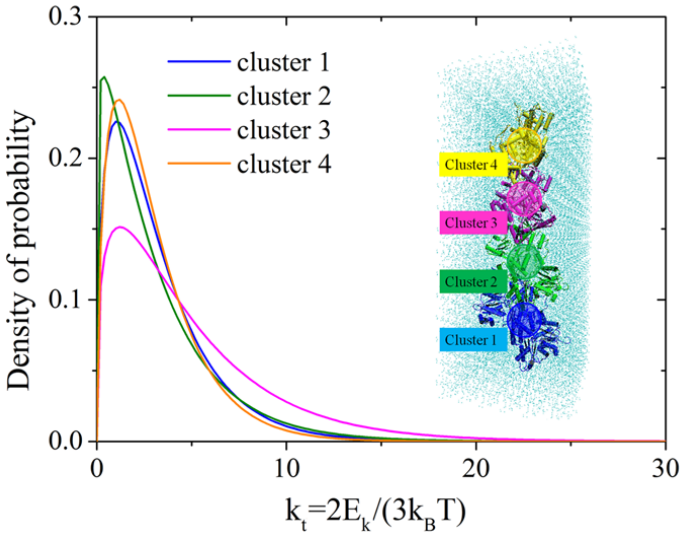

Fig. 5-5. The Gamma distribution fitting for the scattered variable k_t of different G-actin clusters from AA-MD simulation of microfilament fragment with four G-actin clusters.

5.3.3 Stochastic thermostat algorithm

Based on discussions about the distribution rule to which the factor k_t belongs, a new stochastic thermostat algorithm is proposed to predict the thermodynamic motions of G-actin clusters in the CG model of microfilaments. The modified thermostat algorithm is defined as:

$$\begin{cases} E_k = k_t \dfrac{3}{2} k_B T \\ k_t \sim \Gamma(a = 1.53, b = 1.9) \end{cases} \tag{5.4}$$

k_t is a variable that is changing over the modelling time (Fig. 5-3). The variation of this time dependent parameter (k_t) belongs to the aforementioned Gamma distribution, as given in Eq. (5-4). The distribution parameters, i.e. a and b, are obtained by averaging the fitting parameters of distributions in temperature domain (Fig. 5-4). In the current CG-MD simulations, the k_t is changed every one picosecond. It should be noted that, the distribution parameter a and b have dependency on the material and CG strategy, the values of a and b in Eq. (5-4) can only reveal the biophysical characteristics of microfilaments that adopts the aforementioned CG strategy. If the material or CG strategy is changed, proper

modification of these distribution parameters is needed to retain the applicability of this stochastic thermostat algorithm for different soft matters.

5.3.4 Benchmarks and Validation

In order to validate the accuracy and efficiency of this new stochastic thermostat algorithm, the aforementioned question about the longitudinal thermal fluctuations of both short (11nm, 4 G-actin monomers) and long (72nm, 26 G-actin monomers) microfilament fragment is studied by implementing this new thermostat algorithm in the large-scale CG model [12].

According to Section 5.4.2, the variation of distance between G-actin clusters (each cluster denotes two G-actin monomers) is difficult to be accurately extracted from direct CG-MD simulation. In order to validate this newly proposed algorithm, the longitudinal fluctuation of a same microfilament fragment is investigated by the modified CG-MD technique and compared with AA-MD modelling results. As this new thermostat algorithm contains a random factors k_t, three different modified CG-MD simulation cases are conducted to illustrate the reliability of this new algorithm. These modified CG-MD simulation cases are of different k_t indexes that are randomly generated. Comparing with CG-MD technique with unmodified thermostat algorithm (pink open circle), the modelling results of microfilament thermal fluctuation in this modified thermostat algorithm simulation presents larger variability, which is more close to AA-MD characterization (blue open square). The variation of amplitude with respects to modelling time would directly lead to random movements of microfilament fragments due to the thermal inputs to biological materials. However, the dynamic information would be lost in the direct CG-MD characterization, leading to the insufficiency of direct CG-MD strategy in modelling the thermomechanical properties of microfilament like, hierarchical soft materials.

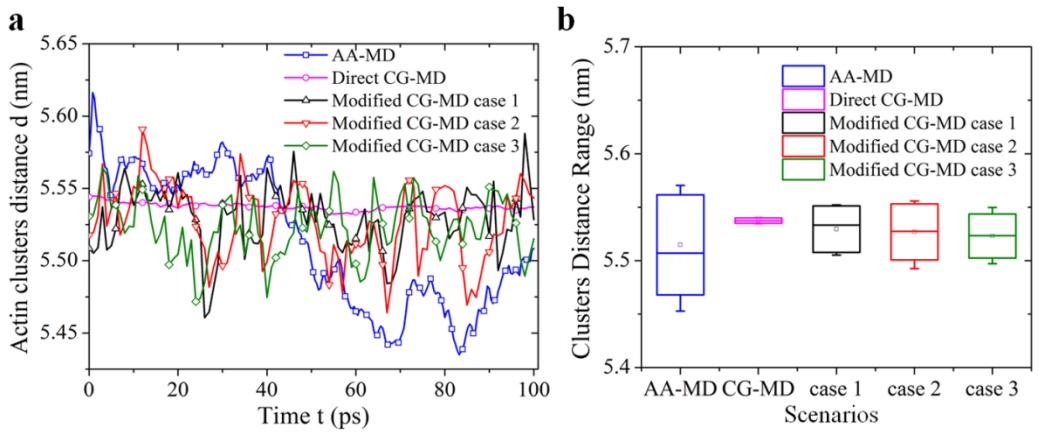

Fig. 5-6. Microfilament CG-MD modelling results by adopting the newly developed stochastic thermostat algorithm. a: the variation of G-actin clusters distance evaluated from different simulation strategies; b: the clusters distance ranges in a double clusters simulation system obtained from different simulation techniques.

As introduced, the three modified CG-MD cases (black up triangle, red down triangle and olive diamond) are of different k_t indexes, however, all lead to similar profiles of fluctuation ranges, indicating that the stochastic thermostat is reliable, even brought in randomly generated indexes of factor k_t. The computational duration of this simulation with modified CG-MD technique is less than one second on single processer for this small microfilament fragment. Comparing with the computational recourses needed by AA-MD method, this modified CG modelling strategy can used limited resources to obtain relatively reliable thermomechanical evaluation of a small microfilament fragment that consists of four G-actin monomers.

Another benchmark study is conducted to validate the accuracy and efficiency of this modified algorithm for longer microfilaments. Two F-actin helical repeats that includes 26 G-actin monomers are chosen for these scenarios. The total length of the filament is 72nm, and we chose the distance between the two G-actin clusters on microfilament ends as the reference variable. The absolute value of this distance is around 5.5nm less than the length of microfilament because of the size of the cluster (Fig. 5-7). The simulation conditions are all the same with abovementioed AA-MD simulation, except that the modelling time is extended to 1ns. The full atom simulation model consists of more than one million (1, 171, 472) atoms. The duration of AA-MD calculation is 49.5 hours with 12 CPUs on HP Z600 workstation (Intel X5620, 2.67CHz). Three sets of k_t indexes are adopted to study the numerical reliability of this newly developed algorithm (Fig. 5-7, black, red and olive). This

results from CG-MD modelling scenarios with modified thermostat algorithm shows larger variation of thermal fluctuation, which is more consistent with AA-MD characterization results (blue solid square) compared with direct CG-MD modelling (magenta solid circle).

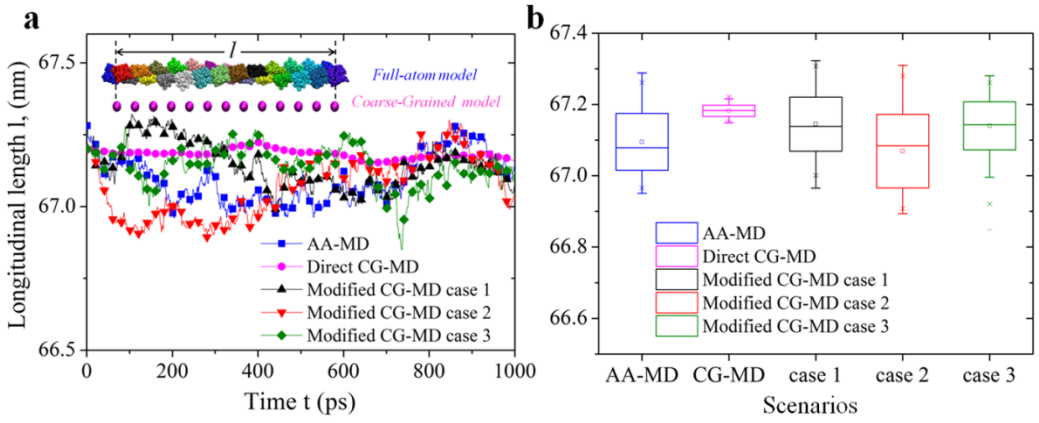

Fig. 5-7. The longitudinal thermal fluctuation of 72nm long microfilament from both AA-MD simulation and CG-MD simulation. a: the variation of longitudinal length from different simulation strategies; b: the thermal fluctuation ranges of a 72nm long microfilament obtained from different simulation techniques.

The computational time for the CG-MD simulation is only 10 seconds with one CPU (Intel E8600, 3.3GHz), which is far less than the 49 hours computational time of AA-MD simulation. The efficiency of this modified CG-MD method indicated that, this simulation strategy can be applied to large-scale, complex microfilament networks to investigate its dynamic behaviours due to thermal energy inputs. This CG model of microfilaments can be extended to three dimensional networks at microscale that is the actual size of cell structure, which is difficult for AA-MD method to handle with nowadays computational capability.

5.4 DISCUSSION

MD simulation of soft matters has advantages in investigating their dynamic characteristics by considering the random motions of independent atoms due to thermal excitation. However, AA-MD simulation is inadequate to be applied to large-scale soft matters for studying thermodynamic behaviours due to the limit of computational capability. Continuum mechanics modelling has advantages in characterizing mechanical deformation of micro/macro scale materials, but is inadequate in capturing the associated internal entropic motions. As a bridging method, CG level granular simulation is necessary for the biophysical modelling of

soft matters based on its natures in both static and dynamic characterizations. By simplifying the definition of simulation beads, CG models can improve the computational efficiency of MD simulation. Take the CG model of microfilaments for example: this CG model ignores conformational changes in each G-actin monomer while only focusing on the global motion of a G-actin cluster that consists of two monomers, approximately seven thousand atoms. Even though the computational efficiency of biophysical simulation can be improved, direct CG model is limited in the characterization of internal thermodynamic motions, because the dynamic behaviours of simulation beads in MD simulation have both enthalpic and entropic effects.

While upgrading the length scale of simulation models by decomposing stress fibres to be strings of CG beads, the information of high frequency motion of atoms inside each simulation bead will be obscured in CG methods. These stochastic motions of single atoms can lead to spontaneous behaviours of macromolecules, which is a long term response of biological materials. However, these time dependent properties of gel like soft matters are still challenges for different modelling methods, such as MD method and soft glass rheology (SGR) [170]. The challenge mainly lies in the following two points. First, the temporal scale of the methods is not large enough to describe the slow and time dependent properties of materials. Compared to picosecond scale of AA-MD method, the temporal scale of this CG method can be extended to a few microseconds. However, there is still a long way to go for solving the long term response of soft matters which can take a few hours to finish. Second, another challenge for the modelling of soft matters lies in the local energy traps, whose depth are much larger than the thermal energy k_BT [171]. With understandings of the characteristics of macromolecular thermodynamics in this paper, the thermal fluctuations of the molecular clusters in soft matters are usually underestimated by adopting classical thermostat algorithm. This underestimation can weaken the ability of flexible materials to transform between local energy traps, which explains the reason why ‘noise’ or ‘effective temperature’ is needed to excite the material in SGR modelling. We note that, with assistance of the aforementioned kinetic energy ratio k_t, the thermodynamic behaviours of soft matters can be efficiently amplified to overcome the corresponding local energy traps in the thermomechanical modelling. In summary, our modified CG method can

improve the ability of the prediction of phase changes in soft matter from the viewpoints of both energy and temporal scale. However, the method still has difficulties in fully exploring the rheology properties of gel like soft matters due to the limit of their absolutely large temporal scale, at which slow dynamics happens.

Based on the above-mentioned claims, similar modification of thermostat algorithm should be made in all other attempts of building oversimplified CG models for soft matters at extra-large scales. This new algorithm can improve the capability of CG modelling in capturing thermomechanical properties of biological materials with hierarchical structures. Using this newly developed stochastic thermostat algorithm, CG-MD modelling method is competent to model the thermodynamic properties of soft matters in association tp the mechanical deformation modelling. Compared to AA-MD characterization, this modified CG-MD modelling strategy can significantly reduce the computational cost while efficiently retaining the ability of biophysical properties of soft biological materials with hierarchical structures.

5.5 CONCLUSIONS

A new stochastic thermostat algorithm is proposed to overcome the incapability of highly coarse-grained (CG) models of microfilaments in thermodynamic prediction. This newly developed algorithm can efficiently predict the thermodynamic properties of microfilament in association to the modelling of mechanical deformation. A statistical factor k_t, which belongs to Gamma distribution, is implemented in the relationship between temperature and kinetic energy. According to the characterization of longitudinal thermal fluctuations of both short (11nm, 4 G-actin monomers) and long (72nm, 26 G-actin monomers) microfilament fragments, this modified method can obtain more reliable thermodynamic behaviours compared to direct CG-MD modelling. By using this new stochastic thermostat algorithm, the computational efficiency can be significantly improved. This new stochastic thermostat algorithm provides an efficient and accurate way to investigate the biophysical properties of large-scale soft matters with hierarchical structures.

5.6 ACKNOWLEDGEMENTS

Support from the ARC Future Fellowship grant (FT100100172) is gratefully acknowledged.

Chapter 6: Mechanical Stability of F-actin Bundles in CSK (Paper 4)

Research paper four:

Li, T., Oloyede, A., Gu, Y.T., 2013. F-actin crosslinker: a key player for the mechanical stability of filopodial protrusion. ***Journal of Applied Physics*** 114, 214701-214705.

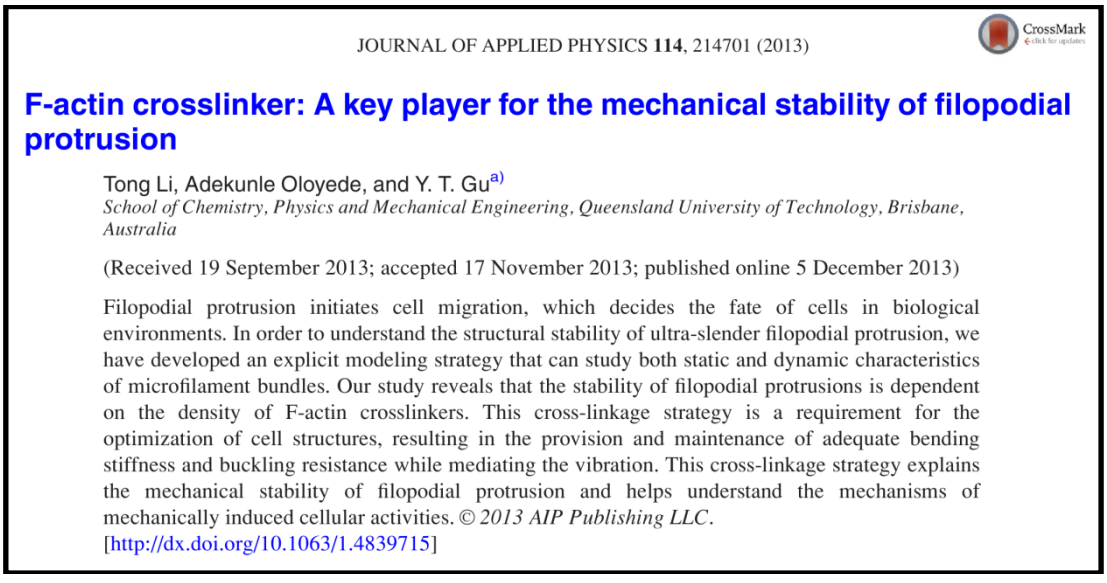

JOURNAL OF APPLIED PHYSICS **114**, 214701 (2013)

F-actin crosslinker: A key player for the mechanical stability of filopodial protrusion

Tong Li, Adekunle Oloyede, and Y. T. Gu[a)]
School of Chemistry, Physics and Mechanical Engineering, Queensland University of Technology, Brisbane, Australia

(Received 19 September 2013; accepted 17 November 2013; published online 5 December 2013)

Filopodial protrusion initiates cell migration, which decides the fate of cells in biological environments. In order to understand the structural stability of ultra-slender filopodial protrusion, we have developed an explicit modeling strategy that can study both static and dynamic characteristics of microfilament bundles. Our study reveals that the stability of filopodial protrusions is dependent on the density of F-actin crosslinkers. This cross-linkage strategy is a requirement for the optimization of cell structures, resulting in the provision and maintenance of adequate bending stiffness and buckling resistance while mediating the vibration. This cross-linkage strategy explains the mechanical stability of filopodial protrusion and helps understand the mechanisms of mechanically induced cellular activities. © *2013 AIP Publishing LLC*.
[http://dx.doi.org/10.1063/1.4839715]

Statement of Contribution of Co-Authors for Thesis by Published Paper

The following is the format for the required declaration provided at the start of any thesis chapter which includes a co-authored publication.

The authors listed below have certified* that:

1. they meet the criteria for authorship in that they have participated in the conception, execution, or interpretation, of at least that part of the publication in their field of expertise;
2. they take public responsibility for their part of the publication, except for the responsible author who accepts overall responsibility for the publication;
3. there are no other authors of the publication according to these criteria;
4. potential conflicts of interest have been disclosed to (a) granting bodies, (b) the editor or publisher of journals or other publications, and (c) the head of the responsible academic unit, and
5. they agree to the use of the publication in the student's thesis and its publication on the QUT ePrints database consistent with any limitations set by publisher requirements.

In the case of this chapter:

Li, T., Oloyede, A., Gu, Y.T., 2013. F-actin crosslinker: A key player for the mechanical stability of filopodial protrusion. Journal of Applied Physics 114, 214701-214705.

Contributor	Statement of contribution*
Tong Li Signature 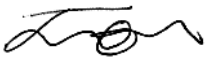 Date 24/11/2014	Designed and conducted numerical model. Conducted data analysis. Wrote the manuscript.
Kunle Oloyede	Designed and conducted numerical model. Involved in the conception and design of the project. Assisted data analysis. Provided feedback on manuscript.
YuanTong Gu*	Involved in the conception and design of the project. Assisted data analysis. Provided feedback on manuscript.

Principal Supervisor Confirmation

I have sighted email or other correspondence from all Co-authors confirming their certifying authorship.

YuanTong Gu	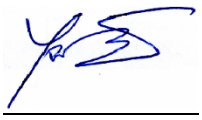	24/11/2014
Name	Signature	Date

6.1 ABSTRACT AND KEYWORDS

Filopodial protrusion initiates cell migration, which decides the fate of cells in biological environments. In order to understand the structural stability of ultra-slender filopodial protrusion, we have developed an explicit modelling strategy that can study both static and dynamic characteristics of microfilament bundles. Our study reveals that the stability of filopodial protrusions is dependent on the density of F-actin crosslinkers. This cross-linkage strategy is a requirement for the optimization of cell structures, resulting in the provision and maintenance of adequate bending stiffness and buckling resistance while mediating the vibration. This cross-linkage strategy explains the mechanical stability of filopodial protrusion and helps understand the mechanisms of mechanically induced cellular activities.

Keywords: F-actin crosslinker, Filopodial protrusion, Mechanical stability, Biomechanics

6.2 INTRODUCTION

Throughout our life, multicellular organism spatiotemporally coordinates various physiological processes, such as embryonic morphogenesis and tissue formation [172], by elaborating the spreading and migration of cells [173, 174]. Cell migration also initiates with leading edge protrusion, and finalizes with cell movements yielded by intracellular cytoskeleton contraction from cell protrusions [175]. Fig. 6-1 shows the *in vivo* morphology of osteoblasts during cell migration. The flat, sheet like F-actin network in cells is lamellipodia, from where cell protrusion initiates [176]. Various functional proteins comprehensively stimulate the lamellipodia to form needle like, highly dynamic cell protrusions: filopodia [177]. The filopodia is made up of F-actin that are bundled by actin binding proteins [178] and acts as the mechanical unit of cell migration frontier. Abnormal cell protrusions due to improper mechanical properties of filopodia can initiate unhealthy cell migration, which leads to human diseases such as immune disorders and proliferation of tumour cells [179, 180]. Therefore, understandings of the mechanical stability of filopodial protrusions are significant to cell pathology studies.

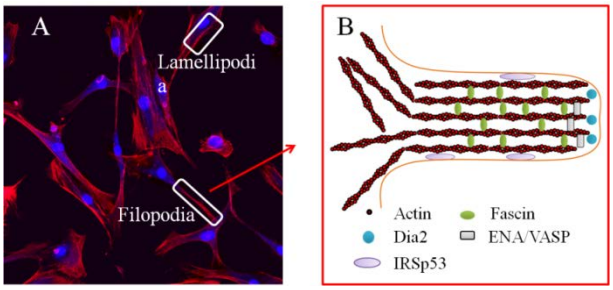

Fig. 6-1. *In vivo* cell migration and the illustration of filopodia structure. A. Osteoblasts morphology evaluation by laser Confocal microscope (Nikon A1R Confocal system) after 24 hours culturing on 22mm×22mm glass cover. DAPI is employed for the visualization of nucleus (in blue) and rhodamine-phalloidin is employed for the visualization of F-actin (in red). B: Molecular structure of filopodia. Dia2 can nucleate the formation of new, unbranched F-actin. ENV/VASP crosslinks F-actin in the tip of protruding filopodia. IRSp53 might sense the negative membrane curvature and initiates new filopodia. Fascin is the major F-actin cross-linkage protein in filopodia.

The physiological environment of living cells includes various potential mechanical loadings, such as extracellular interstitial fluids and intercellular cytoskeleton self-contraction. Fig. 6-2 shows typical loading models on living cell structures: bending model and buckling model. The focal adhesions of living cells are mainly distributed at leading and trailing edges of cells[181], which can be

imaged as mechanical supports to cell structures (e.g. filopodia and lamellipodia) under the condition of mechanical loadings. The diameter of single F-actin is under 10nm [66], while the length of filopodia can be up to 40μm in various organisms [182]. The microscale F-actin length and nanoscale filament cross section result in large aspect ratio, making single F-actin fragile to undergo the challenging mechanical conditions.

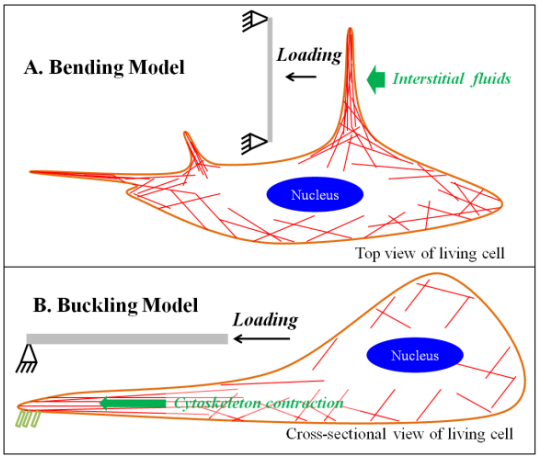

Fig. 6-2. Potential loading models of filopodia in biological environments. A: Bending model of filopodia. The filopodia can be simplified as thin beam. The tip of stress fibre is fixed because of focal adhesions while the other end belongs to the main body of cell. The interstitial fluids can apply transient or continuous transverse loadings to the filopodia. B. Buckling model of stress fibres (F-actin bundle), e.g. filopodia and pseudopodia. Contraction due to myosin II acts as axial compression on the slender beam.

In living cells, single F-actin filaments are tightly bundled by crosslinkers to mediate the mechanical performances of filopodial protrusion [183, 184], and the main cross-linkage protein in filopodia is fascin [8]. The mechanical properties of F-actin bundle have been explored by pure bending theory of slender beam [185] and worm-like chain (WLC) characterization [183]. Based on experimental findings, a mechanics model for this semiflexible biological organism was proposed [186] and numerical simulations successfully predicted the bending stiffness and buckling resistance with respect to the features of F-actin bundle structures [187, 188]. However, these continuum mechanics based models have difficulties in modelling the large, nonlinear deformation of semiflexible F-actin bundles which is comparable to the thickness of filopodia. Also, the dynamic response of filopodia protrusion after excitation is hard to be captured by adopting finite element method based modelling strategy. New modelling technique is needed to meet the requirements in capturing nonlinear deformations and dynamic response of semiflexible filopodia. Recently, multiscale modelling method based on experiments and molecular simulation shows

great potential in the dynamics simulation of bio-inspired materials [145]. A coarse-grained model is specifically developed for the mechanical deformation modelling of F-actin based on atomistic modelling of F-actin filaments [12].

In this paper, crosslinkers are implemented to the coarse-grained model of F-actin bundle [12] to investigate the mechanical performances of filopodial protrusion. This model aims to explicitly extract the complex mechanical behaviours of F-actin bundles considering influences from fascin-actin cross-linkage. The significance of F-actin crosslinkers in stabilizing the filopodial protrusion is evaluated based on static and dynamic characteristics of fascin binding F-actin bundles.

6.3 COMPUTATIONAL MODEL

In the modelling strategy, single filaments are simplified as particle strings that are connected by F-actin crosslinkers, as shown in Fig. 6-3. The interaction between actin clusters on the same F-actin and the cross-linkage between neighbouring F-actin are assumed to be harmonic pair potential energy: $E = \frac{1}{2}k(r - r_0)^2$, where k is the energy scale parameter, r and r_0 correspondingly denote the actual distance and equilibrium distance between actin clusters. Similar characterizations for the angular potential energy functions are defined with respect to the angle between two neighbouring connections. This explicit is capable to obtain dynamic responses of F-actin bundles after mechanical excitation. The stiffness of stress fibres that consists of actin filament has dependency on temperature [189]. However, we only adopt the filament stiffness parameters at human body temperature [12] in this study. The randomly distributed weak interactions between G-actin monomers, e.g. H-bond and disulfide bond, are not considered since they are negligible comparing to mechanical loadings.

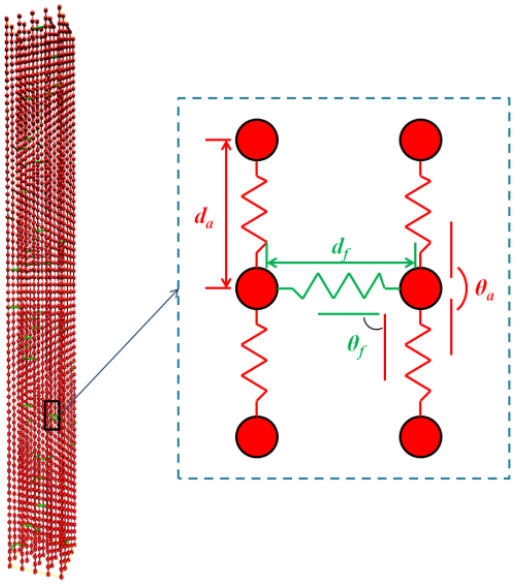

Fig. 6-3. The schematic of granular simulation strategy for F-actin bundle modelling. Each virtual particle (red circle) consists of two actin monomers, and the equilibrium distance between neighboring particles is 5.53nm. The longitude stiffness of a 1μm long F-actin follows the experimental finding of 43pN/nm,**[53]** the equilibrium angle is 180° between actin-actin bonds, and the angular stiffness is characterized to be 7630 kCal/mol·rad^2.[12] The tensile stiffness of 37.5nm long fascin is assumed as 1.5pN/nm, the equilibrium angle is 90° for actin-fascin connection, and the angular stiffness is 500kCal/mol·rad^2.

The cross section of bundle is assumed quadrate, consisting of 25 (5×5) filaments. The length of this actin bundle is 2μm and the transverse distance between filaments is 37.5nm [187], making the total bundle thickness 150nm. The profile of F-actin bundle in this work follows the filopodia length prediction from literature [188]. The cross-linkage randomly occurs between two neighboring particles at the same longitudinal position from different filaments [190]. Five scenarios of F-actin bundles with different crosslinker densities are selected to understand sensitivity of mechanical behaviours with respect to the crosslinker density. The crosslinker density ratio is calculated as $\alpha = n_f / n_a$, where, n_f and n_a respectively denote quantities of F-actin crosslinkers and actin monomers. Canonical ensemble (NVT) is a thermal bath, in which particle numbers, system volume and temperature are constant. Herein, NVT ensemble is employed with a 303K temperature to model the bending and buckling of F-actin bundle. Langevin dynamics algorithm [150] is employed to model the friction from implicit solvent. In the Langevin dynamics algorithm, two terms are added to the force calculation on each particle: viscous damping term due to solvent and a randomly bumping term due to temperature. The combination of these two terms is $F_d = -\frac{m}{C_d} v + \sqrt{\frac{mk_BT}{dtC_d}}$. Where, m is the mass of

particle, v is the velocity, k_B is the Bozeman constant, T is the temperature, dt is the time step and C_d is the damping factor with a time unit. In this simulation, C_d is chosen as 1ps to understand the sensitivity of dissipative force to the density of F-actin crosslinkers.

The size of time step is 0.1ps in bending/buckling simulations and 0.2ps in the vibration simulation. The granular simulations are performed with Lammps [191] on HP Z600 workstation (Intel Xeon X5570) and all the atomistic visualizations are finished on VMD [169].

6.4 RESULTS AND DISCUSSION

The mechanics models of transverse loading conditions and corresponding characterization results are detailed in Fig 4. In the bending test simulation, a rigid cylinder is designed to indent the F-actin bundle to model the transverse bending of F-actin bundle. The velocity of indentation is 150nm per microsecond, which is a slow loading rate in molecular simulations to allow the relaxation of stress-wave. The evaluation of bending stiffness κ_B is based on Euler-Bernoulli beam theory under double clamped boundary condition: $\kappa_B = \frac{Fl^3}{192\delta}$, where, F is the reaction due to rigid cylinder indentation, l is the bundle length and δ is the deflection of F-actin bundle. It should be noted that the distribution of crosslinkers on the F-actin bundle also has effects on the mechanical behaviours of the whole bundle structure (in Supplementary Material). With the same crosslinker density, F-actin bundle with uniformly distributed crosslinkers presents higher mechanical stiffness in bending simulation. Based on the nature of filopodial protrusion, the cases with uniformly distributed crosslinkers are adopted for the mechanical characterization in this paper.

The bending stiffness of F-actin bundles(black solid square in Fig. 6-4) increases with the density of crosslinkers, which is consistent with previous experimental findings [183]. Refer to the interlaminar shear stress in continuum mechanics model, the deformation of actin crosslinkers between different F-actin filaments can store potential energy that is caused by external transverse loadings and increase the bending stiffness of F-actin bundles. Direct indentation tests of *in vivo* F-actin bundles have provided the evaluation of the bending stiffness, which is at the scale of $\kappa_B = 10^{-22}$ to $10^{-21}\,\mathrm{Nm}^2$ [185], while WLC characterization of F-actin

bundles leads to the stiffness evaluation at scale of $\kappa_B = 10^{-23}\,\mathrm{Nm}^2$ [183, 184]. The bending stiffness prediction in this paper, as shown in Fig. 6-4, agrees with these experimental findings and is close to the characterization by direct indentation [185], as our simulation is also based on beam bending model.

Transverse impact is another typical loading on filopodia in cell surviving environments (e.g. from sudden interstitial flow). The capability of filopodia to mediate the violent vibration after transient excitation is significant in stabilizing healthy cell protrusion modes under impacts. We have employed the proposed computational model to capture dynamic responses of F-actin bundles after transient excitation. In the modelling, the F-actin bundle is fixed with the same boundary conditions as aforementioned modelling of transverse indentation. A transient velocity with half sinusoidal profile is applied on the whole bundle, and the velocity amplitude is $10^{-2}\,\mathrm{nm/ps}$.

According to the dynamic response extracted from numerical simulation, the kinetic energy of F-actin bundle decreases while the density of crosslinker increases, indicating that actin crosslinkers can mediate the vibration of ultra-slender filopodia protrusions, which is positive to enhance the stability of cell migration.

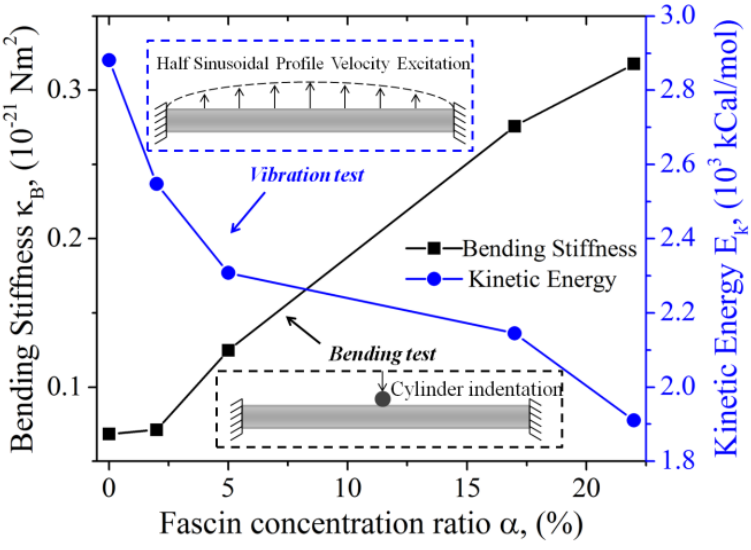

Fig. 6-4. The calculation result from direct bending test and vibration test of F-actin bundles. The mechanics model of both simulation cases are double clamped slender beam. Different from indentation tests, half-sinusoidal profile velocity excitation is applied to the simulation system in vibration tests for 1μs, and the averaging kinetic energy in the last 0.1μs (in which the kinetic energy is steady) is captured to evaluate the dynamic stability of the bundle system.

Fig. 6-5 illustrates the simulation results of free vibration modes of F-actin bundles in different states without and with crosslinker binding. With the assistance of F-actin crosslinkers, F-actin filament is crosslinked to its neighbouring filaments, providing mechanical supports to the filopodia protrusion and mediates the dynamic response of a whole F-actin bundle system. This characteristic improves the resistance of filopodial protrusion to undergo sudden impacts in complex biological environments that includes random transverse loadings.

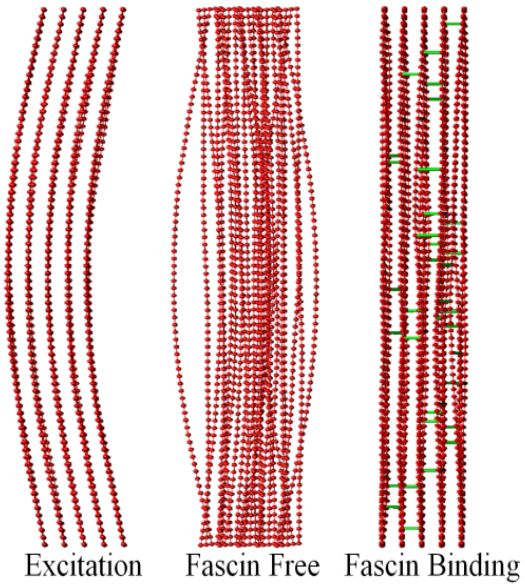

Fig. 6-5. Free vibration modes of F-actin bundles in different crosslinker binding states. The first illustration is the initial excitation applied on the bundle. The second and last illustrations correspondingly represent free vibration modes of F-actin without and with inner cross-linkages.

As a typical biological material, the semiflexible filopodia protrusion also presents highly overdamped property after transient mechanical loadings. By using the aforementioned Langevin dynamics algorithm, the dissipative characteristics of F-actin bundles can be estimated to understand the sensitivity of filopodia dissipation to F-actin crosslinker density. As shown in Fig. 6-6, the kinetic energy dose not converge after 1μs simulation in the scenario of zero F-actin crosslinker while both lower (5.01%) and higher (22.29%) crosslinker densities lead to the convergence of kinetic energy. Moreover, the kinetic energy dissipates faster with higher crosslinker density, indicating that crosslinker density contributes to the dissipative force on filopodia protrusion.

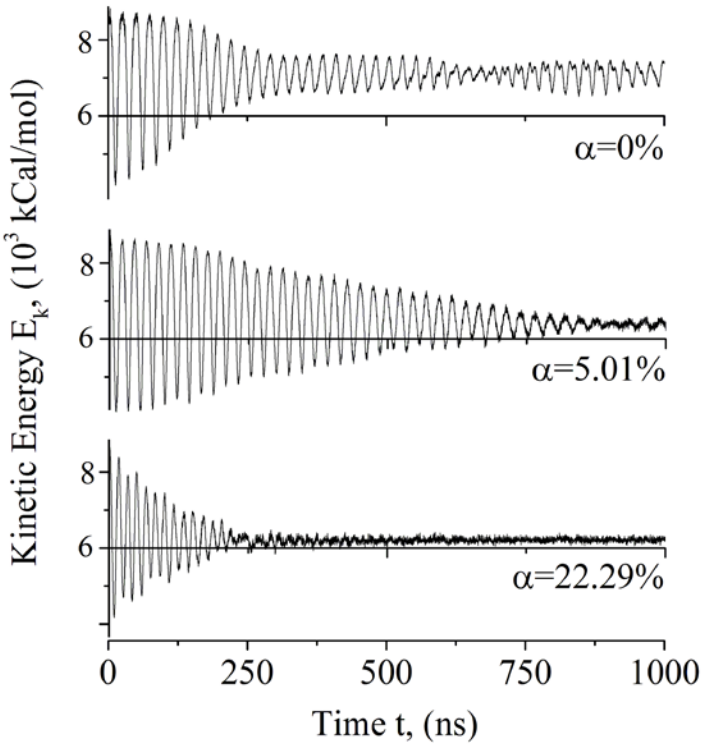

Fig. 6-6. Dissipative kinetic energy profiles of F-actin bundles with different crosslinker densities. The dissipation time for kinetic energy and the residue kinetic energy are both inversely proportional to the density of crosslinkers.

The filopodial protrusion also undergoes axial forces due to the intracellular cytoskeleton contraction from myosin-II [192] or extracellular mechanical loadings. Another set of computational scenarios are set up to investigate the dynamic buckling behaviours of F-actin bundle in filopodia with different F-actin crosslinkers density. In the simulation models, one end of the F-actin bundle is fixed and a constant velocity is applied at the other end to model axial compression. The potential energy profile of F-actin bundle is summarized to characterize the buckling resistance of F-actin bundle model with different F-actin cross-linkage conditions, as shown in Fig. 6-7.

The critical buckling strain of a continuum slender beam with quadrate cross section can be derived from Euler's equation as: $\varepsilon_{cr} = \frac{\pi^2 a^2}{3l^2}$, where, a is the length of quadrant edge and l is the length of slender bundle. Adopting 150nm edge length and 2μm bundle length, theoretical solution of the buckling strain of a nonporous F-actin bundle is 1.85%. The approximate buckling strain for porous F-actin bundle in the modelling can be directly extracted from the transitions on potential energy profile, where the increase of potential energy slows down or even stops. After this

critical loading strain, the F-actin bundle is incapable to fully carry further axial compression. The buckling strain of porous F-actin bundles in modelling increases with the density of crosslinkers, and approaches the theoretical solutions of a continuum beam. Take the scenario of $\alpha = 22.29\%$ for example, by adopting the design strategy of cross-linkage, porous F-actin bundle can approximately reduce 90% of the mass comparing to a nonporous bundle of F-actin filaments. However, the critical buckling strain only decreases 14% (from 1.85% to 1.59%).

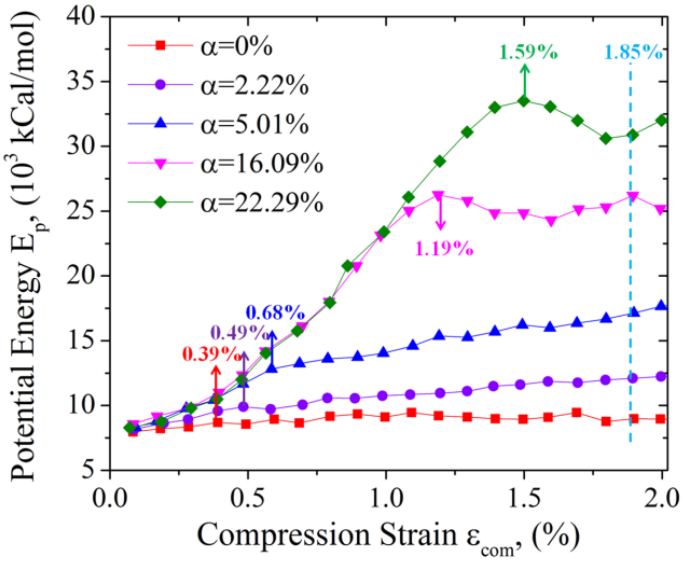

Fig. 6-7. The characterization of F-actin bundles buckling with different crosslinker density. Buckling strain is marked with different colours in corresponding to the computational scenario and the light blue dotted line (1.85%) denotes the theoretical solution of buckling strain of gapless F-actin bundle with the same profile.

Explicit solutions of the buckling behaviours of F-actin bundle with different cross-linkage conditions are provided in Fig. 6-8 to illustrate the molecular mechanisms of strengthened buckling resistance. F-actin bundles without cross-linkage (red bundles) are indeed individual actin filaments whose aspect ratio is too large to resist axial compression. With the help of crosslinkers, single filaments cooperate as a combined bundle to resist extracellular or intracellular mechanical challenges from its surviving environment. The effective lengths l_e (refer to Fig. 6-8) of buckling models decreases with actin crosslinkers density, improving the buckling resistance. The post-buckling behaviours of crosslinked F-actin bundles also demonstrate that, with the assistance from actin crosslinkers (blue and green bundles), F-actin bundles can still partly carry the deformation energy caused by external loadings. Similar findings have been reported for carbon nano materials

[193]. This is another characteristic of ultra-slender filopodia protrusions to undergo complex mechanical conditions in biological environments.

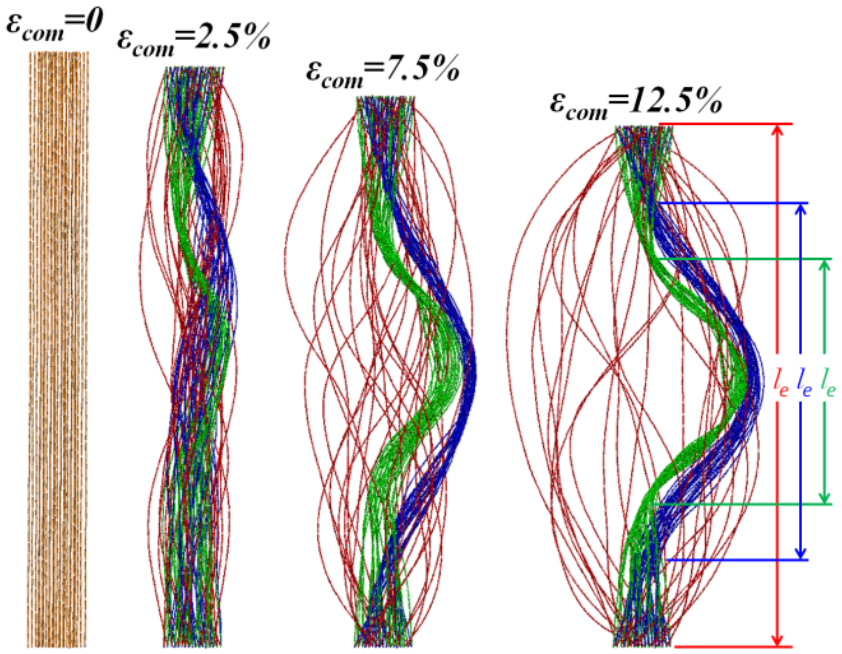

Fig. 6-8. Buckling modes of F-actin bundles with respect to cross-linkage status. The red filaments represent non-bundled individual F-actin filaments, and the blue and green filaments respectively represent F-actin bundles with 5.01% and 22.29% crosslinker density ratios. The effective length of the F-actin bundle (l_e) decreases with the density of crosslinkers, which explains the increase of buckling resistance by crosslinkers.

Mechanics is one of the most primitive signalling systems for multicellular system [1]. The mechanical stability is filopodial protrusion is critical to living cells as it is involved in various dynamic cellular activities, such as spreading [174], migration [194] and adhesion [163]. Take breast cancer cells for example, the high density of fascin can regulate the invasion of cancer cells [195] whose mechanical stiffness is usually higher than normal cells. The modelling results in this paper can theoretically prove that the mechanical performance of filopodial protrusion has dependency on the quantity of crosslinker protein. By adjusting the cross-linkage strategy between F-actin filaments, living cells can sensitively mediate the cytoskeleton mechanical performance, which is significant for the pathological research and physics therapies of cell diseases.

6.5 CONCLUSION

In the present study, the significant role F-actin crosslinkers (fascin) plays in enhancing the mechanical stability of ultra-slender filopodia protrusion is

investigated by developing an explicit granular simulation strategy. The modelling of transverse and axial deformation demonstrates that the bending stiffness and buckling resistance of ultra-slender filopodial protrusion are strengthened by the cross-linkage between single F-actin filaments. The dynamics modelling of crosslinked F-actin bundle also proves that crosslinker protein functions to mediate the vibration of filopodial protrusion after transient excitation. In summary, this cross-linkage design of F-actin bundle in filopodial protrusion can stabilize the mechanical behaviours of cellular activities in complex physiological environment.

6.6 ACKNOWLEDGEMENT

Support from the ARC Future Fellowship grant (FT100100172) is gratefully acknowledged. The authors thank Dr. Ling Liu and Miss J.Q. Li for helpful discussion.

6.7 SUPPLEMENTARY MATERIAL

As described in the paper, the crosslinker distribution has the potential to mediate the mechanical properties of F-actin bundles. Herein, we designed a group of simulation scenarios to investigate the sensitivity of bending stiffness to crosslinker density.

The computational models are of the same geometries with the models in the manuscript. The length is 2μm and there are five layers filaments in the simulation model (5×5). There are three types of crosslinker distributions: first is the top two layers of the filaments are absolutely crosslinked, second is the middle two layers are absolutely crosslinked and the final model has homogeneously distributed crosslinkers. The schematic is provided in Fig. 6-9. It should be noted that, in the first two simulation cases as shown in Fig. 6-9, crosslinkers are only localized on the red regions marked in Fig. 6-9. No crosslinkers are designed in other regions, marked as blank.

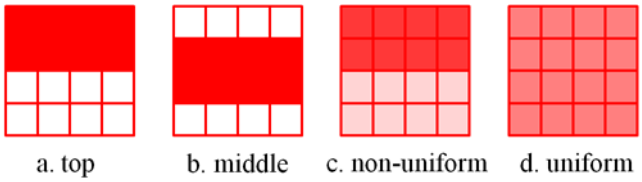

Fig. 6-9. Three different crosslinker distribution strategies. a. top layer crosslinked. b. middle layer crosslinked. c. crosslinkers non-uniformly distributed on the whole bundle. d. crosslinkers uniformed distributed no the whole bundle.

In the model presented by Fig. 6-9(c), the crosslinkers are non-uniformly distributed on the whole bundle. The non-uniform case (c) is an intermediate state whose mechanical properties should be between the characterization from the concentrated case and uniformly distributed cases. Herein, we only focus on the first two cases where crosslinkers are concentrated on certain regions (a and b) and the last case where crosslinkers are uniformed distributed on the structure (d).

The numbers of crosslinkers in these three models are close to each other for the later compilation. The key numbers in simulation are listed in Table 1.

Table 6-1 The model details for different crosslinker distribution cases.

Model	Top layer	Middle layer	Homogeneous
Particle numbers	9075	9075	9075
Actin	18150	18150	18150
Crosslinker	3249	3249	2920
Ratio	0.17	0.17	0.16

The same bending process is applied to these three beams and the force is tracked with respect to the deflection. The result is provided in Fig. 6-10.

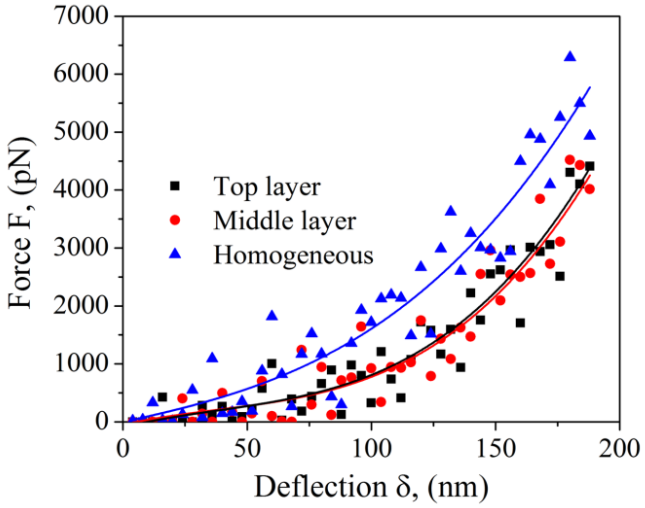

Fig. 6-10. The force profile with respect to deflection during bending.

The stiffness of homogeneously crosslinked bundles are of higher stiffness than the cases in which crosslinkers concentrate only at some certain parts of the bundle. Therefore, the mechanical properties of crosslinked F-actin bundle have dependency on the crosslinker distribution. However, more detailed sensitivity study of crosslinker distribution should be expanded for future design of artificial biomaterials microstructure for better mechanical performances.

Chapter 7: Compressive Response of 3D F-actin CSK (Paper 5)

Research paper five:

Li, T., Hu, D., Yarlagadda, P.K.D.V. and Gu, Y. (2014). Physical mechanism of the compressive response of F-actin networks: significance of crosslinker unbinding events. ***Theoretical and Applied Mechanics Letters*** 4, 051006.

THEORETICAL & APPLIED MECHANICS LETTERS **4**, 051006 (2014)

Physical mechanism of the compressive response of F-actin networks: significance of crosslinker unbinding events

Tong Li,[1, a)] Dean Hu,[1, 2] Prasad K.D.V. Yarlagadda,[1] Yuantong Gu[1, b)]
[1)] *School of Chemistry, Physics and Mechanical Engineering, Queensland University of Technology, Brisbane, Australia*
[2)] *State Key Laboratory of Advanced Design and Manufacturing for Vehicle Body, Hunan University, Changsha 410082, China*

(Received 11 April 2014; revised 17 June 2014; accepted 23 June 2014)

Abstract A model of crosslinker unbinding is implemented in a highly coarse-grained granular model of F-actin cytoskeleton. We employ this specific granular model to study the mechanisms of the compressive responses of F-actin networks. It is found that the compressive response of F-actin cytoskeleton has dependency on the strain rate. The evolution of deformation energy in the network indicates that crosslinker unbinding events can induce the remodelling of F-actin cytoskeleton in response to external loadings. The internal stress in F-actin cytoskeleton can efficiently dissipate with the help of crosslinker unbinding, which could lead to the spontaneous relaxation of living cells.

 [doi:10.1063/2.1405106]

Keywords F-actin cytoskeleton, coarse-grained, crosslinker unbinding, compressive response

Statement of Contribution of Co-Authors for Thesis by Published Paper

The following is the format for the required declaration provided at the start of any thesis chapter which includes a co-authored publication.

The authors listed below have certified* that:

1. they meet the criteria for authorship in that they have participated in the conception, execution, or interpretation, of at least that part of the publication in their field of expertise;
2. they take public responsibility for their part of the publication, except for the responsible author who accepts overall responsibility for the publication;
3. there are no other authors of the publication according to these criteria;
4. potential conflicts of interest have been disclosed to (a) granting bodies, (b) the editor or publisher of journals or other publications, and (c) the head of the responsible academic unit, and
5. they agree to the use of the publication in the student's thesis and its publication on the QUT ePrints database consistent with any limitations set by publisher requirements.

In the case of this chapter:

Li, T., Hu, D., Yarlagadda, P.K.D.V. and Gu, Y. (2014). Physical mechanism of the compressive response of F-actin networks: significance of crosslinker unbinding events. Theoretical and Applied Mechanics Letters 4, 051006.

Contributor	Statement of contribution*
Tong Li Signature  Date 24/11/2014	Designed and conducted numerical model. Conducted data analysis. Wrote the manuscript.
Dean Hu	Designed and conducted numerical model. Involved in the conception and design of the project. Provided feedback on manuscript.
Prasad Yarlagadda	Involved in the conception and design of the project. Provided feedback on manuscript.
YuanTong Gu*	Designed and conducted numerical model. Involved in the conception and design of the project. Assisted data analysis. Provided feedback on manuscript.

Principal Supervisor Confirmation

I have sighted email or other correspondence from all Co-authors confirming their certifying authorship.

YuanTong Gu	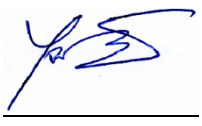	24/11/2014
Name	Signature	Date

7.1 ABSTRACT AND KEYWORDS

F-actin cytoskeleton plays critical roles in a variety of cellular processes. The crosslinker proteins in F-actin networks are responsible for mediating the mechanical properties of cytoskeleton. However, the molecular events in F-actin cytoskeleton are difficult to be tracked experimentally at sub-cellular resolution. In this paper, a model of crosslinker unbinding is implemented in a highly coarse-grained granular model of F-actin cytoskeleton. We have employed this specific granular model to study the mechanisms of the compressive responses of F-actin networks. It can be found that the compressive response of F-actin cytoskeleton has dependency on the strain rate. The evolution of deformation energy in the network indicates that crosslinker unbinding events can induce the remodelling of F-actin cytoskeleton in response to external loadings. The internal stress in F-actin cytoskeleton can efficiently dissipate with the help of crosslinker unbinding, which could lead to the spontaneous relaxation living cells.

Keywords: F-actin cytoskeleton; Coarse-grained; Crosslinker unbinding; Compressive response

7.2 ARTICLE

The cytoskeleton is the material basis for living eukaryotic cells to undergo external mechanical loading.[8] F-actin is an important component of cytoskeleton whose mechanical behaviours can regulate the cellular changes and force generation in cell migration and division.[134, 163, 174] Enormous efforts have been devoted to investigate the cryptic mechanical properties of F-actin networks in living cells for decades.[7, 61, 194] The F-actin network can remodel under mechanical loading, which allows living cells to adjust their cytoskeleton structures for higher mechanical stability.[196] It has been recently reported that, the slow dynamics of F-actin networks is induced by crosslinker unbinding events,[171] which helps living cells to make wise decisions in the evolution of cellular morphology.

The process of dynamical remodelling in F-actin cytoskeleton is significant to understand the mechanisms of cellular morphology changes with respects to the mechanical inputs. Molecular events (e.g. crosslinker unbinding and cytoskeleton remodelling) that happen at sub-cellular resolution can provide insights into the mechanical responses of F-actin cytoskeleton. However, the operation conditions of high resolution microscope (e.g. scanning electron microscope and transmission electron microscope) always have conflicts with the environmental requirements of living cells, which makes it difficult in tracking the aforementioned *in situ* dynamics of F-actin during cellular activities. Therefore, theoretical analysis is needed to explore those molecular events in F-actin cytoskeleton during cellular evolution under mechanical constrains.

Numerical modelling of biological materials can describe the living systems in terms of physics and chemistry, which contributes to the understandings of mechanical behaviours of flexible biological soft matters.[101] Molecular dynamics (MD) simulation of biomacromolecules can provides ultimate details of motional phenomena in principle, which is significant in understanding various biophysical phenomena from the molecular viewpoints.[105] However, all-atom MD modelling system can involve several millions of atoms with nowadays computer power,[160] which can only support the modelling of single F-actin up to hundred nanometres. This computational characteristic of MD modelling limits its application in the direct characterization of mechanical behaviours of F-actin cytoskeleton that consists of thousands of isotropically crosslinked filaments. In order to meet the requirements of

length scale, different coarse-grained (CG) strategies have been developed for F-actin modelling to understand their comprehensive behaviours (thermodynamical and mechanical) from the viewpoint of mechanics.[121, 197] With the help of these CG models, the mechanical modelling of F-actin cytoskeleton can be extended to microscale. Kim, et al., have developed a rod based CG model with empirical parameters for the computational analysis of F-actin networks to explain the significance of actin crosslinkers unbinding in the rheology of F-actin networks.[198] With parameters extracted from all-atom MD simulation and experiments, Li, et al., have developed a bead based CG model of F-actin under the modelling framework of Brownian dynamics for the mechanical simulation of F-actin.[12]

In this paper, a crosslinker unbinding mechanism dominated by mechanical deformation was implemented to the CG model developed in literature[12] to predict the dynamical response of F-actin cytoskeleton that are induced by the transient crosslinker unbinding. Based on the modelling of compressive response of 3D F-actin networks, the mechanisms of internal stress building up and transition were explored by tracking the internal stress distribution. We found that the transient crosslinker unbinding events are responsible to the flexible properties of F-actin cytoskeleton under constant deformation. In living cells, the F-actin filaments are crosslinked to fulfil the ability of transient mechanical resistance. When undergoing constant deformation, the living cells has the ability of spontaneously remodelling in F-actin cytoskeleton with the help of constrains removal at cross-linkage, which is positive for cells to be self-protective under complex conditions.

The 3D F-actin model in this paper was developed based on an *in vitro* characterization crosslinked F-actin networks,[68] in which F-actin filaments were isotropically crosslinked. The filaments in our 3D model were assumed to be orienting around 70^{o}[155] towards the plasma membrane. In a randomly generated network model, crosslinkers can be determined by the distance between G-actin monomers in different F-actin fibres. Fig. 7-1 illustrates a typical network structure in cells and the conformations of cross-linkage in the networks. In order to simplify the calculation, the F-actin network in this paper was assumed to be regular hexahedron. The edge length of square cross-section is 150nm and the thickness of this hexahedron is 60nm.

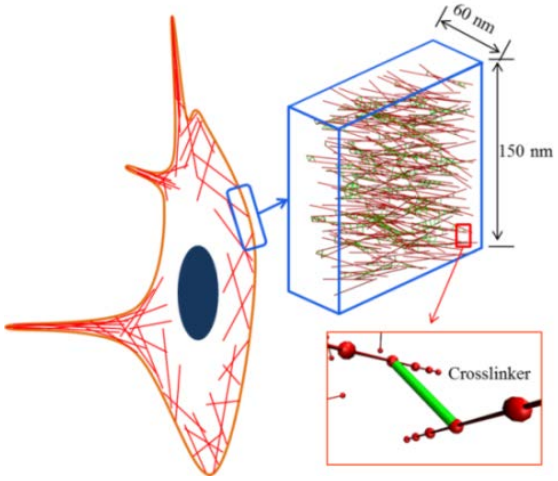

Fig. 7-1. 3D F-actin network model. Cyan dots represent the randomly distributed crosslinkers.

The mechanical deformation models and CG MD simulation models are described in the Supplementary Material. It should be noted that a crosslinker rupture model is developed to understand the significance of crosslinker unbinding in the compression of F-actin cytoskeleton. This rupture model is based on the mechanical testing results from different literatures[199-201].

We respectively carried out the numerical modelling of F-actin networks compression at different strain rates to characterize the mechanical properties of F-actin networks. In order to evaluate the mechanical properties of F-actin networks, compressive stress, modulus and potential energy (deformation energy) are calculated based on the simulation result. Compressive stress was calculated with respect to the pressure on unit area: $\sigma = F/A$. F is the pressure applied on the surface of network and A is the area of cross-section of the network, which is $2.25\times10^4 nm^2$. The modulus was derived from the compressive stress as $E = \partial\sigma/\partial\varepsilon$. ε denotes the strain of F-actin network under compression. The potential energy (P) of F-actin and crosslinker were independently normalized regarding the initial energy state (P_0) to understand the source of energy carrying capability in the F-actin network. Therefore, the deviation of normalized potential energy (P/P_0) from 'one' denotes the degree of energy evolution during the compression.

The crosslinker unbinding in F-actin networks can induce the rearrangement of network structure and positively adjust their mechanical performances under mechanical inputs.[171, 196, 202] We have putatively removed the crosslinker unbinding mechanism in the F-actin model as a reference to normal conditions. The compressive responses of F-actin networks with and without crosslinker unbinding

model were compared to understand the significant of crosslinker unbinding. The simulation results are provided in Fig. 7-2. In the region of low strain (8%), the modulus of F-actin networks with either detachable or non-detachable crosslinkers is quite similar to each other, which indicate that crosslinker unbinding would not take place under this deformation limit (ε=8%). When the deformation exceeds 8%, the F-actin network shows lower modulus when crosslinker unbinding was allowed to take place. This indicates that the crosslinker unbinding can improve the flexibility of F-actin cytoskeleton when the deformation is large. This characteristic is positive for living cells to maintain a healthy phase as one typical characteristic of most cancer cells is their higher stiffness. After the deformation of 13%, a dramatic decrease in modulus can be observed in the networks that are of detachable crosslinkers compared to the saturated modulus of networks with non-detachable crosslinkers.

Both of these two cases present softening phenomenon when the compressive deformation is increased (Fig. 2b, after olive dash line). However, we note that, the compressive modulus of F-actin networks with detachable crosslinkers is lower than relatively rigid networks before softening, which means crosslinker breakage can sensitively mediate the stiffness of F-actin CSK to decrease energy accumulation in cells during deformation. With respect to the region of softening, the stiffness of F-actin CSK with detachable crosslinkers decreases more efficiently. The energy can dissipate more efficiently in the F-actin CSK with detachable crosslinkers, which is more positive for stressed living cells to relieve the pressure under large mechanical deformation.

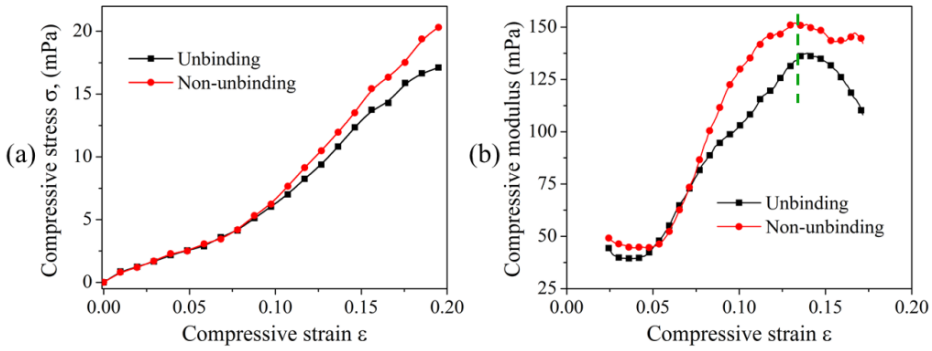

Fig. 7-2. Compressive response of F-actin networks with and without crosslinker unbinding.

In the theoretical model, both longitudinal and rotational stiffness of F-actin in this CG model were assumed to be harmonic, which excluded the possibility that the decrease of modulus is a result of intrinsic material behaviour of F-actin filament.

Therefore, the decrease of modulus can only be the result of microstructure remodelling. Regardless of crosslinker unbinding, the F-actin networks in both models showed softening behaviours. However, when crosslinker unbinding was allowed in the network, F-actin cytoskeleton would present lower stiffness and higher flexibility in response to external loadings, which is a self-protective property of living cells.

It has been widely reported that the mechanics of living cells has dependency on the deformation rates.[203-206] Herein, we tried to quantify this dependency of strain rate by our CG model. The mechanical properties of 3D F-actin networks were studied under different strain rates. In all these modelling cases of rate-dependency, crosslinker unbinding events were allowed to take place during the compression. The compressive strains were all the same in different cases, but the duration of compression varied from 0.1μs to 1μs to achieve different strain rates. It should be noted that, the actual transition time for protein structure change is believed to be at micro-second scale [159], but most of the all atom MD simulation can only play the modelling at nanosecond scale. This indicates that our CG modelling strategy at micro-second scale is capable to improve the capability of molecular modelling in the characterization of time dependent mechanical properties of soft matters at large spatial scale.

The F-actin networks with crosslinkers were all compressed to 80% of its original thickness in the aforementioned durations and the corresponding strain rate ranged from 0.2 /μs to 2 /μs. The compressive stress was tracked during the deformation and the related results are shown in Fig. 7-3.

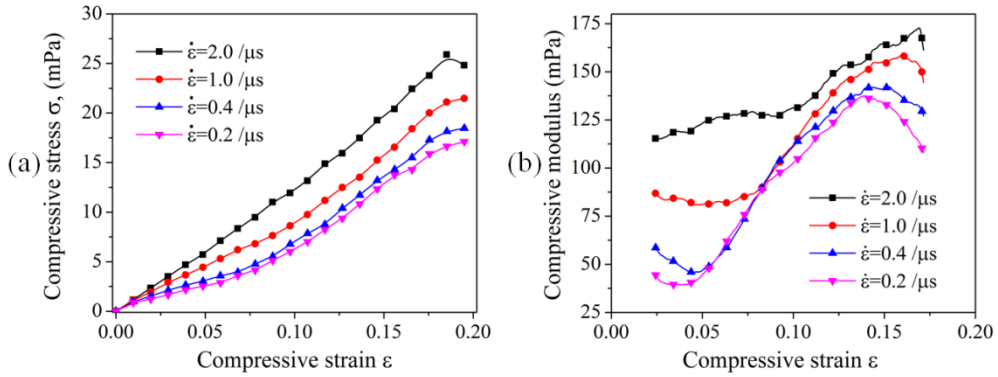

Fig. 7-3. a, Stress-strain relation at different strain rates. b, Compressive modulus at different strain rates.

It can be found that the compressive modulus of F-actin networks increases with the strain rate, which is similar to crystalline inorganic materials.[207] Stiffness changes during compression can be derived from the stress-strain relationship, which is provided in Fig. 7-3(b). Lower strain rate can lead to smaller compressive modulus of F-actin network. In order to understand the mechanism of the rate dependency, the potential energy of network was divided into two parts: deformation energy in F-actin and deformation energy in crosslinkers. These energy profiles with respect to modelling time for both F-actin and crosslinkers at different strain rates are provided in Fig. 7-4.

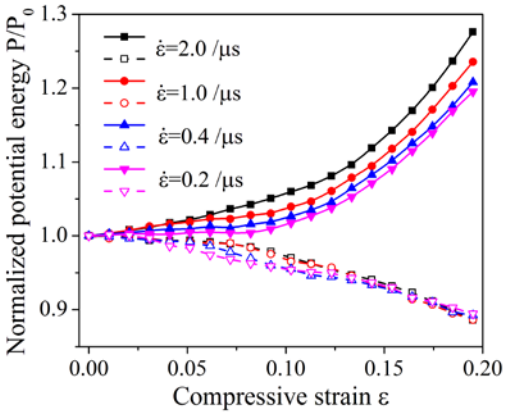

Fig. 7-4. Potential energy profile of F-actin and crosslink during mechanical loading. Solid line and symbol denotes F-actin, dash line and hollow symbol denotes crosslinkers.

Under lower strain rate conditions (0.2/μs), the normalized potential energy on crosslinkers (open and dash marks in Fig. 7-4) is lower than the results of higher strain rate (2/μs) when the compression is smaller than 15%. The decrease of potential energy in crosslinkers denotes that the crosslinkers were unbinding from the network. When the strain rate is low, longer duration is allowed for crosslinkers to unbind from F-actin and the deformation energy due to mechanical loading is more easily to get released. However, when enough time was allowed for the internal stress to build up and transport from F-actin to crosslinker (after the deformation exceeds 15%), the F-actin filaments would reorganize to build more optimized network that is of lower potential energy. Therefore, the macroscopic mechanical properties of F-actin networks are not only results of the inherent material behaviours of F-actin or crosslinkers, but also a result of the dynamic remodelling process of F-actin networks structures during deformation.

The stress dissipation of F-actin networks[208] is another positive aspect for living cells to be self-protective under constant mechanical loadings. We have designed four modelling cases with the abovementioned different strain rates to capture the transient stress dissipation in F-actin networks, which can help study the physical mechanisms of this dissipation process. In the modelling of stress dissipation, after the compression had been finished, the defamation of F-actin network was reserved for a period that is two times of the loading duration, in which the stress was allowed to get released in the F-actin network. The stress evolution in the networks is provided with respect to modelling time in Fig. 7-5. It can be found that the rate of stress dissipation has dependency on the strain rate in the whole process of stress dissipation (as presented by olive dash line in Fig. 7-5) and a saturated stress can be achieved after the transient and dramatic decrease of stress.

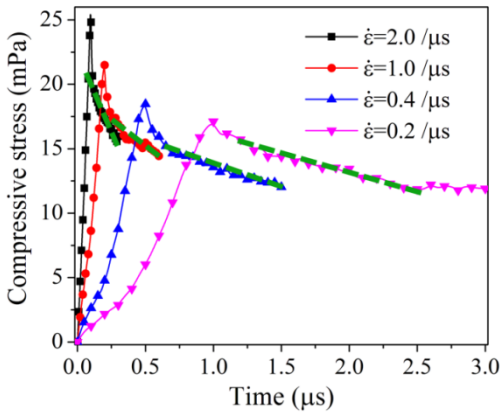

Fig. 7-5. Stress dissipation of F-actin networks after loadings with different strain rates.

As we have already claimed that crosslinker unbinding plays crucial roles in the mechanical mediation of F-actin networks, herein, the significance of crosslinker unbinding events was further investigated by comparing to the results when the crosslinker unbinding events were putatively prohibited. In order to understand the mechanisms of stress dissipation of F-actin networks, the potential energy carried by F-actin and crosslinkers were independently captured for analysis. Only the strain rate of 0.2 per micro-second was studied in this paper without loss of generality. Fig. 6(a) shows the stress dissipation processes of F-actin networks with different crosslinker phases. For networks with non-detachable crosslinkers, the stress becomes saturated efficiently after the loading is stopped, which is different from the network with detachable crosslinkers whose stress keeps decreasing at the same time. The stress dissipation rate of F-actin networks is higher when the crosslinkers are

allowed unbind from F-actin (olive dash line in Fig. 7-6(a)), which further proves the significance of crosslinkers in the stress dissipation of F-actin networks.

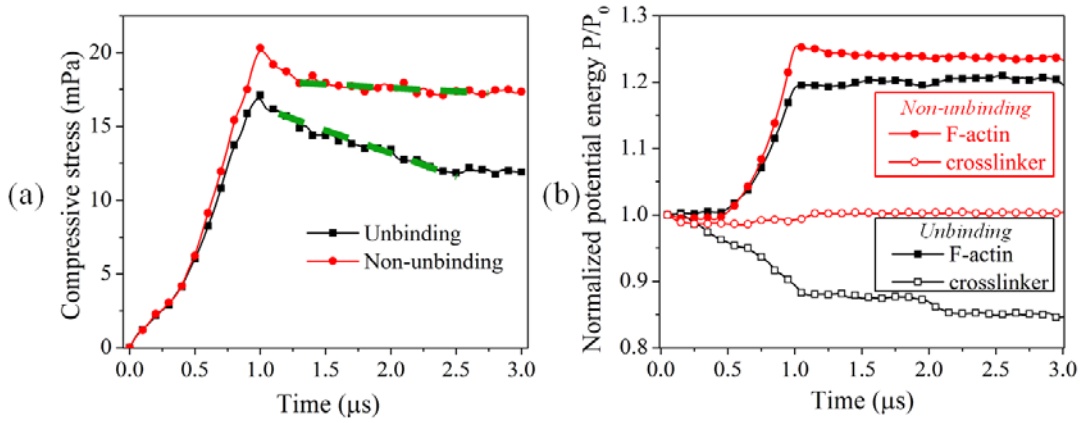

Fig. 7-6. a, Macroscopic stress of F-actin networks. b, Potential energy carried by F-actin and crosslinkers.

From Fig. 7-6(b), it can be seen that F-actin carries less potential energy when crosslinkers can unbind from the network (solid, black square profile). The potential energy in crosslinkers decreases during the mechanical deformation (black, open square in Fig. 7-6(b)), which indicates that the crosslinkers were unbinding from the networks. These unbinding of crosslinkers can improve the remodelling ability of network structures in the optimization of internal stress distribution, making the networks structure more flexible to resist the mechanical deformation that is caused by external mechanical loadings. When crosslinker unbinding were prohibited in the networks, the potential energy carried by crosslinkers are saturated in the period of constant deformation (red, open circle in Fig. 7-6(b)), which indicates that the room for networks remodelling was limited by the rigid cross-linkage between single filaments. On the contrary, obvious energy fluctuation can be found on the profile of potential energy at cross-linkage when crosslinkers can dynamically unbind in the network (black, open square in Fig. 7-6(b)). These fluctuations of energy profiles are related to the dynamical formation and break of crosslinkers in the networks.

In summary, during various cellular activities in mechanical environments, the network structures of F-actin cytoskeleton are naturally optimizing themselves with the help of crosslinker unbinding events. This strategy of dynamical optimization in F-actin cytoskeleton can contribute to the self-protective ability of living cells to undergo challenging mechanical conditions in complex surviving environments.

In this paper, we have implemented a crosslinker unbinding mechanisms to the CG modelling strategy in the mechanical characterization of F-actin networks. Unbinding events were allowed to happen in association to the compressive deformation of F-actin networks. We have quantified the compressive response of F-actin network with different mechanical constraints to study the underlying mechanisms. The following conclusions can be made based on the mechanism study:

- Crosslinkers unbinding events can sensitively mediate the mechanical response of F-actin networks. The networks can be softened in response to deformation due to the unbinding of crosslinkers, making F-actin networks more flexible to undergo external mechanical signals.
- The compressive stiffness of F-actin networks has dependency on the strain rates. Lower strain rate will lead to lower stiffness, which is caused by the transmission of internal stress.
- Deformation energy in F-actin networks can be dissipated efficiently with the help of crosslinker unbinding, which is significant for living cells to avoid highly stressed states under mechanical constrains.

The mechanical performance of living cells is cryptic and should not be handled by implicit material models. Granular model that involves specific physical events is more suitable for the theoretical investigation of the mechanical responses of F-actin networks in time domain. Our explicit model can qualitatively evaluate the compressive response of 3D F-actin networks in time domain while considering the effects of crosslinker unbinding. The transient crosslinker unbinding events are proved to be significant for the mechanical mediation of F-actin cytoskeleton. Under mechanical deformation, the dynamics of crosslinkers in F-actin networks can associate the dissipation of potential energy and the remodelling of networks structural, which is positive for living cells to be self-protective in constantly changing mechanical environments.

Support from the ARC Future Fellowship grant (FT100100172) is gratefully acknowledged. The authors also thank the technical supports from HPC group at QUT.

7.3 SUPPLEMENTARY MATERIAL

Supplementary Materials for: '***Physical Mechanism of the Compressive Response of F-actin Networks: Significance of Crosslinker Unbinding Events***'

7.3.1 Mechanical loading and boundary conditions

Fig. 7-7 provides the schematics of loading and boundary conditions in the modelling of compression. In the compressive modelling, the displacement of bottom surface in *z* direction was fixed and a uniform compression was applied on the top surface towards negative z direction.

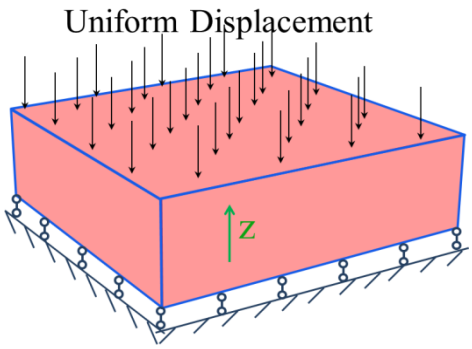

Fig. 7-7. Schematics of the boundary conditions and loadings under compressive loading condition.

7.3.2 Coarse-grained molecular dynamics model

In order to extract the dynamical behaviours of this crosslinked biological network, a highly coarse-grained (CG) granular model of F-actin networks was developed under the framework of MD method. The F-actin network was simplified to be a network of particle chains that are connected by crosslinkers and the configurations can be found in Fig. 7-8.

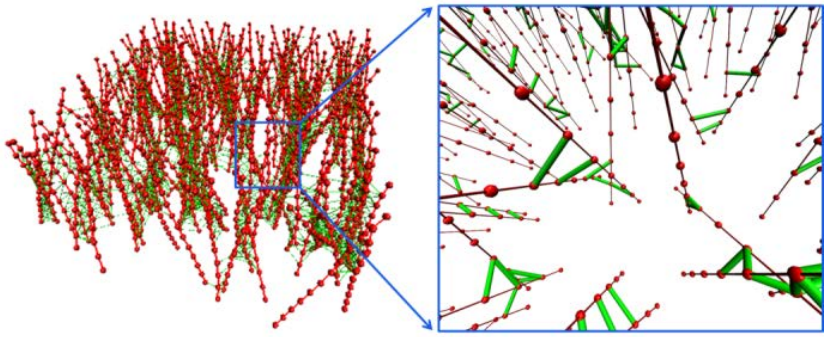

Fig. 7-8. Schematic of the 3D F-actin networks CG model

The interaction between particles in the same F-actin and at the cross-linkage between neighbouring F-actin are both assumed to be harmonic pair potential energy

[89]: $E = k(r - r_0)^2/2$, where k is the energy scale parameter, r and r_0 respectively denotes the actual distance and equilibrium distance between simulation particles. Each particle (red dot) consists of two G-actin monomers, and the distance between neighbouring particles is 5.6nm. [93] The harmonic longitudinal stiffness between adjacent particles in the same F-actin is 43pN/nm (1 μm material), which is obtained from the modulus of F-actin from experiments. [53] The angular potential of F-actin was also simplified as harmonic equations, and the stiffness constant has been characterized from all atom MD simulation, the details can be found in published work. [12] The equilibrium distance for crosslinker is 6nm, and the harmonic longitudinal stiffness of crosslinkers is 10pN/nm (1μm material), [209] which is also at the same scale with experimental characterization [210] and F-actin modulus. [53] This longitudinal (tensile) and transverse (bending) deformation properties of F-actin filament have been validated by experimental results of tensile behaviour and transverse vibration modes in previous publication. [12]

Energy equipartition theorem was employed to control the temperature, in which the kinetic energy of a simulation particle can be defined as $E_k = 3k_B T/2$, where, k_B is the Bozeman constant, T is the temperature. Langevin dynamics algorithm [150] was employed to implicitly model the effects of solvent. In the Langevin dynamics algorithm, two terms are added to the force calculation on each particle: viscous damping term due to solvent and a randomly bumping term due to temperature. The combination of these two terms is $F_d = -mv/C_d + \sqrt{mk_B T/dtC_d}$. Where, m is the mass of particle, v is the velocity of particle, dt is the time step and C_d is the damping factor with a time unit, which was chosen as 1ps in this paper.

This highly ‘coarse-grained’ F-actin model was specifically designed for the analysis of mechanical behaviours of F-actin cytoskeleton, which has similar characteristic with previous contributions to the state of the art in actin CG modelling. [197, 211] In the literature [197], each G-actin monomer was simplified as four particles with respect to the conformational domains in G-actin monomers. Differently, each simulation particle in our model consists of two G-actin monomers, which can improve the computational efficiency by ignoring the conformational details inside each G-actin monomers and the sliding between helical chains in the same F-actin. Moreover, as no binding site between G-actin and crosslinker at

atomistic level is needed, the complexity of the mechanical properties of cross-linkage can be simplified in our CG strategy. Based on these simplifications, the scale of networks model can be extended to 3D geometry that is up to hundreds of nanometres. Moreover, compared to implicit modelling methods (e.g. implicit continuum mechanics modelling) that are widely adopted in the mechanical modelling of biological material, this explicit granular simulation method also has the advantages in solving dynamical responses of soft matters with complex microstructures.

We note that, the stiffness of crosslinkers was putatively set up in this paper to understand the mechanical responses of F-actin networks that are induced by crosslinker unbinding events under compression. The parameters were generalized from experimental findings. [199, 200] The setting of crosslinker in this model was not specifically designed for a particular type of crosslinker protein. In fact, there are hundreds of crosslinker proteins in F-actin networks (e.g. Arp2/3, filamin, fascin and α-actinin), whose mechanical behaviours are different to each other and have significant dependency on their surviving environments. Our model only focused on the significance of cross-linkage break in the network, the sensitivity of F-actin network performance to crosslinker properties is not the focus of this paper. However, by specifying the mechanical behaviours of crosslinkers, our generalized model can benefit the future study in the effects of crosslinker properties, which can provide the insights into the diversity of crosslinker proteins in F-actin cytoskeleton.

7.3.3 Crosslinker unbinding model

The mechanical properties of crosslinkers were also simplified as linear elastic as introduced, whose constitutive law can be found in Fig. 7-9. As the transient unbinding of crosslinker is a result of mechanical loading,[196] the crosslinker unbinding mechanism in this model was developed based on the rupture strength of crosslinker element, which was reported to be at the scale of hundreds of pico-Newton.[199-201] In this crosslinker rupture model, once the force applied on the crosslinker exceeds 500pN, the crosslinker will unbind from the F-actin. However, mechanical testings on the critical unbinding force and the constitutive relationship of crosslinker protein are still limited and it is also arguable whether the unbinding or unfolding of actin binding protein is the dominating factor of crosslinker failure.[199] Therefore, the unbinding mechanism cannot fully account the above-

mentioned biological factors mathematically. In this model, the mechanical parameters were straight forwardly set up based on the statistical result of both crosslinker unbinding and unfolding forces.[199, 200] However, our mechanics based crosslinker unbinding model of crosslinker unbinding is capable to represent the molecular rupture behaviours happening in F-actin networks. With advanced molecular manipulator in future, specific characterization of the aforementioned mechanical parameters of crosslinker proteins can be obtained to provide more convincing quantification of the crosslinker unbinding mechanism in remodelling of F-actin networks.

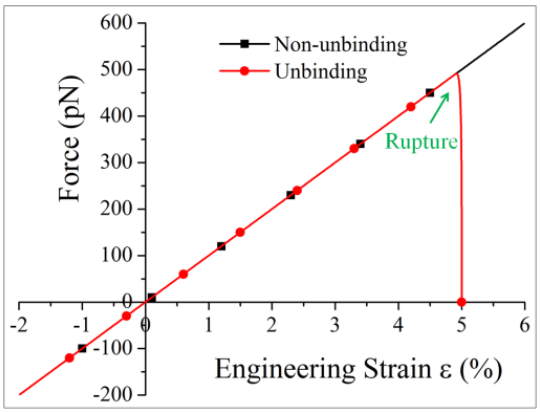

Fig. 7-9. Deformation controlled crosslinker unbinding mechanism.

7.3.4 Simulation set up

Each simulation started with a geometry optimization and 0.5 micro-second relaxation of the simulation system was performed sequentially in canonical (NVT) ensemble to get a dynamically equilibrated molecular configuration for mechanical loading simulation. The temperature was maintained at 310K by using Langevin dynamics,[150] which can implicitly consider the friction from the liquid environment as introduced. The time step in the simulation is 0.1ps. The profile of potential energy during system relaxation is given in Fig. 7-10. The potential energy is saturated after the system relaxation of 0.5μs. It should be noted that, incomplete relaxation of simulation system could also result in stress dissipation during the modelling of mechanical deformation, which is a numerical phenomenon instead of a physical property of material. Therefore, a system relaxation in a sufficient duration is necessary for a stable modelling that can exclude numerical effects in the characterization. As indicated in Fig. 7-10, for this case, the minimum relaxation duration should be no less than 0.4 μs in this model.

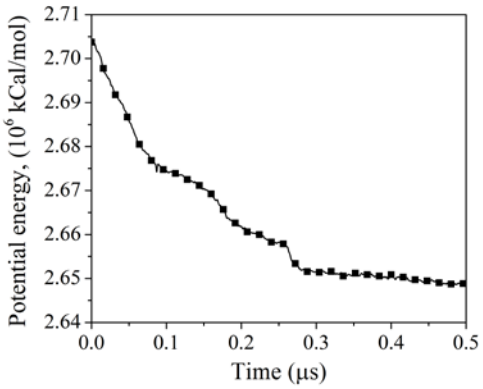

Fig. 7-10. Potential energy of the modelling system during system relaxation

The strain rates in the model can directly affect the simulation results and will be discussed in details in the following sections. The molecular simulation was performed with Large-scale Atomic/Molecular Massively Parallel Simulator (Lammps)[149] and all atomic visualizations were conducted by Visual Molecular Dynamics (VMD).[169] Each simulation would take 4 to 24 hours on 8 processers (1472x E5-2670@2.66(GHz) 64 bit Intel Xeon processor cores).

7.3.5 Crosslinker Unbinding Effects

In order to directly validate the effects of crosslinker unbinding, the configuration of the aforementioned F-actin CSK after 3μs relaxation is provided in Fig. 7-11. The loading rate in this case is 0.2/μs.

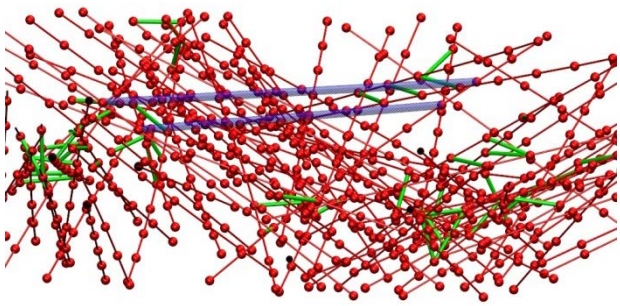

Fig. 7-11. Illustration of the crosslinker unbinding effects. Green bonds denotes the crosslinkers that are not unbinding from the network. The green transparent bond denotes the crosslinkers that are unbinding from the network.

It can be found that with the help of crosslinker unbinding, the network structure is more flexible to deform under specific large compressions. This structural flexibility is positive for F-actin CSK to get adapted to the living environments.

Chapter 8: Mechanobiological Energy Dissipation in F-actin CSK (Paper 6)

Research paper six:

Li, T., Liu, L., Hu, D., Oloyedea, A., Xiao, Y., Yarlagadda, P., and Gu, Y.T. Comprehensive Contribution of Filament Thickness and Crosslinker Failure to the Rheological Property of F-actin Cytoskeleton. (Accepted by **Cellular and Molecular Bioengineering,** DOI :10.1007/s12195-015-0382-y)

Statement of Contribution of Co-Authors for Thesis by Published Paper

The following is the format for the required declaration provided at the start of any thesis chapter which includes a co-authored publication.

The authors listed below have certified* that:

1. they meet the criteria for authorship in that they have participated in the conception, execution, or interpretation, of at least that part of the publication in their field of expertise;
2. they take public responsibility for their part of the publication, except for the responsible author who accepts overall responsibility for the publication;
3. there are no other authors of the publication according to these criteria;
4. potential conflicts of interest have been disclosed to (a) granting bodies, (b) the editor or publisher of journals or other publications, and (c) the head of the responsible academic unit, and
5. they agree to the use of the publication in the student's thesis and its publication on the QUT ePrints database consistent with any limitations set by publisher requirements.

In the case of this chapter:

This paper is accepted by 'Cellular and Molecular Bioengineering' DOI :10.1007/s12195-015-0382-y**.**

Contributor	Statement of contribution*
Tong Li Signature  Date 24/11/2014	Designed and conducted numerical model. Conducted data analysis. Wrote the manuscript.
Ling Liu	Designed and conducted numerical model. Involved in the conception and design of the project. Provided feedback on manuscript.
Dean Hu	Involved in the conception and design of the project. Provided feedback on manuscript.
Kunle Oloyede	Involved in the conception and design of the project. Provided feedback on manuscript.
Yin Xiao	Involved in the conception and design of the project. Provided feedback on manuscript.
Prasad Yarlagadda	Involved in the conception and design of the project. Provided feedback on manuscript.
YuanTong Gu*	Designed and conducted numerical model. Involved in the conception and design of the project. Assisted data analysis. Provided feedback on manuscript.

Principal Supervisor Confirmation

I have sighted email or other correspondence from all Co-authors confirming their certifying authorship.

YuanTong Gu 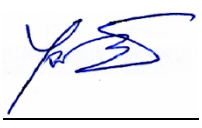 24/11/2014

Name Signature Date

8.1 ABSTRACT AND KEYWORDS

Rheological property of F-actin cytoskeleton is significant to the restructuring of cytoskeleton under a variety of cell activities. This study numerically validates the rheological property of F-actin cytoskeleton is not only a result of kinetic energy dissipation of F-actin, but also greatly depends on the configuration remodeling of networks structure. Both filament geometry and crosslinker properties can affect the remodeling of F-actin cytoskeleton. The crosslinker unbinding is found to dissipate energy and induce prominent stress relaxation in the F-actin adjacent to cross-linkages. Coupled with F-actin elasticity, the energy dissipation and stress relaxation are more significant in bundled F-actin networks than in single F-actin networks.

Keywords: F-actin networks, Crosslinker, Energy dissipation, Mechanics

8.2 INTRODUCTION

One of the most important characteristics of living eukaryotic cells is that they can adapt their mechanical properties at multiple timescales to best respond to external stimuli [8, 163]. Such changes of cellular mechanical properties are underpinned by the mechanobiological response of the cell cytoskeleton, a complex network consisting of thick (microtubule), intermediate (intermediate filament) and thin (F-actin) biological filaments. Among these cytoskeleton components, actin has been identified to serve a critical role in the mechanical responses of living cells [196, 212]. The mechanical toughness of living cells is collectively fulfilled by the high tensile stiffness of single F-actin which is typically at the GPa scale [53], and the rheological properties of actin gels which maintain the flexibility of living cells at long timescales [68]. This adaptability of cells with respect to timescale is achieved by complex mechanosensing rearrangements of F-actin cytoskeleton, which is a composite network with constantly changing chemical components. Various functional and structural proteins work in conjunction to archive the phase change of cells under physical forces, which is significant to their self-protective properties in chemical environments.

The underlying structural rearrangements in living cells can be promptly accelerated once the cells are exposed to physical forces. Subsequent cell relaxation would result in a significant phase change [18] in which the local stress relaxation of cellular structure plays critical roles. This cryptic physiological phenomenon is known to depend on the remodeling properties of F-actin cytoskeleton. Dynamically synthesized by cytoplasm [69], the F-actin in living cells has multiple states varying from single filaments to filament bundles [68]. It has been demonstrated that, in bundled F-actin networks, the potential energy slowly dissipates with the structural remodeling of the networks [171]. Compared with single F-actin networks, the F-actin bundle networks feature enhanced stiffness and strength, both favored for living cells to resist transient mechanical deformation.

As well known, one of the most typical characteristics of tumor cells is their different mechanical stiffness compared with the normal ones [1, 213]. These mechanical properties change can reflect the health of living cells. It is crucial for a living cell to mediate its stiffness and releasing the deformation energy induced by mechanical inputs. A previous experiment treated isotropically crosslinked actin

networks with glutaraldehyde to fix the binding interaction between actin and heavy meromyosin, and discovered that the critical ability of energy dissipation was significantly diminished [214]. Crosslinker unbinding events were therefore proposed to be responsible for the temporal, spontaneous stress relaxation in bundled F-actin networks. Despite the progress in the observation of actin networks remodeling at microscale [171], the resolution of in-situ experiments is still limited to directly characterize the molecular events happening during the structural remodeling of F-actin networks. To improve the understandings of the important dissipative properties of F-actin networks, a granular modelling strategy is developed to explicitly track the dynamical behaviors of F-actin networks in association with crosslinkers. This granular modelling strategy has been adopted to study the compression of F-actin CSK and explained the significance of transient crosslinker failure to the mechanical deformation properties of CSK [215]. However, the temporal scale in this granular model is limited by today's computer power and it is impossible to fully track the physiological process of CSK remodeling, which happens at the time scale of hours. In this paper, we putatively fixed the crosslinkers in CSK to achieve relatively stable configuration and then suddenly allow the crosslinkers to fail. The transient remodeling of networks is caused by the sudden crosslinker failure. The potential energy evaluations are quantified with respects to filament thickness to understand the contribution of fiber properties in the networks.

8.3 MODEL

In the present investigation, we have developed an actin networks with isotropic configuration of F-actin network. This is similar to the experimental characterization by Lieleg, et al [171], in which F-actin bundles are isotropically oriented (Fig. 1). A prescribed shear strain γ, ranging from 0.05 to 0.2, is applied to the 4μm×4μm network to mimic the boundary constraints in rheology measurements. Assuming the line elements in Fig. 1 to be single F-actin filaments or F-actin bundles generates two models, i.e. a single F-actin network model and a bundled F-actin network model. The F-actin bundle in this study is considered to have 10 parallel single filaments, which is a fair assumption based on both experimental and theoretical studies [185, 187]. It needs to be noted that, the filament length in this network model is not strictly controlled and the length ranges from a few hundreds nanometer to 4 micrometer. In the granular modeling, every two adjacent G-actin

monomers in a single filament are merged and simplified as one bead. The same model is also employed for modelling the bundled F-actin, where the harmonic elasticity is increased by 10 times to reflect the enlarged cross-section. It should be noted that, there are also crosslinker inside each F-actin bundle. However, due to the computational cost, the effects of bundle state are implicitly presented by the mechanical parameters changes. From the viewpoint of mechanics, the internal crosslinkers are of less chance to fail comparing to those crosslinkers connecting different F-actin bundles, as stress intensity usually happens near the connection. As a result, these crosslinkers are assumed to be fixed in the process of deformation to simplify the calculation. The timescale resolution is controlled as 0.1ps to fully extract the trajectory of macromolecules. More details about the model and simulation parameters can be found in supplementary material.

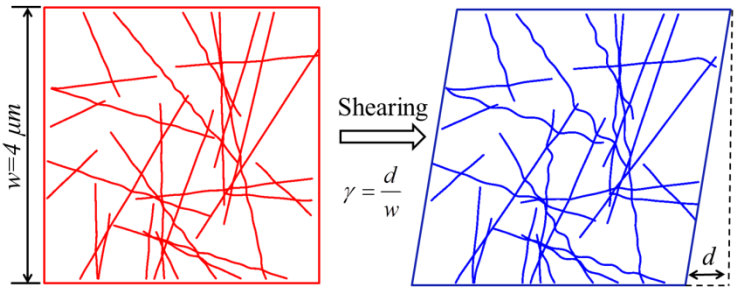

Fig. 8-1 Shear deformation of the F-actin network in modelling

During the simulations, crosslinkers are allowed to form when any two G-actin clusters (from different filaments) are separated less than 20nm. The transient crosslinker unbinding takes place when the force on the cross-linkage exceeds a threshold of σult. We have designed different modellings considering this ultimate force as constant, Gaussian distribution and uniform distribution. It has been found that, the stochasticity has effects on the mechanical performance of cytoskeleton (CSK). However, the difference between uniform distribution and Gauss distribution is not significant. Hence, this ultimate strength is assumed to follow Gauss distribution of $\sigma_{ult} \sim N(180,10)$ in this paper, which is at the level of many experimental findings such as α-actinin unfolding[210] and filamin unbinding [199, 200]. The comparison between different strength distributions can be found in the supplementary material (Figs. S3 and S4).

The sheared F-actin networks are first relaxed by geometric optimization and 20μs granular dynamics simulations (temperature of 300K) in which the crosslinkers

are not allowed to fail. This 20μs system relaxation is just numerical relaxation for us to obtain a relatively stable molecular configuration of actin networks that can be used for later dynamics simulation. After the system relaxation, network models are differently treated regarding crosslinker conditions and these dynamics simulations last for another one micro-seconds to study the evolution of stress and energy with respects to different cross-linkage conditions. For the purpose of comparison, two cases are considered for each of the modelled F-actin networks. In the first case, the crosslinkers are allowed to form and break when the corresponding criteria be satisfied, which mimics the real physical processes. In the second case, crosslinkers are not allowed to fail from the network, which simulates F-actin networks treated with glutaraldehyded [171]. The impact of crosslinker failure can be then reflected by the difference of those dissipation curves due to different crosslinker treatments. It should be noted that, even 20μs takes long computation time to accomplish, it is still not long enough for a fully system relaxation of this nature event. Slight energy dissipation still happens after the 20μs relaxation, as is provided in supplementary material (Figs. S2). However, we only focus on the difference between these curves to understand the significance of crosslinker dynamics in the stress relaxation of F-actin CSK.

The micro-second level simulations performed in this study are enabled by the highly coarse-grained granular modeling of the F-actin networks. The large timescale is very important for capturing time-dependent material properties such as stress relaxation. Moreover, by not allowing the crosslinkers to fail during the relaxation, we exclude the loading-rate effect so the present computational study can mimic the quasi-static loading in experiments.

Results and discussion

With the aforementioned explicit modelling strategy, we are able to capture the potential energy carrying ability of F-actin networks with both detachable and non-detachable crosslinkers. According to conventional thermostat theory, the kinetic energy only have dependency on the temperature, therefore, only potential energy of the network is tracked in this study to understand the energy evolution in time domain. Bundled F-actin networks and single F-actin networks have been independently studied to investigate the effects of filament thickness on the dissipative properties of F-actin networks. The profiles of potential energy in

different modeling scenarios are provided in Fig. 2. All values are normalized by the initial potential energy before stress relaxation. The normalized potential energy serves as a quantitative characterization of the energy dissipation in the network.

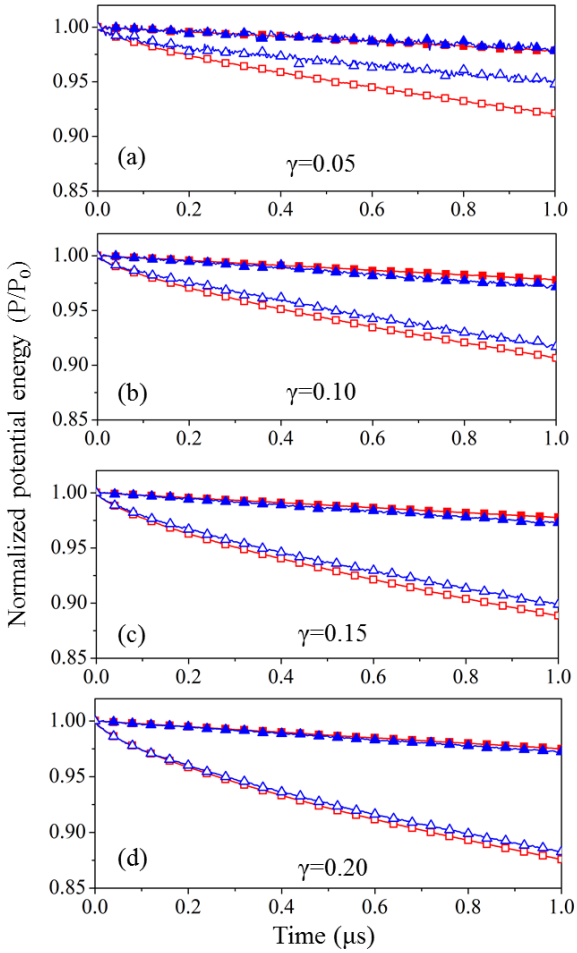

Fig. 8-2 The energy dissipation in F-actin networks under different deformation conditions. (a) to (d) relatively represent the situation of shear strain (γ) from 0.05 to 0.2. In all these sub-figures: red solid square denotes bundled F-actin networks with non-detachable crosslinkers; red open square is the bundled F-actin networks with detachable crosslinkers; blue solid triangle is single F-actin networks with non-detachable crosslinkers; blue open triangle is single F-actin networks with detachable crosslinkers.

From the modelling results, neither bundled nor single F-actin networks show significant energy dissipation when crosslinker unbinding is putatively prohibited. The dissipation of deformation energy in F-actin networks is the reflection of cellular remodeling. This inconspicuous change of energy indicates that networks with rigid crosslinkers are insufficient to release the stress caused by mechanical inputs. However, when crosslinkers are allowed to unbind, the energy dissipation rate can be 3-8 times higher, leading to about 10% energy dissipation in 1μs. We note that, the energy dissipation mainly happens on F-actin filaments or bundles, not on the

crosslinkers. For example in the simulation of single filament networks under shear strain of 0.1, the energy dissipation in the 1μs simulation is 5601.88 kcal/mol. However, the change of potential energy stored in crosslinkers is only 94.49 kcal/mol. Therefore, the energy dissipation is more related to the structural rearrangement of CSK networks, instead of the direct loss of potential energy in the crosslinkers.

In the whole shear strain range (γ=0.05~0.2), bundled F-actin networks exhibit higher energy dissipation compared to the networks of single filaments. The rate of energy dissipation has proportional dependency on the shear deformation. The more F-actin network deforms, the more deformation energy will be released by the material in unit duration. However, the rate of energy dissipation in single F-actin networks would approach bundled F-actin networks with the increase of shear deformation. We have independently extracted the potential energy carried by F-actin and crosslinkers to further explain these specific characteristics of F-actin cytoskeleton. The separated potential energy is also normalized with respects to the initial energy state for the purpose of comparison, as shown in Fig. 3. Without loss of generality, we only tracked the energy profiles for the case with a shear strain of 0.05.

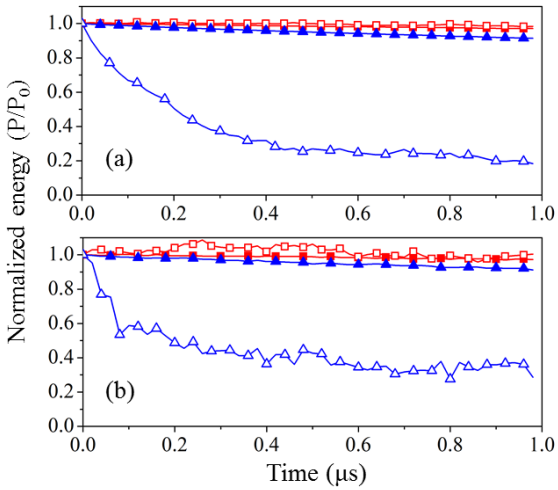

Fig. 8-1 The energy separation for F-actin and crosslinkers when γ=0.05. (a) represents a network with bundled F-actin; (b) represent a network of single filaments. In all sub-figures: red, solid square and red open square respectively denotes the energy carried by F-actin and crosslinkers on a network with non-detachable crosslinkers; blue, solid and open triangle respectively denotes the energy carried by F-actin and crosslinker on a network with detachable crosslinkers.

Neither of the deformation energy carried by F-actin or crosslinker shows significant energy dissipation phenomenon when the crosslinker unbinding events

are prohibited, which is consistent with conclusions from the energy profiles in Fig. 2. For bundled F-actin network, the potential energy carried by crosslinker reduces promptly after crosslinkers are allowed to fail in the network. This energy deduction physically illustrates that the crosslinkers are unbinding from F-actin. As the mechanical constrains (cross-linkage) in the network structure are removed due to the unbinding events, the network is more flexible to self-remodel and release the concentrated deformation energy stored near F-actin cross-linkage. Compared to networks with detachable crosslinker, the network with non-detachable crosslinkers lacks this flexibility to remodel its structure in response to external mechanical signals.

When the network is structured by single filaments, the potential energy carried by crosslinkers also has a chance to be released. However, due to the low stiffness of the element in single F-actin networks, the stress-level at cross-linkage would not be as significant as that in bundled F-actin networks. The lower stress-level promises that the deflection of filaments on the network would be flexible and not as sensitive to limited deformation as bundled F-actin networks. Correspondingly, the crosslinkers still reserve the possibility to rebind on actin after temporary unbinding, which is the reason of the increasing zigzag energy profile of crosslinkers. However, with the increase of deformation, the stress–level would be amplified at the cross-linkage, making the unbinding events of crosslinkers more irreversible and the energy releasing behaviors of single F-actin networks would approach that of bundled F-actin networks. When the strain is large (γ=0.2), the deformation energy carried by crosslinkers in single F-actin networks also present monotonous downtrend, instead of the zigzag profile when the strain is small (γ=0.05 or γ=0.1). This also explains why the energy dissipation rate of single F-actin networks can approach the performance of bundled F-actin networks with the increase of shear strain is (Fig. 2(d)). The result of energy separation of F-actin and crosslinkers under large strain conditions (γ=0.15~0.2) is consistent with our conclusions (see supplementary material, Fig. S5-S6).

The potential energy distribution at a local cross-linkage in the network is extracted to illustrate the energy dissipation process in bundled F-actin networks with different cross-linking conditions, as shown in Fig. 4. After the crosslinkers are allowed to fail in the F-actin CSK, the potential energy will be efficiently released at

the cross-linkage, which provides favorable conditions for living cells to perform flexible with respect to saturated mechanical inputs. Note that, there is still some residual potential energy at the cross-linkage, which is stored by the deformation of actin filaments and cannot be released immediately after the crosslinker breaks. However, without the constraints of crosslinkers, the F-actin network can gradually release this residual potential energy in longer duration by restructuring the cellular structures. This slow dynamics is caused by the time dependent behaviors of macromolecules and can take up to a few hours [171]. As introduced, this granular modelling strategy still keeps the high frequency oscillation of particles due to temperature ($E_k = 3k_B T/2$, Ek is the kinetic energy, kB is the Boltzmann constant and T is the absolute temperature), which weakens the ability of long-term prediction from the viewpoint of integration algorithm [159]. On the other hand, from physics, only thermal dynamic diffusion is usually insufficient for the network to overcome the barriers on energy landscape [171], living cells still need non-thermal origin of energy (such as ATP dependent protein conformational changes) to overcome the energy barriers during the phase change [18], which further limits the ability of long-term prediction of the granular modeling strategy in this letter. Therefore, we only track the transient changes of F-actin networks that are induced by transient crosslinker unbinding events instead of the long-term spontaneous responses. The degree of energy dissipation in single F-actin networks is not as significant as bundled F-actin networks. Please refer to Fig. S7 for further information of the energy distribution in single F-actin networks before and after crosslinker unbinding happens.

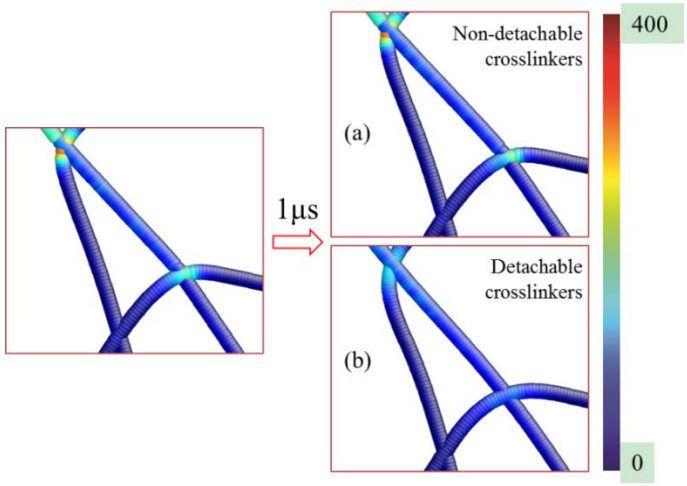

Fig. 8-2 The contour of energy distribution in bundled F-actin networks under the circumstance of γ=0.05. The energy unit for this contour is kCal/mol.

Moreover, in order to investigate the effects of crosslinker strength, another group of modeling scenarios is designed in which the rupture force of crosslinkers is decreased to 100pN from the aforementioned limit of 180pN. The energy dissipation processes are still tracked under different strain conditions. Herein, we only provide the result of small deformation condition as an illustration, which has been shown in Fig. 5. The energy dissipation efficiency of single F-actin networks is increased when the fracture limit of crosslinkers is decreased. However, this change of rupture limit of crosslinker has no significant effects on the behaviors of bundled F-actin networks. This is because the stress-levels are different between bundled F-actin networks and single F-actin networks. Bundle F-actin networks exhibits less sensitivity to the crosslinker strength as the stress–level at cross-linkage is usually sufficient to break even tougher crosslinkers. However, for single F-actin networks, the stress-level could be lower than the critical rupture force. Therefore, the unbinding events can more easily happen with the decrease of crosslinker strength in single F-actin networks. It is therefore arguable that, the rate of energy dissipation in F-actin networks depends not only on the absolute value of crosslinker rupture force, but also on the hierarchical structures of actin filament in the network. It can be concluded that, for single F-actin network, the dependency of energy dissipation ability on crosslinker strength would be weakened with the increase of shear strain (i.e. γ=0.15~0.2). This can be validated by modelling results under large strain conditions (see Figs. S8-S9).

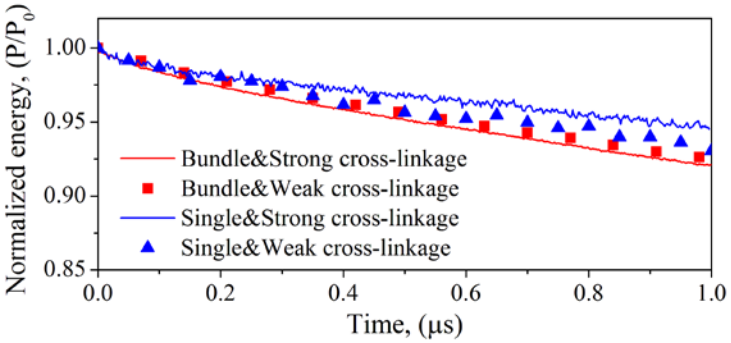

Fig. 8-3 The energy dissipation profile for both bundled and single F-actin networks when the crosslinker ultimate strength is reduced (γ=0.05). The efficiency of energy dissipation in single F-actin networks is dramatically changed compared to bundled F-actin networks.

8.4 CONCLUSION

In summary, the mechanobiological behaviors of F-actin networks are dynamical performances that depend on both intrinsic material behaviors of actin and

the physiological behaviors of various functional actin binding proteins. By using granular simulation technique, we have designed a highly coarse-grained model to understand the physical mechanisms of energy dissipation in F-actin cytoskeleton. Our investigation numerically validates the critical role that crosslinker protein plays in the process of phase changes of F-actin cytoskeleton with respect to physical forces. According to the numerical analysis, crosslinker protein in the F-actin cytoskeleton are dynamically unbinding or rebinding in response to mechanical conditions, which sensitively mediates the mechanical performances of F-actin cytoskeleton. The flexible responses of F-actin cytoskeleton induced by crosslinker unbinding events can help living cells to maintain a healthy phase while being exposed to constantly changing mechanical signals. This mechanosensing characteristic of F-actin cytoskeleton is significant to the mechanical adaptability of living cells.

8.5 ACKNOWLEDGEMENT

The authors thank Dr. Oliver Lieleg and Prof. Xi-Qiao Feng for stimulating suggestions. This work is supported by ARC Future Fellowship grant (FT100100172).

8.6 SUPPLEMENTARY MATERIAL

Supplementary Materials for 'Mechanobiological Energy Dissipation of F-actin Networks by Transient Crosslinker Unbinding'.

8.6.1 Granular model and package used

The network model in this paper is single layer and the simulations are performed with Lammps [149]. The molecular visualization are finished by VMD [169] and AtomEye [216].

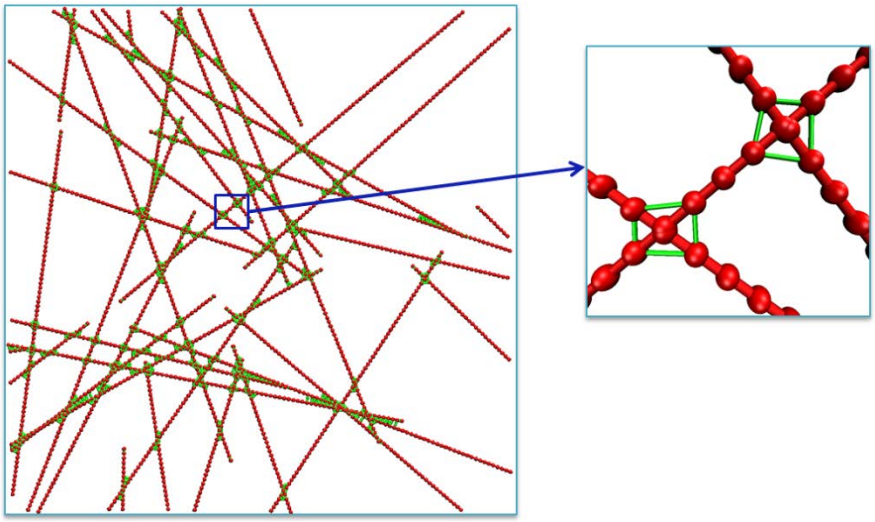

Fig. 8-3. Illustration of the single layer F-actin networks. Red dot denotes actin cluster which includes two G-actin monomers, and green bond denotes the cross-linkage

The cross-linkage positions are determined by the distance between actin clusters (red dot in Fig. 8-6). In the modelling strategy, single filaments are simplified as particle strings that are connected by F-actin crosslinkers, as shown in Fig 8-6. The interaction between actin clusters on the same F-actin and the cross-linkage between neighboring F-actin are both assumed to be harmonic pair potential energy: $E = \frac{1}{2}k(r - r_0)^2$, where k is the energy scale parameter, r and r_0 respectively denotes the actual distance and equilibrium distance between actin clusters. For G-actin clusters in the same F-actin, the stiffness is adopted as 43pN/nm (1μm material) [53], and the equivalent distance is 5.6nm. The equilibrium distance for crosslinker is 20 nm, which is larger than the equilibrium distance between G-actin clusters on the same filament. The harmonic stiffness of crosslinkers are adopted as 7pN/m (1μm material), which is at the scale of experimental characterization [210]. Langevin dynamics algorithm [150] is employed to model the friction from implicit solvent. In

the Langevin dynamics algorithm, two terms are added to the force calculation on each particle: viscous damping term due to solvent and a randomly bumping term due to temperature. The combination of these two terms is $F_d = -\frac{m}{C_d}v + \sqrt{\frac{mk_BT}{dtC_d}}$.

Where, m is the mass of particle, v is the velocity, k_B is the Bozeman constant, T is the temperature, dt is the time step and C_d is the damping factor with a time unit. In this simulation, C_d is chosen as 1ps. The size of time step in the highly coarse-grained molecular dynamics modelling is 0.1ps.

8.6.2 Energy carrying ability of F-actin and crosslinkers under different strains

The energy carried by F-actin and crosslinker are indecently quantified to track the energy flow in the networks. This energy distribution in the networks provides good evidence of the physical events related to crosslinker unbinding events. Figure s in the Supplementary Material respectively presents the energy profile under the strain conditions of γ=0.1 and γ=0.2.

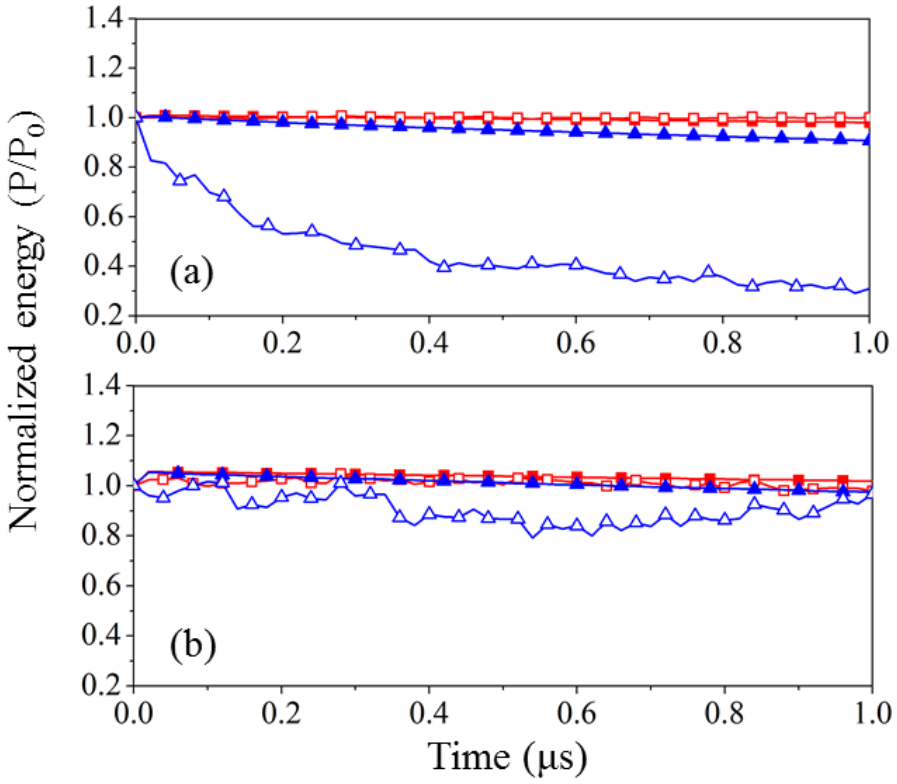

Fig. 8-4. The energy separation for F-actin and crosslinkers when γ=0.1. (a) represents a network with bundled F-actin; (b) represent a network of single filaments. In all sub-figures: red, solid square and red open square respectively denotes the energy carried by F-actin and crosslinkers on a network with non-detachable crosslinkers; blue, solid and open triangle respectively denotes the energy carried by F-actin and crosslinker on a network with detachable crosslinkers.

Similar to strain condition γ=0.05, in the case of γ=0.1, the crosslinkers on single F-actin networks still reserve possibility to rebind to the F-actin, which can constraint the F-actin in remodelling and stops the energy to be released in the networks.

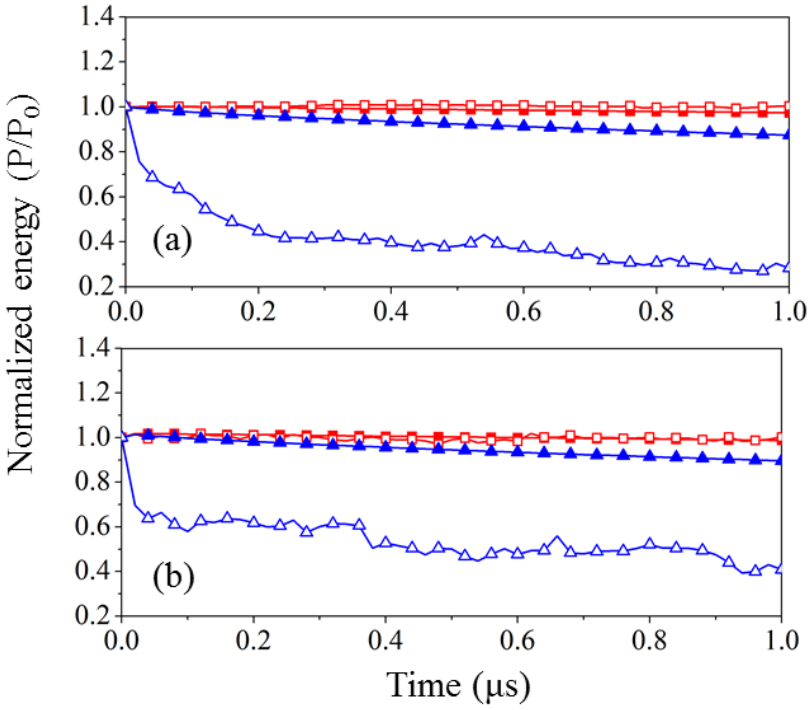

Fig. 8-5. The energy separation for F-actin and crosslinkers when γ=0.2. The details about plotting are all the same with Fig. 8-7.

However, when the deformation approaches γ=0.2, the energy carried by crosslinkers in single F-actin networks also shows monotonous down trend. This is because the deformation of cross-linkage is relatively large and lead to larger stress at the cross-linkage. The crosslinkers lost its ability to rebind to the F-actin and the relative constraints on F-actin networks is released and the energy can dissipate easily.

8.6.3 Energy concentration on the cross-linkage in the F-actin networks

We have quantified the energy distribution on the F-actin networks in the phases of both bundled and single filaments. It can be found that, the degree of energy concentration is more significant on bundled F-actin networks comparing to single filament networks. Herein, we provide the energy concentration at a typical venue in the networks to support this claim. As the contour of energy distribution of

bundled F-actin networks is already provided in the paper, herein, we only provided the energy contour of single F-actin networks when γ=0.05.

For single F-actin networks, the energy concentration also happened at the cross-linkage, however, not as significant as bundled F-actin networks. This can effectively explain the different mechanical responses of bundled and single F-actin networks.

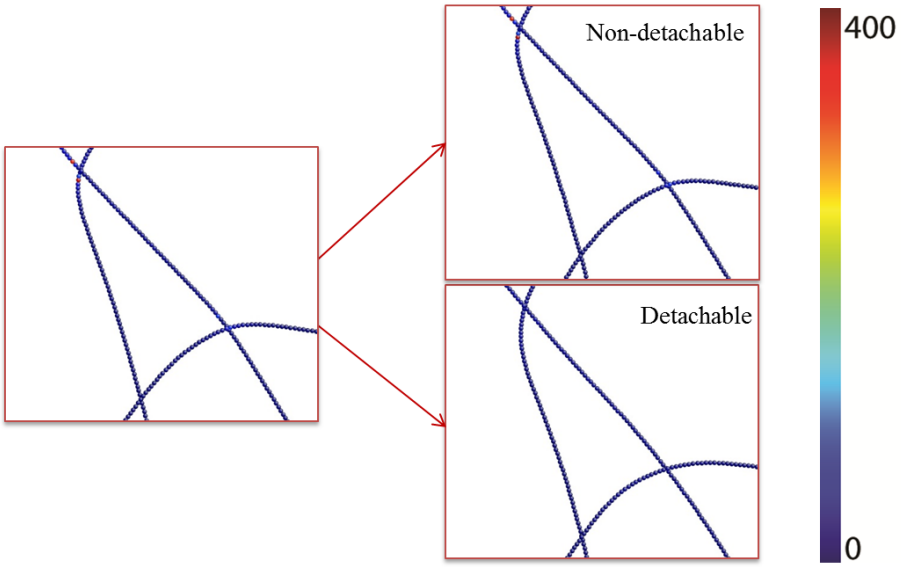

Fig. 8-6. The energy contour of single F-actin networks during energy dissipation. The energy unit for the contour is kCal/mol.

8.6.4 The mechanical response when crosslinker binding is weaken

We have investigated the effects of crosslinker strength by reducing the rupture force set up in the model. In the manuscript, it is claimed that, the crosslinker strength sensitivity would be reduced by increasing the deformation applied on the networks. Herein, we provide the modelling result of loading conditions of γ=0.1 and γ=0.2.

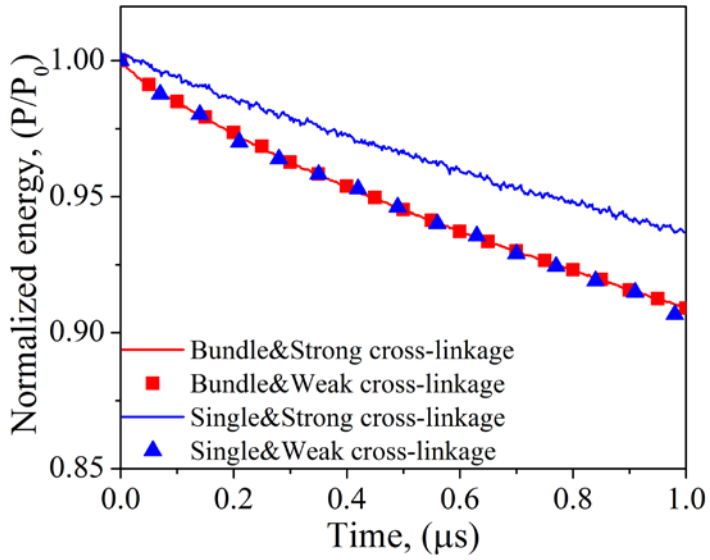

Fig. 8-7. The stress dissipation profile for both bundled and single F-actin networks when the crosslinker ultimate strength is reduced (γ=0.1). The efficiency of energy dissipation in single F-actin networks is dramatically changed comparing to bundled F-actin networks.

Different from the result of when γ=0.05, the energy dissipation efficiency of single F-actin networks approaches the bundled F-actin networks when the crosslinker strength is reduced.

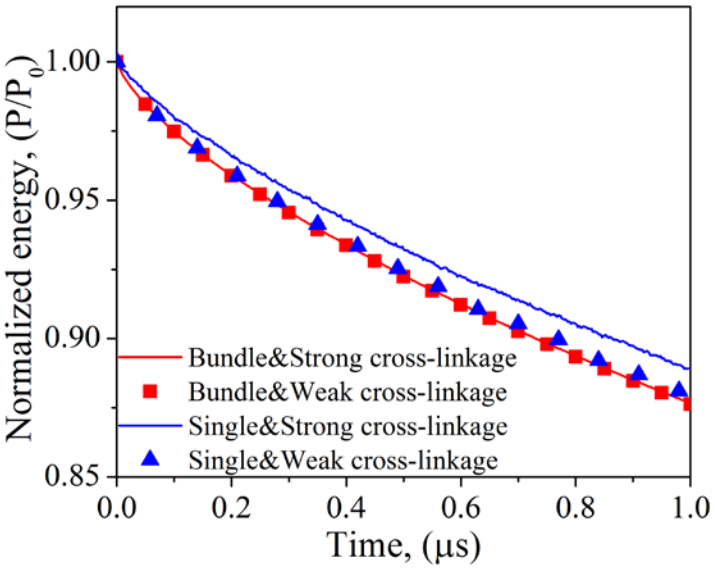

Fig. 8-8. The stress dissipation profile for both bundled and single F-actin networks when the crosslinker ultimate strength is reduced (γ=0.2). The efficiency of energy dissipation in single F-actin networks is dramatically changed comparing to bundled F-actin networks.

For the case of γ=0.2, the energy dissipation efficiency of single F-actin networks is similar to bundled F-actin networks. It is therefore arguable that, it is the degree of stress concentration that decides the sensitivity of energy dissipation efficacy to crosslinker strength.

Chapter 9: Mechanisms of muscular contraction (Paper 7)

Research paper seven:

Li, T., Gu, Y.T., Oloyede, A., 2014. Molecular Sliding Filament Model for Muscular Contraction based on Multiscale Investigation. **Science of Advanced Material** 6, 1346-1350(1345).

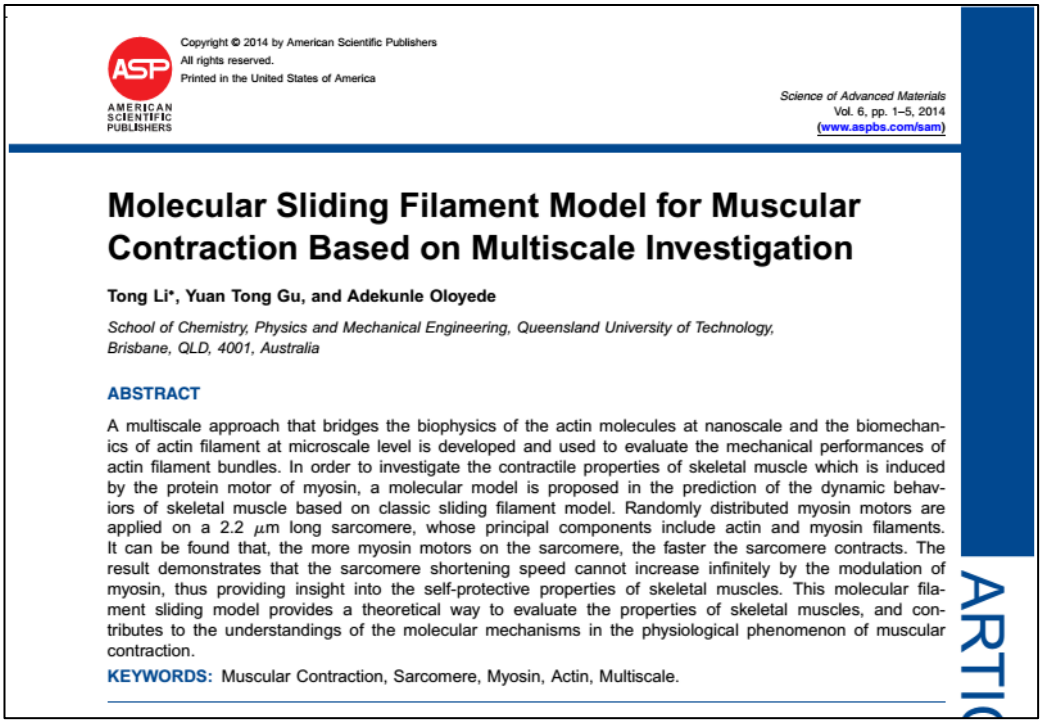

AMERICAN SCIENTIFIC PUBLISHERS

Science of Advanced Materials
Vol. 6, pp. 1–5, 2014
(www.aspbs.com/sam)

Molecular Sliding Filament Model for Muscular Contraction Based on Multiscale Investigation

Tong Li*, Yuan Tong Gu, and Adekunle Oloyede

School of Chemistry, Physics and Mechanical Engineering, Queensland University of Technology, Brisbane, QLD, 4001, Australia

ABSTRACT

A multiscale approach that bridges the biophysics of the actin molecules at nanoscale and the biomechanics of actin filament at microscale level is developed and used to evaluate the mechanical performances of actin filament bundles. In order to investigate the contractile properties of skeletal muscle which is induced by the protein motor of myosin, a molecular model is proposed in the prediction of the dynamic behaviors of skeletal muscle based on classic sliding filament model. Randomly distributed myosin motors are applied on a 2.2 μm long sarcomere, whose principal components include actin and myosin filaments. It can be found that, the more myosin motors on the sarcomere, the faster the sarcomere contracts. The result demonstrates that the sarcomere shortening speed cannot increase infinitely by the modulation of myosin, thus providing insight into the self-protective properties of skeletal muscles. This molecular filament sliding model provides a theoretical way to evaluate the properties of skeletal muscles, and contributes to the understandings of the molecular mechanisms in the physiological phenomenon of muscular contraction.

KEYWORDS: Muscular Contraction, Sarcomere, Myosin, Actin, Multiscale.

Statement of Contribution of Co-Authors for Thesis by Published Paper

The following is the format for the required declaration provided at the start of any thesis chapter which includes a co-authored publication.

The authors listed below have certified* that:

6. they meet the criteria for authorship in that they have participated in the conception, execution, or interpretation, of at least that part of the publication in their field of expertise;
7. they take public responsibility for their part of the publication, except for the responsible author who accepts overall responsibility for the publication;
8. there are no other authors of the publication according to these criteria;
9. potential conflicts of interest have been disclosed to (a) granting bodies, (b) the editor or publisher of journals or other publications, and (c) the head of the responsible academic unit, and
10. they agree to the use of the publication in the student's thesis and its publication on the QUT ePrints database consistent with any limitations set by publisher requirements.

In the case of this chapter:

Li, T., Gu, Y.T., Oloyede, A., 2014. Molecular Sliding Filament Model for Muscular Contraction based on Multiscale Investigation. Science of Advanced Material 6, 1346-1350(1345).

Contributor	Statement of contribution*
Tong Li Signature 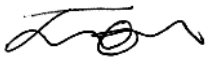 Date 24/11/2014	Designed and conducted numerical model. Conducted data analysis. Wrote the manuscript.
YuanTong Gu*	Designed and conducted numerical model. Involved in the conception and design of the project. Assisted data analysis. Provided feedback on manuscript.
Kunle Oloyede	Involved in the conception and design of the project. Provided feedback on manuscript.

Principal Supervisor Confirmation

I have sighted email or other correspondence from all Co-authors confirming their certifying authorship.

YuanTong Gu 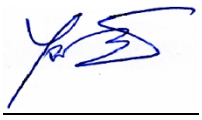 24/11/2014

Name Signature Date

9.1 ABSTRACT AND KEYWORDS

A multiscale approach that bridges the biophysics of the actin molecules at nanoscale and the biomechanics of actin filament at microscale level is developed and used to evaluate the mechanical performances of actin filament bundles. In order to investigate the contractile properties of skeletal muscle which is induced by the protein motor of myosin, a molecular model is proposed in the prediction of the dynamic behaviours of skeletal muscle based on classic sliding filament model. Randomly distributed myosin motors are applied on a 2.2μm long sarcomere, whose principal components include actin and myosin filaments. It can be found that, the more myosin motors on the sarcomere, the faster the sarcomere contracts. The result demonstrates that the sarcomere shortening speed cannot increase infinitely by the modulation of myosin, thus providing insight into the self-protective properties of skeletal muscles. This molecular filament sliding model provides a theoretical way to evaluate the properties of skeletal muscles, and contributes to the understandings of the molecular mechanisms in the physiological phenomenon of muscular contraction.

Keywords: Muscular contraction, Sarcomere, Myosin, Actin, Multiscale.

9.2 INTRODUCTION

The contraction of skeletal muscle is due to mechanisms that generate relative sliding forces between partially overlapping arrays of actin and myosin filaments [217]. The interaction between actin and myosin (motor protein) has been proposed to be the driving force for muscular contraction [218-220]. However, this classic sliding filament model is inadequate to quantify the mechanical properties of skeletal muscles during muscular contraction. In order to understand the mechanisms of muscular contraction, the quantification of the contractile force and the stroke size caused by myosin motion have been subject of focus for decades [221-223]. The contractile force generated by each myosin motor is around 6pN [224] with a stroke size up to 30nm [225]. Recently, Gabriella, et al, reported that, the skeletal muscle performance is determined by the modulation of myosin motors number, rather than the motor force or stroke size [224]. This research extends our understanding of the dynamic motion of actin filament bundles in skeletal muscle. Hence, more detailed molecular level muscular contraction mechanisms should be studied to facilitate further understanding of the role of this physiological phenomenon at the microscale level.

According to the discoveries in complex in-vivo cell mechanics, a better understanding of physiological behaviours is necessary as complementary knowledge to in-vitro cell biomechanics [62]. Due to the difficulties in the in-vivo cell experiments, biophysical models at nanoscale level, based on physical concepts, have been proposed to explain the mechanical performance of protein networks in living cells. Molecular dynamics (MD) method has been widely adopted to evaluate the properties of protein filaments [72, 106]. However, as atomistic molecular dynamics simulation is computationally time-consuming, coarse-grained molecular dynamics (CGMD) models have been proposed to analyze the biomechanical features of protein filaments [121, 122, 226]. The principal components of skeletal muscle include thin actin filaments and thick myosin filaments. In the classic sliding filament model, actin filaments are the contractile elements while myosin filaments providing the driving force for the contraction. A specific CGMD model of actin filament based on multiscale investigations of actin molecules interactions is adopted in this paper to reveal the mechanical behaviours of skeletal muscle unit: sarcomere. The biological functions of myosin motors are simplified as dynamic loads applied to

the sarcomere. The sliding interaction between actin filaments and myosin filaments are of the same mechanical properties according to experimental findings [224, 225].

9.3 CGMD MODEL OF ACTIN FILAMENT

Fig. 9-1(a) shows the 'Oda 2009' F-actin model [93] (pdb ID: 2ZWH) which is used to investigate the interaction between adjacent actin clusters. The multiscale model for actin filament is proposed based on these interactions between neighboring actin clusters and the properties of the model are extracted from the results of MD simulations, as shown in Fig. 9-1 (b). The ensuring model is used to investigate the behaviour of a two-dimensional actin filament bundle, as shown in Fig. 9-1(c).

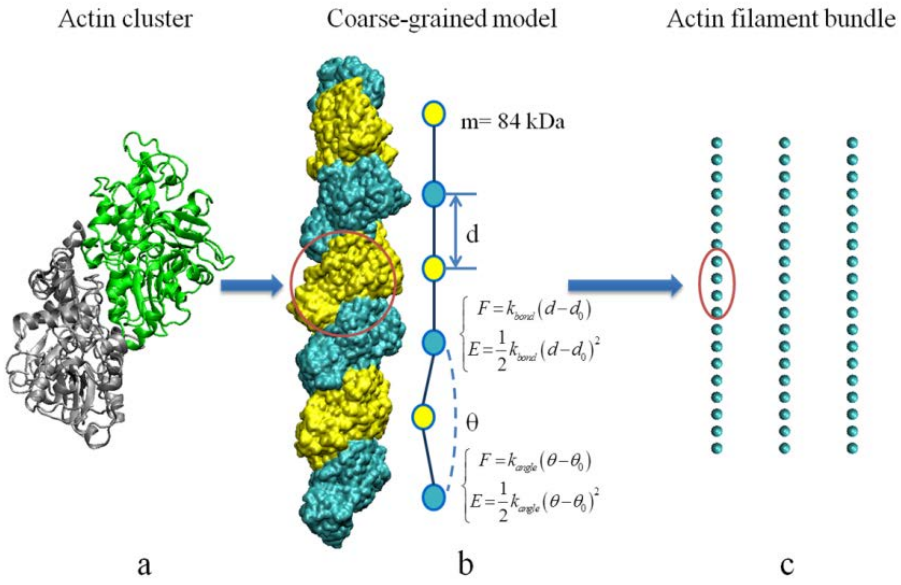

Fig. 9-1. The multiscale approach for actin filaments. a: Actin cluster which contains two 'Oda 2009' actin model. b: A single F-actin built from 'Oda 2009' actin model following the nature from globular actin to filamentous actin [93]. c: Sarcomere model built from actin filament bundles.

Every two neighbouring actin monomers from different helical chains are constituted as one particle for simplification. The equilibrium distance between adjacent particles is 5.53nm according to the crystallography of F-actin from X-ray diffraction experiments [92, 93]. The MD simulations were performed with MARTINI [108, 109] force field instead of full atom MD simulation to save computational cost. All molecular simulations are performed on GROMACS [136]. The force-displacement relationship for the actin filament is provided in Fig. 9-2.

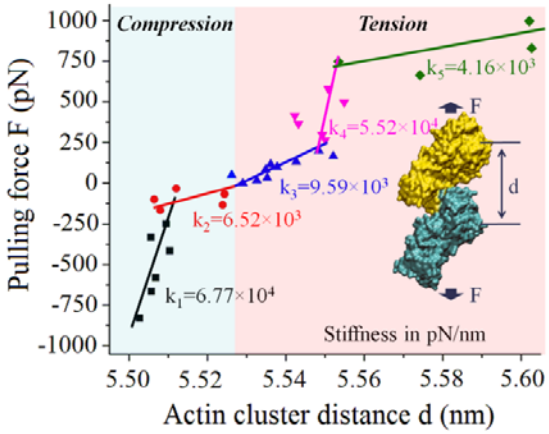

Fig. 9-2. The force-displacement relation between actin clusters from the tensile and compression numerical simulations. In the compression region, there is a stiffness transition at 5.51 nm. The balance distance for the whole curve is 5.53 nm. In the tension region, there are two stiffness transitions respectively at 5.55 nm and 5.56 nm.

9.4 MOLECULAR SLIDING FILAMENT MODEL

Electron-microscopy [227] has revealed that, striated skeletal muscle consists of a single set of longitudinal filaments that extends continuously through each sarcomere. Each sarcomere starts with one Z disk and ends at the next Z disk. Hence, our model focuses on only one sarcomere in the continuous skeletal muscle, from which the performances of the skeletal muscle is derived. Every sarcomere contains an H zone, where there is no actin filaments, leaving only myosin filaments as the structural component. Fig. 9-3 shows the structure of a striate sarcomere and the mechanism of the sliding filament model for muscular contraction. In the classic sliding filament model, the myosin heads (in purple) on myosin filament (in cyan) drag the actin filament (in red) towards the H zone, resulting in the shortening of the sarcomere.

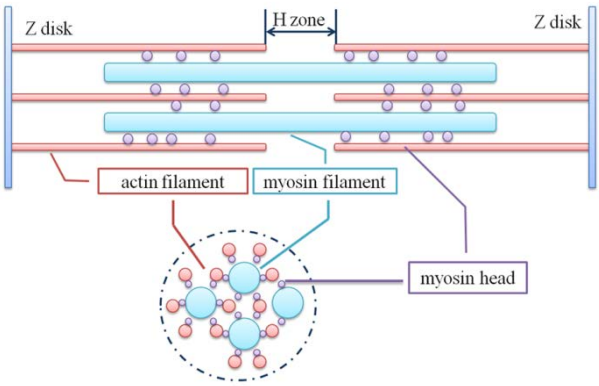

Fig. 9-3**.** Diagram of the structure of sarcomere, which contains both thick myosin filament and thin actin filament, and the myosin head induced sliding-filament model of sarcomere contraction. For convenience of representation, the structure is drawn with only one sarcomere which ends with Z disks. The dash-dot circle represents the hypothetical cross section of sarcomere.

The interaction between myosin head and actin filament is crucial to the understanding of the molecular mechanisms underlying muscular contraction according to the classic sliding filament model. Gabriella, etc. reported that, the contractile properties of skeletal muscle are determined by the modulation of myosin number, rather than the force generated or the stroke size caused by myosin. The force generated by each protein motor is approximately 6pN [224] and the stroke size is around 6nm. The most recent research provided crystallographic details at nanoscale for myosin-actin interaction [228]. The crystallography of rigor actin-tropomyosin-myosin complex (pdb ID: 4A7F) is provided in Fig. 9-4. The myosin heads and actin filament are within the scope of van der waals and Coulomb interactions. Complex domain motions only occur in myosin [228], which further verifies that it is the myosin head motion which triggers the muscular contraction by dragging the actin filament towards H zone in the molecular sliding filament model.

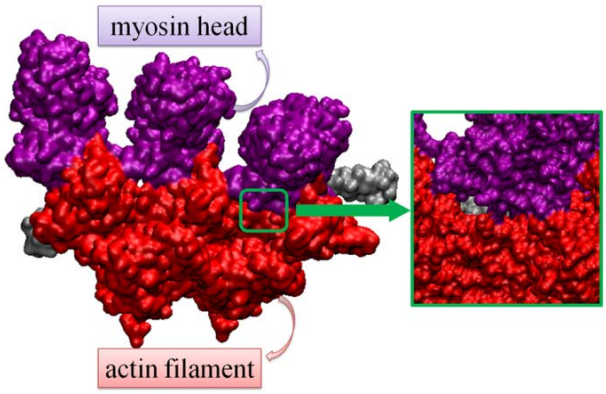

Fig. 9-4. The crystallography of rigor actin-tropomyosin-myosin complex. The purple protein clusters represent myosin heads from the myosin filament; the red protein clusters represent a part of the actin filament (five actin molecules in this example); the silver protein cluster represents tropomyosin filament which is not discussed in our current model.

It should be noted that, the tropomyosin filament also plays a role in the mechanical performance of the actin bundle. However, our model only considers the mechanical performances for pure actin filament as tropomyosin does not exist in all skeletal muscle[66]. Future study which focuses on the mechanical performances of actin filaments with tropomyosin should be conducted to adapt our molecular model to the prediction of behaviours of those tropomyosin containing skeletal muscles.

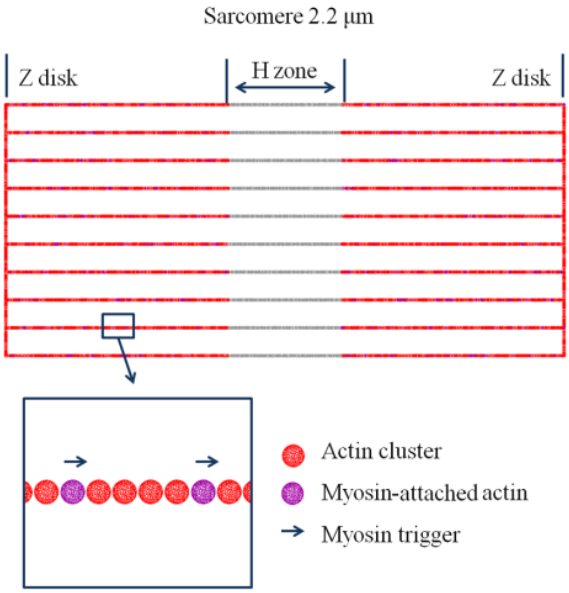

Fig. 9-5. Molecular filament sliding model for muscular contraction. The length of this typical sarcomere is assumed to be 2.2μm. The myosin motors are uniformly distributed on the sarcomere, and 10% of the actin clusters are attached by myosin motors. The distance between neighbouring actin clusters is 5.529nm.

The biophysical properties of the myosin head motion is quite complex as this physiological process is related to the chemical environments. In our particle method based molecular model, these chemical backgrounds are included by the phenomenological mechanical motions, which can be determined experimentally [224, 225, 228, 229]. Fig. 9-5 shows the molecular sliding filament model, which is based on the aforementioned multiscale investigation of actin filament's mechanical properties and the experimental results of myosin head motions.

The mechanical and biological performances of sarcomere would vary with the sarcomere length, and typical sarcomere is of a length between 1.8μm and 2.3μm [218, 230]. In order to study the physiological phenomenon of muscular contraction, the length of sarcomere in our model is assumed to be 2.2μm. However, the sarcomere length in our model is adjustable according to real problems. The largest scale of atomistic actin filament modelling cannot exceed hundreds of nanometres due to the enormous computational cost[72]. With this molecular sliding filament model, the simulation could be performed at microscale level, while the actin filament still follows nanoscale biophysical fundamentals. The attachment rate of myosin motors on the filament has dependency on the chemical environments of the sarcomere according to experiments [224]. In order to simplify the modelling, myosin motors are randomly distributed on the actin bundle in our model. However,

this random distribution would result in the uncertainty of the dynamic behaviours of sarcomere, and the distribution of myosin motors should be considered during modelling. Noting that the chemical nature of the myosin motor distribution is complex, we acknowledge that the assumption in our model that myosin motors are uniformly distributed on the actin bundle could be a significant idealization. Thus, further analysis should be conducted in the future to determine the effect of this idealization relative to the physiological responses of this system.

9.5 CASE STUDY AND DISCUSSION

In order to validate the adequacy of this molecular sliding filament model, different hypothetical cases were studied in this research. As was mentioned before, the myosin triggered mechanical motion of actin clusters can be quantified experimentally. From a classic myosin head motion study, we can find that a single myosin head moves towards the H zone by 5.3nm in 20ms on sarcomere [225]. Therefore, in our molecular sliding filament model, we define a constant velocity for the actin clusters which are attached by myosin motors besides their thermal dynamic motions. This velocity is 0.265nm/ms, which is consistent with earlier findings[8]. The CGMD simulations are performed on LAMMPS [191]. The potential field proposed in section 2 is adopted to describe the mechanical performance of actin filament bundles. The simulations are taken in microcanonical ensemble (NVE), and the temperature is controlled at 303K by using Langevin dynamics [150] algorithm, which implicitly incorporates the friction from solvent.

Five different simulations with 2%, 4%, 6%, 8% and 10% of the actin clusters attached by myosin heads respectively are represent cases 1 to 5 (Figs. 9-6 and 9-7). The sarcomere shortening speed can be extracted from our molecular sliding filament model. Fig. 9-6 shows the sarcomere length change relative to simulation time during muscular contraction in the aforementioned sarcomere models.

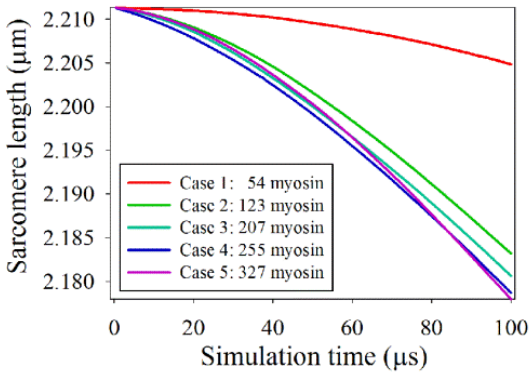

Fig. 9-6. The length of sarcomere with different myosin motor number during muscular contraction.

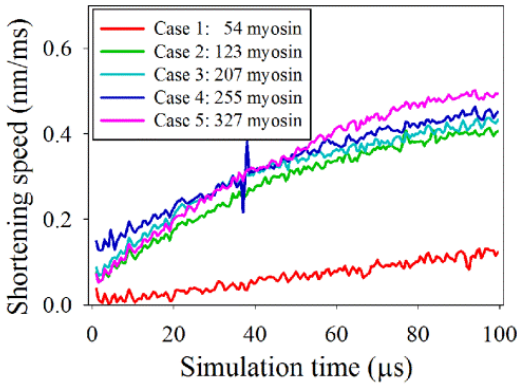

Fig. 9-7 The shortening speed of sarcomere with different myosin numbers during the muscular contraction.

The shortening speed of sarcomere increases during the muscular contraction and becomes reliable after 80μs. It can be seen that the more myosin motors are attached to the actin filament bundles, the faster this sarcomere contracts. The speed increase for sarcomere from case 4 to case 5 is not as large as the increase from case 1 to case 2, while the same amount of myosin motors are added to the simulation systems. This means that the shortening speed of sarcomere cannot increase infinitely by the modulation of myosin motors, which also verifies the self-protective properties of skeletal muscle. The skeletal muscle would adjust its contractile properties by the modulation of myosin motors, while preventing itself from being ruptured due to biological changes.

It should be noted that future studies can be conducted to understand the roles that sliding force and stroke size play in muscular contraction by using this new molecular sliding filament model.

9.6 CONCLUSION

In this paper, a new molecular sliding filament model is proposed based on classic sliding filament model and multiscale investigation of the mechanical properties of actin filaments. The mechanical behaviours of skeletal muscle due to the modulation of myosin motors are theoretically analysed with this new model. From the above studies, the following conclusions can be drawn:

- The mechanical properties of actin filaments can be evaluated by multiscale analysis from microscopic point of view.
- A new molecular sliding filament model is proposed to evaluate the microscale mechanical properties of skeletal muscle during muscular contraction.
- With this molecular sliding filament model, the relations between the modulation of myosin motors and the sarcomere shortening speed can be quantified.
- The shortening speed of sarcomere cannot increase infinitely by the modulation of myosin motors, which explains the self-protective properties of skeletal muscle.

In conclusion, this molecular sliding filament model is efficient in predicting the dynamic behaviours of sarcomere that is crucial to the understandings of the contractile properties of skeletal muscles. This molecular model provides a new means of investigating the mechanisms of muscular contraction from the microscopic point of view.

9.7 ACKNOWLEDGMENTS

Support from the ARC Future Fellowship grant (FT100100172) is gratefully acknowledged.

Chapter 10: Interaction between F-actin CSK and graphene (Paper 8)

Research paper eight:

Li, T., Oloyede, A., Gu, Y.T, 2014. Adhesive characteristics of low dimensional carbon nanomaterial on actin. **Applled Physics Letters** 104, 023702.

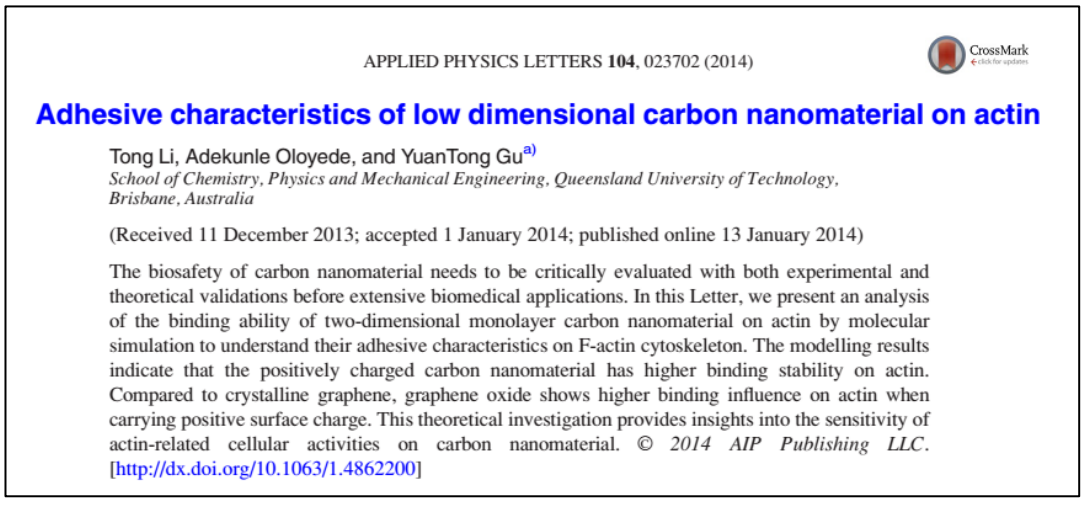

APPLIED PHYSICS LETTERS **104**, 023702 (2014)

Adhesive characteristics of low dimensional carbon nanomaterial on actin

Tong Li, Adekunle Oloyede, and YuanTong Gu[a)]
School of Chemistry, Physics and Mechanical Engineering, Queensland University of Technology, Brisbane, Australia

(Received 11 December 2013; accepted 1 January 2014; published online 13 January 2014)

The biosafety of carbon nanomaterial needs to be critically evaluated with both experimental and theoretical validations before extensive biomedical applications. In this Letter, we present an analysis of the binding ability of two-dimensional monolayer carbon nanomaterial on actin by molecular simulation to understand their adhesive characteristics on F-actin cytoskeleton. The modelling results indicate that the positively charged carbon nanomaterial has higher binding stability on actin. Compared to crystalline graphene, graphene oxide shows higher binding influence on actin when carrying positive surface charge. This theoretical investigation provides insights into the sensitivity of actin-related cellular activities on carbon nanomaterial. © *2014 AIP Publishing LLC*.
[http://dx.doi.org/10.1063/1.4862200]

Statement of Contribution of Co-Authors for Thesis by Published Paper

The following is the format for the required declaration provided at the start of any thesis chapter which includes a co-authored publication.

The authors listed below have certified* that:

11. they meet the criteria for authorship in that they have participated in the conception, execution, or interpretation, of at least that part of the publication in their field of expertise;
12. they take public responsibility for their part of the publication, except for the responsible author who accepts overall responsibility for the publication;
13. there are no other authors of the publication according to these criteria;
14. potential conflicts of interest have been disclosed to (a) granting bodies, (b) the editor or publisher of journals or other publications, and (c) the head of the responsible academic unit, and
15. they agree to the use of the publication in the student's thesis and its publication on the QUT ePrints database consistent with any limitations set by publisher requirements.

In the case of this chapter:

Li, T., Oloyede, A., Gu, Y., 2014. Adhesive characteristics of low dimensional carbon nanomaterial on actin. Applled Physics Letters 104, 023702.

Contributor	Statement of contribution*
Tong Li Signature 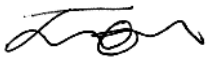 Date 24/11/2014	Designed and conducted numerical model. Conducted data analysis. Wrote the manuscript.
Kunle Oloyede	Involved in the conception and design of the project. Provided feedback on manuscript.
YuanTong Gu*	Designed and conducted numerical model. Involved in the conception and design of the project. Assisted data analysis. Provided feedback on manuscript.

Principal Supervisor Confirmation

I have sighted email or other correspondence from all Co-authors confirming their certifying authorship.

YuanTong Gu 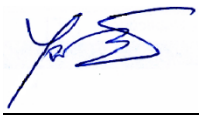 24/11/2014

Name Signature Date

10.1 ABSTRACT AND KEYWORDS

The biosafety of carbon nanomaterial needs to be critically evaluated with both experimental and theoretical validations before extensive biomedical applications. In this letter, we present an analysis of the binding ability of two-dimensional monolayer carbon nanomaterial on actin by molecular simulation to understand their adhesive characteristics on F-actin cytoskeleton. The modelling results indicate that the positively charged carbon nanomaterial has higher binding stability on actin. Compared to crystalline graphene, graphene oxide shows higher binding influence on actin when carrying positive surface charge. This theoretical investigation provides insights into the sensitivity of actin-related cellular activities on carbon nanomaterial.

Keywords: Actin, Graphene, Graphene oxide, Adhesion

10.2 ARTICLE

Inorganic materials are widely applied in biomedical engineering for tissue regeneration and surgical replacement, therefore critical insight into their biosafety is required before extensive applications in this area of growing need [231]. Among the potential inorganic biomaterials, graphene is a two-dimensional monolayer carbon nanomaterial on which carbon atoms are packed into honeycomb lattice that provides it with exceptional physical and chemical properties [232]. Graphene oxide (GO) is the disordered analogue of crystalline graphene and allows higher interaction with a wide range of organic and inorganic materials because of its oxygen-containing functional groups [233].

Various biomedical applications were proposed based on the physical and chemical properties of graphene and GO [234]. However, experiments have shown that a significant high uptake of graphene nanomaterials by tumour cells occur *in vivo* [235]. GO also exhibits dose-dependent cytotoxicity on both human and animal cells [236]. A recent experiment demonstrated that GO particles can localize on F-actin networks when living cells are cultured in GO solution [237]. Among the various bio-macromolecules, actin is the most abundant structural protein in the human body, whose biophysical behaviours can alternate cell cycles by adjusting the mechanical behaviours of living cells [163, 174]. Therefore, the adhesion of low dimensional carbon nanomaterial on F-actin networks can potentially mediate the cellular activities of living cells. It is therefore imperative to understand the adhesive characteristics of graphene/GO on actin for the purpose of reliable biomedical applications.

Experimental techniques have been utilized to investigate the micro/nanoscale interactions between living organisms and inorganic materials. For example, atomic force microscopy has been used to characterize the adhesion between living cells and an inorganic substrate [124]. However, the inorganic particles to which in cells attach are often nanoscopic in size, thereby rendering it difficult to perform physical or experimental characterization involving the micromanipulation of proteins to gain quantitative insight. In combination with experimental characterization, molecular modelling provides a powerful tool for probing the mechanism of the interaction between organic macromolecules and inorganic materials. Systematic molecular dynamics (MD) exploration have been conducted to investigate the mechanical

properties carbon nanomaterials. The small scale vibrational characteristics of multi-walled carbon nanotube have been investigate with respect to elastic and thermal properties [238, 239]. The failure properties of carbon nanotube and graphene have been further explored insightfully [240, 241]. Moreover, the mechanical instability of carbon nanomaterials have been studied at nanoscale [242, 243]. Despite these numerical explorations of the mechanical behaviours of carbon nanomaterials, their adhesive characteristics on biomolecules need further theoretical studies. ab initio and MD modelling strategies have been applied to characterize the interaction between biomolecules (e.g. protein, amino acids and nuclei acids) and inorganic materials (i.e. graphene and hydroxyapatite) [125, 126]. However, the computational investigation is very limited in understanding the mechanisms underlying the interfacial relationships between actin and an inorganic material, which is important for gaining insights of how inorganic biomaterials sensitively mediate cytoskeleton-related cellular activities in biological environments.

This letter presents a modelling technique that can assist the study of the physics of the interaction between actin and graphene/GO based on MD simulation approach. Different charge states of carbon atoms on graphene/GO are studied leading to an understanding of the sensitivity of cell adhesion to atomic charge states. This molecular level investigation provides insight that can elucidate the nature of the physical events occurring at the rigor binding sites between monolayer carbon nanomaterial and F-actin cytoskeleton.

G-actin is the macromolecular monomer of F-actin cytoskeleton that is adopted in the biophysical model presented; where the 2ZWH G-actin model [93] is selected as the starting condition in our approach. A square graphene nanomaterial is developed with armchair boundaries and an edge length of 18 nm. The general simulation model is presented in Fig. 10-1(a); the graphene/GO layer is located above the actin and approaches it during simulation/sampling. To start with, geometry minimization was performed for each macromolecule's configuration in vacuum to ensure dimensional reliability for the MD simulation. After geometry optimization, 100ps relaxation was first performed in canonical (NVT) ensemble by using Berendsen method [137], with the temperature maintained at 303 K. Subsequently, another 100ps relaxation was performed in isothermal-isobaric (NPT) ensemble at a constant pressure of 1atm by using Parinello-Rahman method [167]. A

dynamically equilibrated configuration of the molecular system can be obtained for later sampling simulations after these relaxation processes. Particle mesh Ewald (PME) method is adopted to calculate the coulomb potentials, and the cut off radius for van der Waals interaction is 2.0 nm. Umbrella sampling was performed with the stable molecular configuration obtained from aforementioned relaxation process. The sprint constant for umbrella sampling is 1000 kJ/mol·nm2. The OPLS-AA force field [166] was utilized in the MD simulation and implicit solution strategy [244] was adopted to limit the computational cost of MD simulations. All MD simulations were finished using Gromacs [136], with molecular visualization conducted with VMD [169]. The time step for all MD simulations is 2 fs and the modelling time for umbrella sampling is 1 ns. We note that the PME in the calculation of coulomb potentials significantly increased the computational cost. However, this treatment is important to the characterization of long-distance electrostatic interaction that is crucial to the phenomenon of biosorption.

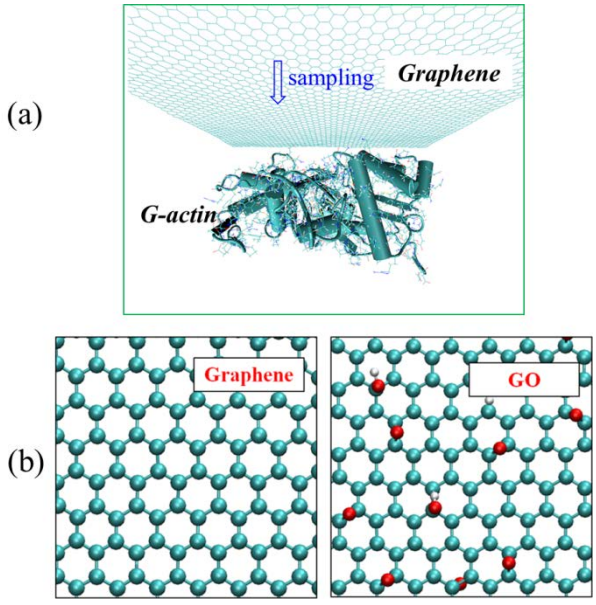

Fig. 10-1. Molecular modelling details. (a) General MD simulation model that consists of monolayer graphene and single G-actin monomer. (b) Molecular conformation of graphene and GO. Cyan dots denote carbon, red dots denote oxygen and silver dots denote hydrogen.

The non-bonded interaction energy between two sub-groups (graphene and G-actin) was extracted from the MD simulation trajectory results. This interaction energy denotes weak chemical interactions, which mainly includes van der Waals interaction, electrostatic interaction and H-bond interaction. According to the

principle of minimum potential energy, molecular configuration with lower interaction energy corresponds to higher binding stability in the process of adhesion.

Oxidization of graphene can result in various functional groups that might change the physical properties of monolayer carbon nanomaterial. In order to study how these functional groups can change the adhesive characteristics of carbon nanomaterial on G-actin, we also designed a molecular structure of monolayer honeycomb carbon materials in association with oxygen-containing functional groups (i.e. epoxy, C-OH and C-COOH), as is shown in Fig. 10-1(b).

The interaction energy profiles between G-actin and graphene/GO are provided in Fig. 10-2. When the distance between graphene and G-actin is about 1.41 nm, the potential energy is minimum, which indicates the highest binding stability of graphene on G-actin. For GO structure, the minimum interaction energy corresponds to a distance of 1.55 nm, which is larger than the distance for graphene. This difference in distance is arguably due to the additional oxygen-containing functional groups on the surface of honeycombed carbon lattice.

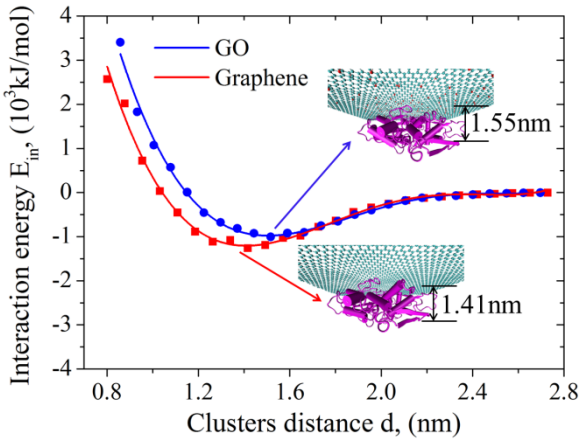

Fig. 10-2. Interaction energy between actin and carbon nanomaterials with respect to distance between nanomaterial and G-actin

When approaching the carbon nanomaterial, the additional oxygen containing groups would provide van der Waals forces to resist this approaching body. Therefore, compared to graphene, the saturated binding energy of GO occurs at a further distance from the actin. Therefore, the degree of van der Waals interaction from the carbon nanomaterial on the G-actin will be reduced.

According to chemical theories, the adherence characteristic of an inorganic material with protein in the biological environment is a function of the interaction forces between protein molecules and the surface of the inorganic material. Also the electrostatic force plays a critical role in the adhesion between protein and inorganic materials[245]. Experimental findings have verified that many biological attachments such as cell attachment and drugs binding are pH sensitive [246], as the cellular pH value can alter the electrostatic states of protein in biological environments. The normal pH value for living cells to survive in the human body is 7.4 and the isoelectric point of actin is 4.8 [247], which makes actin usually negatively charged. It is presumable that when exposed to positively charged carbon materials, actin would present higher absorption ability due to the strong electrostatic interaction.

Recent experimental findings demonstrate that the surface charge of graphene can be mediated by controlling the chemical component of the surrounding organic solution [248]. Similarly, GO can be either positively or negatively charged according to the chemical conditions [249]. It can therefore be argued that studying neutral carbon nanomaterial alone would not produce a full insight on biological adhesion. Consequently, we have developed a model that accounts for the influence of the charge condition of carbon atoms on biological adhesion. The biological environment in human body for living cells to survive is quite complex and can therefore lead to different charge states of the carbon atoms in carbon nanomaterials, leading to the conclusion that the charge carried by a carbon atom is significant in determining the nature of the contact between G-actin and graphene/GO substrates. Based on the potential charging characteristics, we have considered numerical modelling scenarios, in which the charge of each carbon atom ranges from -0.1e to +0.1e. The interaction force results for graphene in different charge states are provided in Fig. 10-3(a).

When the graphene is negatively charged, the interaction force between G-actin and graphene is smaller compared to positively charged nanomaterials, indicating that the crystalline graphene is more difficult to be localized on F-actin networks (whose principal component is actin), because they are repel the negatively charged protein as they approach the surface. For positively charged carbon atoms, the graphene shows higher attractive force on G-actin, indicating the propensity for higher binding on F-actin cytoskeleton. Similar characteristics have been found in

the study of interaction force between F-actin and positively charged lipids membrane [250].

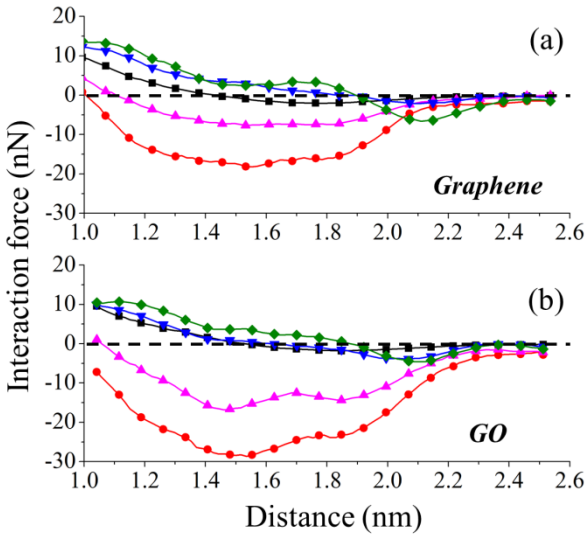

Fig. 10-3. Interaction force between G-actin and graphene/GO relative to carbon atom charge state. In both figures, red circle, magenta up triangle, black square, blue down triangle and olive diamond respectively denotes the charge states from +0.1e, +0.05e, 0e, -0.05e and -0.1e. Negative force means attracting while positive force means repelling.

The interaction force between GO and G-actin is also extracted for different carbon atom charge states and the corresponding interaction force profiles are provided in Fig. 10-3(b). Similar to crystalline graphene, positively charged carbon material also shows higher binding ability on actin compared to negatively charged material. Moreover, the binding stability increases with the positive charge of carbon atom, which indicates that, the GO absorption on F-actin cytoskeleton can be mediated by changing the charge of atoms on carbon nanomaterial.

We further compare the interaction forces between actin, graphene and GO when their carbon atoms are both positively charged (Fig. 10-4). The larger attractive force obtained from the GO model indicates that GO has a larger chance of localizing on F-actin cytoskeleton than graphene when the carbon atom equally carries positive charge, which is consistent with classic chemical theories [233] and experimental findings [237]. The absorption ability increases with the positive charge of carbon nanomaterial.

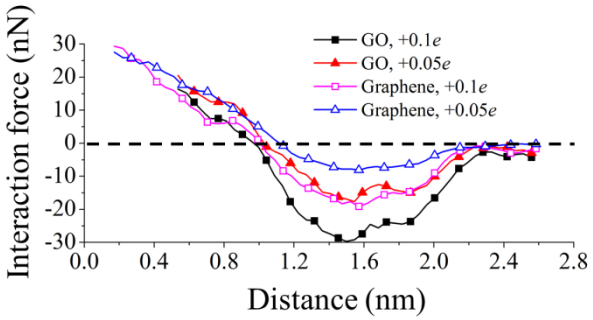

Fig. 10-4. Interaction force as a function of the distance between G-actin and positively charged GO/graphene

The molecular configuration of GO binding on actin with lowest interaction energy (highest binding stability) is extracted to study the mechanisms of the physical interaction between actin and carbon nanomaterial (Fig. 10-5). We have tracked only the H-bond and electrostatic interactions subject to the scientific knowledge that van der Waals interaction is much weaker than electrostatic bonding, and that this bond type is always present regardless of whether or not functional groups are involved. Two typical residues (e.g. GLU270 and LYS284) on actin are extracted as examples to investigate typical long range interactions. The nitrogen atom on GLU270 can potentially form an H-bond with the epoxy on carbon lattice. This H-bond interaction can partly contribute to an increase in the interaction force of carbon nanomaterial with the help of oxygen containing functional groups. Moreover, the electrostatic interaction between actin and GO is significantly responsible for the increase in the attraction force. For example, the hydrogen atom in protein residues usually carries a positive charge of 0.06~0.3e (i.e. the hydrogen atoms in LYS284), which will effectively increase the force of attraction on negatively charged carbon atoms. The oxygen atom in a functional group also carries a positive charge, which will further increase the interaction force on actin.

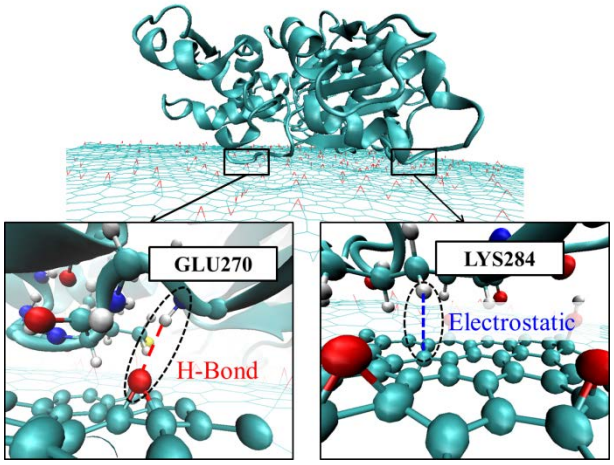

Fig. 10-5. Physical mechanism of the interaction between GO and actin. Cyan dots denote carbon, red dots denote oxygen and silver dots denote hydrogen.

However, the surface charge of nanomaterial is characterised with uncertainty, especially in respect of the oxygen containing functional groups. Therefore, more investigation about the charge states of functional groups needs to be conducted in future by both experiments and theoretical evaluation to understand the biocompability and biosorption ability of functionalized carbon nanomaterial.

In summary, the interaction between actin and low dimensional carbon nanomaterial has been investigated by molecular modelling method to understand the adhesive characteristics of monolayer carbon nanomaterial (i.e. graphene and GO) on F-actin cytoskeleton. For neutral condition, oxidation on the carbon monolayer can slightly decrease the interaction force of monolayer carbon nanomaterial on actin. The positive charge of carbon atoms on graphene/GO can significantly improve their binding ability on actin, and the binding affinity of carbon nanomaterial is proportional to the positive charge it carries.

The theoretical investigation of interaction mechanisms offers clues that can assist in exploring the biosorption and biocompability of carbon nanomaterial. In the future, with further developed sub-cellular manipulation techniques, accurate characterization of the interaction between graphene/GO and proteins can be conducted to better understand the interaction mechanisms.

The authors thank Prof. Xi-Qiao Feng for stimulating suggestions. This work is supported by the Australian Research Council Future Fellowship grant (FT100100172).

Chapter 11: Conclusions and Future Works

11.1 CONCLUSION

In this thesis, the biophysical properties of F-actin CSK were systematically investigated from the viewpoints of granular modelling across different scales. These biophysical properties include the mechanical deformation of F-actin CSK and the interaction between F-actin CSK and newly-developed inorganic materials. These biophysical modelling results can provide insight into the biological behaviours of living cells in different environments and contribute to the bio-safety evaluation of newly developed nano-biomaterials for their potential biomedical applications.

The feasibility of continuum mechanics modelling was evaluated in this study of F-actin CSK at first. It can be found that the continuum mechanics models can be conditionally used to describe the mechanical properties of F-actin CSK. Based on the characteristics of F-actin CSK, a new multiscale approach is developed to understand the biomechanics and mechanobiology of F-actin CSK. This method is designed under the bottom-up philosophy, from an atomic physics basis to a continuum mechanics description. It can provide a bridge between nanoscale biophysical and microscale biomechanical events that are occurring in the F-actin CSK. This new method can be applied in the analysis of mechanical performances of F-actin CSK, which is significant to the cellular responses under external stimuli. As a multiscale method, it provides a powerful theoretical tool to study the mechanobiology of F-actin CSK.

A new stochastic thermostat algorithm was proposed to facilitate this new, highly coarse-grained (CG) model of F-actin CSK for thermodynamic prediction. This newly developed algorithm can efficiently predict the thermodynamic properties of microfilament in association to the modelling of mechanical deformation. By using this new stochastic thermostat algorithm, computational efficiency can be significantly improved. This algorithm also provides an efficient way to investigate the biophysical properties of large-scale soft matters with typical hierarchic structures.

By using the newly developed multiscale method, the mechanical responses of F-actin CSK have been analysed, such as the mechanical stabilisation of filopodial protrusion during cell migration, the compressive responses of F-actin CSK under external pressure and the energy dissipation in F-actin CSK induced by structural

remodelling. The detailed conclusions of each of the biophysical properties of F-actin CSK are expanded as following.

The F-actin crosslinkers (fascin) were proved to be playing significant roles in enhancing the mechanical stability of ultra-slender filopodia. The modelling of transverse and axial deformation demonstrated that the bending stiffness and buckling resistance of ultra-slender filopodial protrusion are strengthened by the cross-linkage between single F-actin filaments. The dynamics modelling of a cross-linked F-actin bundle also proved that crosslinker protein functions to mediate the vibration of filopodial protrusion after transient excitation.

A linear crosslinker unbinding mechanism is implemented to the CG modelling strategy in the mechanical characterisation of F-actin CSK. Unbinding events were allowed to happen in association to the compressive deformation of F-actin networks. We have quantified the compressive response of the F-actin network with different mechanical constraints to study the underlying mechanisms. Crosslinkers' unbinding events can sensitively mediate the mechanical response of F-actin networks. The networks can be softened in response to deformation due to the unbinding of crosslinkers, making F-actin networks more flexible to undergo external mechanical stimuli. The compressive stiffness of F-actin networks has dependency on the strain rates. A lower strain rate will lead to lower stiffness, which is caused by the transmission of internal stress. Deformation energy in F-actin networks can be dissipated efficiently with the help of crosslinker unbinding, which is significant for living cells to avoid highly stressed states under mechanical constraints. Under mechanical deformation, the dynamics of crosslinkers in F-actin CSK can associate the remodelling of network structure, which is positive for living cells to be self-protective in constantly changing mechanical environments.

The mechanobiological behaviours of F-actin networks are dynamical performances that depend on both intrinsic material behaviours of actin and the physiological behaviours of various functional actin binding proteins. By using the newly-developed multiscale method, we tried to understand the physical mechanisms of energy dissipation in an F-actin cytoskeleton. Our investigation validates the critical role that crosslinker protein plays in the process of phase changes of F-actin cytoskeleton with respect to physical forces. According to the modelling analysis, crosslinker protein in the F-actin cytoskeleton are dynamically unbinding or

rebinding in response to mechanical constraints, which sensitively mediates the mechanical performances of the F-actin cytoskeleton. The flexible responses of the F-actin cytoskeleton, induced by crosslinker unbinding events, can help living cells to maintain a healthy phase while being exposed to constantly changing mechanical signals. This mechanosensing characteristic of the F-actin cytoskeleton is significant to the mechanical adaptability of living cells.

A new molecular sliding filament model for muscular contraction is developed based on a classic sliding filament model and a multiscale investigation of the mechanical properties of actin filaments. The mechanical behaviours of skeletal muscle due to the modulation of myosin motors are theoretically analysed. The mechanical properties of actin filaments can be evaluated by multiscale analysis from a microscopic point of view. With this molecular sliding filament model, the relations between the modulation of myosin motors and the sarcomere shortening speed can be quantified. The shortening speed of sarcomere cannot increase infinitely by the modulation of myosin motors, which explains the self-protective properties of skeletal muscle. This molecular sliding filament model is efficient in predicting the dynamic behaviours of sarcomere that is crucial to the understandings of the contractile properties of skeletal muscles. This molecular model provides a new means of investigating the mechanisms of muscular contraction from the microscopic point of view.

The interaction between actin and graphene was investigated in this project, which is a newly developed functional material. In summary, the interaction between actin and graphene/GO has been investigated by a molecular modelling method to understand the adhesive characteristics graphene/GO on F-actin cytoskeleton. For neutral condition, oxidation on the carbon monolayer can slightly decrease the interaction force of monolayer carbon nanomaterial on actin. The positive charge of carbon atoms on graphene/GO can significantly improve their binding ability on actin, and the binding affinity of carbon nanomaterial is proportional to the positive charge it carries. The theoretical investigation of interaction mechanisms offers clues that can assist in exploring the biosorption and biocompability of carbon nanomaterial. In the future, with further developed sub-cellular manipulation techniques, accurate characterisation of the interaction between graphene/GO and proteins need to be conducted to better understand the interaction mechanisms.

To sum up, we have developed a modelling framework for the biophysics modelling of F-actin CSK, based on the multiscale concept to overcome the difficulties of physical modelling in conventional continuum mechanics modelling and the computational challenges in all-atom molecular dynamics simulation. The thermostat algorithm was modified in this method to better predict the thermodynamic properties of F-actin CSK. This multiscale method framework has been applied to explain various physical mechanisms of F-actin CSK responses to external load and materials.

11.2 LIMITATIONS AND FUTURE WORKS

Despite the modelling findings of the biophysical properties of F-actin CSK, there still exist limitations and knowledge gaps in the physics of F-actin CSK behaviors and more work needs to be done in future to improve understanding of the biological events happening in F-actin CSK.

The extension of this research can be mainly divided into two parts: the improvement of the multiscale method and the dynamical modelling of F-actin CSK polymerisation under mechanical loading.

The nonlinear interactions between G-actin monomers were not fully presented at different loading rates. More detailed characterisations about the rate-dependent behaviours of F-actin filaments are needed to provide perdition with higher accuracy. In addition, the mechanical behaviours of F-actin have dependency on the chemical environments in which living cells survive. Therefore, the rules to adjust the modelling parameters with respect to the chemical environment will be the focus of future study on this multiscale method.

Along with the mechanical properties of static F-actin filaments, the dynamic polymerisation of F-actin filaments is proved to be significant to the physiological behaviours of F-actin CSK. However, our current model cannot predict this significant biological activity. The dynamical branching of F-actin CSK has dependency on the mechanical inputs according to statistical studies of the morphologies of F-actin in the CSK [67, 251]. This indicates that the formation of F-actin CSK is a natural optimisation of cellular structures with respect to external loadings. However, the mechanism is still cryptic to understand. Monte Carlo simulation was used to characterise the polymerisation behaviour of F-actin based on

statistical analysis [123]. However, more detailed physical laws about the way that F-actin polymerises under external stimuli should be defined to understand the process of cellular optimisation of CSK when the cell is exposed to mechanical loadings.

These methodology studies can contribute to understand the biological events that are happening in F-actin CSK. With further insight into mechanisms of physiological behaviours of F-actin CSK, it would be possible to physically control the behaviours of functional cells, which will be significant to the physical therapies of cell related diseases [1].

Bibliography

1. Jonietz, E., *Mechanics: The forces of cancer.* Nature, 2012. **491**(7425): p. S56-S57.

2. Bao, G. and S. Suresh, *Cell and molecular mechanics of biological materials.* Nat Mater, 2003. **2**(11): p. 715-725.

3. Uhal, B.D., et al., *Cell size, cell cycle, and α-smooth muscle actin expression by primary human lung fibroblasts.* American Journal of Physiology - Lung Cellular and Molecular Physiology, 1998. **275**(5): p. L998-L1005.

4. Janmey, P.A. and C.A. McCulloch, *Cell mechanics: integrating cell responses to mechanical stimuli.* Annu. Rev. Biomed. Eng., 2007. **9**: p. 1-34.

5. Kasza, K.E., et al., *The cell as a material.* Current Opinion in Cell Biology, 2007. **19**(1): p. 101-107.

6. Ingber, D.E., *Tensegrity I. Cell structure and hierarchical systems biology.* Journal of Cell Science, 2003. **116**(7): p. 1157-1173.

7. Lim, C., E. Zhou, and S. Quek, *Mechanical models for living cells--a review.* Journal of Biomechanics, 2006. **39**(2): p. 195-216.

8. Fletcher, D.A. and R.D. Mullins, *Cell mechanics and the cytoskeleton.* Nature, 2010. **463**(7280): p. 485-492.

9. Zhu, C., G. Bao, and N. Wang, *Cell mechanics: mechanical response, cell adhesion, and molecular deformation.* Annual review of biomedical engineering, 2000. **2**(1): p. 189-226.

10. Pollard, T.D. and J.A. Cooper, *Actin, a central player in cell shape and movement.* Science, 2009. **326**(5957): p. 1208-1212.

11. Li, T., et al., *Molecular investigation of the mechanical properties of single actin filaments based on vibration analyses.* Computer Methods in Biomechanics and Biomedical Engineering, 2014. **17**(6): p. 616-622.

12. Li, T., et al., *Hierarchical multiscale model for biomechanics analysis of microfilament networks.* Journal of Applied Physics, 2013. **113**(19): p. 194701-7.

13. Li, T. and Y. Gu, *A stochastic thermostat algorithm for coarse-grained thermomechanical modeling of large-scale soft matters: Theory and application to microfilaments.* Journal of Computational Physics, 2014. **263**(0): p. 177-184.

14. Li, T., A. Oloyede, and Y.T. Gu, *F-actin crosslinker: A key player for the mechanical stability of filopodial protrusion.* Journal of Applied Physics, 2013. **114**(21): p. 214701-5.

15. Wood, M.D.K., et al., *Failure of Stitched Composite L-Joints Under Tensile Loading – Experiment and Simulation.* Journal of Reinforced Plastics and Composites, 2008.

16. Li, T., Y.T. Gu, and A. Oloyede, *Molecular Sliding Filament Model for Muscular Contraction based on Multiscale Investigation.* Science of Advanced Material, 2014. **6**(7): p. 1346-1350.

17. Li, T., A. Oloyede, and Y. Gu, *Adhesive characteristics of low dimensional carbon nanomaterial on actin.* Applied Physics Letters, 2014. **104**(2): p. 023702.

18. Trepat, X., et al., *Universal physical responses to stretch in the living cell.* Nature, 2007. **447**(7144): p. 592-595.

19. Wang, N., J. Butler, and D. Ingber, *Mechanotransduction across the cell surface and through the cytoskeleton.* Science, 1993. **260**(5111): p. 1124-1127.

20. Buschmann, M.D., et al., *Mechanical compression modulates matrix biosynthesis in chondrocyte/agarose culture.* Journal of Cell Science, 1995. **108**(4): p. 1497-1508.

21. Liu, S.Q., *Influence of Tensile Strain on Smooth Muscle Cell Orientation in Rat Blood Vessels.* Journal of Biomechanical Engineering, 1998. **120**(3): p. 313-320.

22. Wang, H., et al., *Cell orientation response to cyclically deformed substrates: Experimental validation of a cell model.* Journal of Biomechanics, 1995. **28**(12): p. 1543-1552.

23. Du, J., et al., *Integrin activation and internalization on soft ECM as a mechanism of induction of stem cell differentiation by ECM elasticity.* Proceedings of the National Academy of Sciences, 2011. **108**(23): p. 9466.

24. Van Vliet, K.J., G. Bao, and S. Suresh, *The biomechanics toolbox: experimental approaches for living cells and biomolecules.* Acta Materialia, 2003. **51**(19): p. 5881-5905.

25. Crick, F.H.C. and A.F.W. Hughes, *The physical properties of cytoplasm: A study by means of the magnetic particle method Part I. Experimental.* Experimental Cell Research, 1950. **1**(1): p. 37-80.

26. Mitchison, J.M. and M.M. Swann, *The Mechanical Properties of the Cell Surface: I. The Cell Elastimeter.* Journal of Experimental Biology, 1954. **31**(3): p. 443-460.

27. Hochmuth, R.M., *Micropipette aspiration of living cells.* Journal of Biomechanics, 2000. **33**(1): p. 15-22.

28. Petersen, N.O., W.B. McConnaughey, and E.L. Elson, *Dependence of locally measured cellular deformability on position on the cell, temperature, and cytochalasin B.* Proceedings of the National Academy of Sciences, 1982. **79**(17): p. 5327-5331.

29. Geerts, H., et al., *Nanovid tracking: a new automatic method for the study of mobility in living cells based on colloidal gold and video microscopy.* Biophysical Journal, 1987. **52**(5): p. 775-782.

30. Maksym, G.N., et al., *Mechanical properties of cultured human airway smooth muscle cells from 0.05 to 0.4 Hz.* Journal of Applied Physiology, 2000. **89**(4): p. 1619-1632.

31. Hoh, J.H. and C.A. Schoenenberger, *Surface morphology and mechanical properties of MDCK monolayers by atomic force microscopy.* Journal of Cell Science, 1994. **107**(5): p. 1105-1114.

32. Thoumine, O. and A. Ott, *Time scale dependent viscoelastic and contractile regimes in fibroblasts probed by microplate manipulation.* Journal of Cell Science, 1997. **110**(17): p. 2109-2116.

33. Lo, C.-M. and J. Ferrier, *Electrically measuring viscoelastic parameters of adherent cell layers under controlled magnetic forces.* European Biophysics Journal, 1999. **28**(2): p. 112-118.

34. Hénon, S., et al., *A New Determination of the Shear Modulus of the Human Erythrocyte Membrane Using Optical Tweezers.* Biophysical Journal, 1999. **76**(2): p. 1145-1151.

35. Dao, M., C.T. Lim, and S. Suresh, *Mechanics of the human red blood cell deformed by optical tweezers.* Journal of the Mechanics and Physics of Solids, 2003. **51**(11–12): p. 2259-2280.

36. Miyazaki, H., Y. Hasegawa, and K. Hayashi, *A newly designed tensile tester for cells and its application to fibroblasts.* Journal of Biomechanics, 2000. **33**(1): p. 97-104.

37. Schmid-Schönbein, G.W., et al., *Passive mechanical properties of human leukocytes.* Biophysical Journal, 1981. **36**(1): p. 243-256.

38. Fabry, B., et al., *Scaling the Microrheology of Living Cells.* Physical Review Letters, 2001. **87**(14): p. 148102.

39. Nguyen, T.D. and Y. Gu, *Exploration of mechanisms underlying the strain-rate-dependent mechanical property of single chondrocytes.* Applied Physics Letters, 2014. **104**(18): p. -.

40. *Passive material behavior of granulocytes based on large deformation and recovery after deformation tests*, ed. E. Evans and B. Kukan. Vol. 64. 1984. 1028-1035.

41. Dong, C., R. Skalak, and K. Sung, *Cytoplasmic rheology of passive neutrophils.* Biorheology, 1990. **28**(6): p. 557-567.

42. Tsai, M.A., R.S. Frank, and R.E. Waugh, *Passive mechanical behavior of human neutrophils: power-law fluid.* Biophysical Journal, 1993. **65**(5): p. 2078-2088.

43. Dong, C. and R. Skalak, *Leukocyte deformability: Finite element modeling of large viscoelastic deformation.* Journal of Theoretical Biology, 1992. **158**(2): p. 173-193.

44. Mow, V.C., et al., *Biphasic Creep and Stress Relaxation of Articular Cartilage in Compression: Theory and Experiments.* Journal of Biomechanical Engineering, 1980. **102**(1): p. 73-84.

45. Shin, D. and K. Athanasiou, *Cytoindentation for obtaining cell biomechanical properties.* Journal of Orthopaedic Research, 1999. **17**(6): p. 880-890.

46. Charras, G.T. and M.A. Horton, *Single Cell Mechanotransduction and Its Modulation Analyzed by Atomic Force Microscope Indentation.* Biophysical Journal, 2002. **82**(6): p. 2970-2981.

47. Pollard, T.D. and G.G. Borisy, *Cellular motility driven by assembly and disassembly of actin filaments.* Cell, 2003. **112**(4): p. 453-465.

48. Wessells, N., et al., *Microfilaments in cellular and developmental processes.* Science, 1971. **171**(3967): p. 135.

49. Wrighton, K.H., *Cytoskeleton: JMY: actin up in cell motility.* Nature Reviews Molecular Cell Biology, 2009. **10**(5): p. 304-304.

50. Frixione, E., *Recurring views on the structure and function of the cytoskeleton: A 300 Year Epic.* Cell motility and the cytoskeleton, 2000. **46**(2): p. 73-94.

51. Murakami, K., et al., *Structural basis for actin assembly, activation of ATP hydrolysis, and delayed phosphate release.* Cell, 2010. **143**(2): p. 275-287.

52. Kim, S. and P.A. Coulombe, *Emerging role for the cytoskeleton as an organizer and regulator of translation.* Nature Reviews Molecular Cell Biology, 2010. **11**(1): p. 75-81.

53. Kojima, H., A. Ishijima, and T. Yanagida, *Direct measurement of stiffness of single actin filaments with and without tropomyosin by in vitro nanomanipulation.* Proceedings of the National Academy of Sciences, 1994. **91**(26): p. 12962-12966.

54. Yasuda, R., H. Miyata, and K. Kinosita Jr, *Direct measurement of the torsional rigidity of single actin filaments.* Journal of molecular biology, 1996. **263**(2): p. 227-236.

55. Dupuis, D.E., et al., *Actin filament mechanics in the laser trap.* Journal of muscle research and cell motility, 1997. **18**(1): p. 17-30.

56. Gittes, F., et al., *Flexural rigidity of microtubules and actin filaments measured from thermal fluctuations in shape.* The Journal of cell biology, 1993. **120**(4): p. 923-934.

57. Higuchi, H., T. Yanagida, and Y.E. Goldman, *Compliance of thin filaments in skinned fibers of rabbit skeletal muscle.* Biophysical journal, 1995. **69**(3): p. 1000-1010.

58. Janmey, P.A., J.X. Tang, and C.F. Schmidt, *Actin filaments.* Supramolecular Assemblies, 2001.

59. Åström, J.A., et al., *Strain hardening, avalanches, and strain softening in dense cross-linked actin networks.* Physical Review E, 2008. **77**(5): p. 051913.

60. Chaudhuri, O., S.H. Parekh, and D.A. Fletcher, *Reversible stress softening of actin networks.* Nature, 2007. **445**(7125): p. 295.

61. Gardel, M., et al., *Elastic behavior of cross-linked and bundled actin networks.* Science, 2004. **304**(5675): p. 1301-1305.

62. Gardel, M.L., et al., *Stress-Dependent Elasticity of Composite Actin Networks as a Model for Cell Behavior.* Physical Review Letters, 2006. **96**(8): p. 088102.

63. Janmey, P.A., et al., *Viscoelasticity of F-actin and F-actin/gelsolin complexes.* Biochemistry, 1988. **27**(21): p. 8218-8227.

64. Liu, X. and G.H. Pollack, *Mechanics of F-actin characterized with microfabricated cantilevers.* Biophysical journal, 2002. **83**(5): p. 2705-2715.

65. Huxley, H.E., et al., *X-ray diffraction measurements of the extensibility of actin and myosin filaments in contracting muscle.* Biophysical journal, 1994. **67**(6): p. 2411-2421.

66. Sharma, S., et al., *Atomic force microscopy reveals drebrin induced remodeling of F-actin with subnanometer resolution.* Nano letters, 2011.

67. Risca, V.I., et al., *Actin filament curvature biases branching direction.* Proceedings of the National Academy of Sciences, 2012. **109**(8): p. 2913-2918.

68. Lieleg, O., M.M.A.E. Claessens, and A.R. Bausch, *Structure and dynamics of cross-linked actin networks.* Soft Matter, 2010. **6**(2): p. 218-225.

69. Luo, T., et al., *Molecular mechanisms of cellular mechanosensing.* Nat Mater, 2013. **12**(11): p. 1064-1071.

70. Ghoniem†, N.M., et al., *Multiscale modelling of nanomechanics and micromechanics: an overview.* Philosophical Magazine, 2003. **83**(31-34): p. 3475-3528.

71. Bausch, A.R. and K. Kroy, *A bottom-up approach to cell mechanics.* Nat Phys, 2006. **2**(4): p. 231-238.

72. Splettstoesser, T., et al., *Structural modeling and molecular dynamics simulation of the actin filament.* Proteins: Structure, Function, and Bioinformatics, 2011.

73. Rudd, R.E. and J.Q. Broughton, *Coarse-grained molecular dynamics and the atomic limit of finite elements.* Physical Review B, 1998. **58**: p. 5893-5896.

74. Tozzini, V., *Coarse-grained models for proteins.* Current opinion in structural biology, 2005. **15**(2): p. 144-150.

75. Ortiz, C. and M.C. Boyce, *Bioinspired Structural Materials.* Science, 2008. **319**(5866): p. 1053-1054.

76. Omary, M.B., et al., *'Heads and tails' of intermediate filament phosphorylation: multiple sites and functional insights.* Trends in biochemical sciences, 2006. **31**(7): p. 383-394.

77. Wang, N. and D. Stamenovic, *Mechanics of vimentin intermediate filaments*, in *Mechanics of Elastic Biomolecules*. 2003, Springer. p. 535-540.

78. Wang, N. and D. Stamenović, *Contribution of intermediate filaments to cell stiffness, stiffening, and growth.* American Journal of Physiology - Cell Physiology, 2000. **279**(1): p. C188-C194.

79. Herrmann, H., et al., *Intermediate filaments: from cell architecture to nanomechanics.* Nat Rev Mol Cell Biol, 2007. **8**(7): p. 562-573.

80. Kreplak, L., et al., *Exploring the Mechanical Behavior of Single Intermediate Filaments.* Journal of Molecular Biology, 2005. **354**(3): p. 569-577.

81. Qin, Z. and M. Buehler, *Computational and theoretical modeling of intermediate filament networks: Structure, mechanics and disease.* Acta Mechanica Sinica, 2012. **28**(4): p. 941-950.

82. Qin, Z., M.J. Buehler, and L. Kreplak, *A multi-scale approach to understand the mechanobiology of intermediate filaments.* Journal of Biomechanics, 2010. **43**(1): p. 15-22.

83. Ackbarow, T., et al., *Alpha-Helical Protein Networks Are Self-Protective and Flaw-Tolerant.* PLoS ONE, 2009. **4**(6): p. e6015.

84. Shen, J.-W., et al., *Molecular simulation of protein adsorption and desorption on hydroxyapatite surfaces.* Biomaterials, 2008. **29**(5): p. 513-532.

85. Sun, Y., C. Zhang, and K.M. Liew, *Higher-order Constitutive Relationship for Microtubules Based on the Higher-order Cauchy-Born Rule.* Procedia Engineering, 2012. **31**(0): p. 973-978.

86. Hatami-Marbini, H., A. Shahsavari, and R.C. Picu, *Multiscale modeling of semiflexible random fibrous structures.* Computer-Aided Design, 2013. **45**(1): p. 77-83.

87. Peter, S.J. and M.R.K. Mofrad, *Computational Modeling of Axonal Microtubule Bundles under Tension.* Biophysical Journal, 2012. **102**(4): p. 749-757.

88. Theisen, K.E., et al., *Multiscale Modeling of the Nanomechanics of Microtubule Protofilaments.* The Journal of Physical Chemistry B, 2012. **116**(29): p. 8545-8555.

89. Ji, X.-Y. and X.-Q. Feng, *Coarse-grained mechanochemical model for simulating the dynamic behavior of microtubules.* Physical Review E, 2011. **84**(3): p. 031933.

90. Straub, F. and G. Feuer, *Adenosinetriphosphate the functional group of actin.* Biochimica et Biophysica Acta, 1950. **4**: p. 455-470.

91. Holmes, K.C., et al., *Atomic model of the actin filament.* Nature, 1990. **347**(6288): p. 44-49.

92. Holmes, K.C., *Structural biology: actin in a twist.* Nature, 2009. **457**(7228): p. 389-390.

93. Oda, T., et al., *The nature of the globular-to fibrous-actin transition.* Nature, 2009. **457**(7228): p. 441-445.

94. Oda, T. and Y. Maéda, *Multiple Conformations of F-actin.* Structure, 2010. **18**(7): p. 761-767.

95. Dominguez, R. and K.C. Holmes, *The Structure of G and F Actin Filaments.* Annual Review of Biophysics, 2011. **40**(1): p. 169-186.

96. Fujii, T., et al., *Direct visualization of secondary structures of F-actin by electron cryomicroscopy.* Nature, 2010.

97. Akola, J. and R. Jones, *Density functional calculations of ATP systems. 1. Crystalline ATP hydrates and related molecules.* The Journal of Physical Chemistry B, 2006. **110**(15): p. 8110-8120.

98. Akola, J. and R.O. Jones, *Density Functional Calculations of ATP Systems. 2. ATP Hydrolysis at the Active Site of Actin.* The Journal of Physical Chemistry B, 2006. **110**(15): p. 8121-8129.

99. McCammon, J.A., B.R. Gelin, and M. Karplus, *Dynamics of folded proteins.* Nature, 1977. **267**(5612): p. 585-590.

100. Herschbach, D.R., *Molecular dynamics of elementary chemical reactions (Nobel lecture).* Angewandte Chemie International Edition in English, 1987. **26**(12): p. 1221-1243.

101. Karplus, M., *Molecular dynamics simulations of biomolecules.* Accounts of Chemical Research, 2002. **35**(6): p. 321-323.

102. Kolahi, K.S. and M.R.K. Mofrad, *Molecular mechanics of filamin's rod domain.* Biophysical journal, 2008. **94**(3): p. 1075-1083.

103. Splettstoesser, T., et al., *A Comparison of Actin Filament Models by Molecular Dynamics Simulation.* Biophysical journal, 2010. **98**: p. 154.

104. Chu, J.W. and G.A. Voth, *Allostery of actin filaments: molecular dynamics simulations and coarse-grained analysis.* Proceedings of the National Academy of Sciences of the United States of America, 2005. **102**(37): p. 13111.

105. Pfaendtner, J., et al., *Structure and Dynamics of the Actin Filament.* Journal of molecular biology, 2010. **396**(2): p. 252-263.

106. Matsushita, S., et al., *Evaluation of extensional and torsional stiffness of single actin filaments by molecular dynamics analysis.* Journal of Biomechanics, 2010. **43**(16): p. 3162-3167.

107. Deriu, M.A., et al., *Biomechanics of actin filaments: A computational multi-level study.* Journal of Biomechanics, 2011. **44**(4): p. 630-636.

108. Marrink, S.J. and A.E. Mark, *Molecular dynamics simulation of the formation, structure, and dynamics of small phospholipid vesicles.* Journal of the American Chemical Society, 2003. **125**(49): p. 15233-15242.

109. Marrink, S.J., et al., *The MARTINI force field: coarse grained model for biomolecular simulations.* The Journal of Physical Chemistry B, 2007. **111**(27): p. 7812-7824.

110. Stricker, J., T. Falzone, and M.L. Gardel, *Mechanics of the F-actin cytoskeleton.* Journal of Biomechanics, 2010. **43**(1): p. 9-14.

111. MacKintosh, F.C., J. Käs, and P.A. Janmey, *Elasticity of Semiflexible Biopolymer Networks.* Physical Review Letters, 1995. **75**(24): p. 4425-4428.

112. Janmey, P.A., et al., *Resemblance of actin-binding protein/actin gels to covalently crosslinked networks.* Nature, 1990. **345**(6270): p. 89-92.

113. Wachsstock, D., W. Schwarz, and T. Pollard, *Cross-linker dynamics determine the mechanical properties of actin gels.* Biophysical journal, 1994. **66**(3): p. 801-809.

114. You, L., et al., *A model for strain amplification in the actin cytoskeleton of osteocytes due to fluid drag on pericellular matrix.* Journal of Biomechanics, 2001. **34**(11): p. 1375-1386.

115. Mogilner, A. and G. Oster, *Force generation by actin polymerization II: the elastic ratchet and tethered filaments.* Biophysical journal, 2003. **84**(3): p. 1591-1605.

116. Chen, P. and V.B. Shenoy, *Strain stiffening induced by molecular motors in active crosslinked biopolymer networks.* Soft Matter, 2010. **7**(2): p. 355-358.

117. Ghoniem, N.M., et al., *Multiscale modelling of nanomechanics and micromechanics: an overview.* Philosophical Magazine, 2003. **83**(31-34): p. 3475-3528.

118. Bausch, A. and K. Kroy, *A bottom-up approach to cell mechanics.* Nature Physics, 2006. **2**(4): p. 231-238.

119. Ayton, G.S., W.G. Noid, and G.A. Voth, *Multiscale modeling of biomolecular systems: in serial and in parallel.* Current opinion in structural biology, 2007. **17**(2): p. 192-198.

120. Yamaoka, H., et al., *Multiscale modeling and mechanics of filamentous actin cytoskeleton.* Biomechanics and Modeling in Mechanobiology, 2012: p. 1-12.

121. Chu, J.W. and G.A. Voth, *Coarse-grained modeling of the actin filament derived from atomistic-scale simulations.* Biophysical journal, 2006. **90**(5): p. 1572-1582.

122. Deriu, M.A., et al., *Multiscale modelling of cellular actin filaments: From atomistic molecular to coarse grained dynamics.* Proteins: Structure, Function, and Bioinformatics, 2012.

123. Shimada, Y., et al., *Coarse-grained modeling and simulation of actin filament behavior based on Brownian dynamics method.* Molecular & Cellular Biomechanics, 2009. **6**(3): p. 161-174.

124. Benoit, L. and N. Alice, *Physically based principles of cell adhesion mechanosensitivity in tissues.* Reports on Progress in Physics, 2012. **75**(11): p. 116601.

125. Rimola, A., et al., *Ab Initio Modeling of Protein/Biomaterial Interactions: Glycine Adsorption at Hydroxyapatite Surfaces.* Journal of the American Chemical Society, 2008. **130**(48): p. 16181-16183.

126. Jin, K., X. Feng, and Z. Xu, *Mechanical Properties of Chitin–Protein Interfaces: A Molecular Dynamics Study.* BioNanoScience, 2013. **3**(3): p. 312-320.

127. Mayes, J.S. and A.C. Hansen, *A comparison of multicontinuum theory based failure simulation with experimental results.* Composites Science and Technology, 2004. **64**(3–4): p. 517-527.

128. Martin, P., *Wound healing--aiming for perfect skin regeneration.* Science, 1997. **276**(5309): p. 75-81.

129. Pantaloni, D., C.L. Clainche, and M.F. Carlier, *Mechanism of actin-based motility.* Science, 2001. **292**(5521): p. 1502-1506.

130. Pollard, T.D., *Mechanics of cytokinesis in eukaryotes.* Current opinion in cell biology, 2010. **22**(1): p. 50-56.

131. Cossart, P., *Cellular microbiology*. 2005: ASM Press, Washington DC.

132. Stossel, T.P., et al., *Filamins as integrators of cell mechanics and signalling.* Nat Rev Mol Cell Biol, 2001. **2**(2): p. 138-145.

133. Pollard, T.D., *Cytoskeletal functions of cytoplasmic contractile proteins.* Journal of supramolecular structure, 1976. **5**(3): p. 317-334.

134. Pollard, T.D., L. Blanchoin, and R.D. Mullins, *Molecular mechanisms controlling actin filament dynamics in nonmuscle cells.* Annual Review of Biophysics and Biomolecular Structure, 2000. **29**(1): p. 545-576.

135. Shin, J.H., et al., *Bending stiffness of a crystalline actin bundle.* Journal of molecular biology, 2004. **337**(2): p. 255-261.

136. Van Der Spoel, D., et al., *GROMACS: fast, flexible, and free.* Journal of computational chemistry, 2005. **26**(16): p. 1701-1718.

137. Berendsen, H.J.C., et al., *Molecular dynamics with coupling to an external bath.* The Journal of Chemical Physics, 1984. **81**(8): p. 3684-3690.

138. Car, R. and M. Parrinello, *Unified approach for molecular dynamics and density-functional theory*. Physical Review Letters, 1985. **55**(22): p. 2471-2474.

139. David, S., L. Erik, and B. Hess, *Gromacs user manual. version 4.0.* Netherlands: University of Groningen, 2006.

140. Boresi, A.P., R.J. Schmidt, and O.M. Sidebottom, *Advanced mechanics of materials*. Vol. 5. 1993: Wiley.

141. Rao, S.S., *Vibration of continuous systems*. 2007: John Wiley & Sons, Inc., Hoboken, New Jersey.

142. Oda, T., et al., *Effect of the length and effective diameter of F-actin on the filament orientation in liquid crystalline sols measured by x-ray fiber diffraction.* Biophysical journal, 1998. **75**(6): p. 2672-2681.

143. Gu, Y.T. and L. Zhang, *A concurrent multiscale method based on the meshfree method and molecular dynamics analysis.* Multiscale Modeling & Simulation, 2006. **5**(4): p. 1128-1155.

144. Gu, Y.T. and P.K. Yarlagadda, *A multiscale deformation analysis for mono-crystalline copper under dynamic uniaxial tension.* Advanced Materials Research, 2008. **32**: p. 241-244.

145. Liu, L., L. Zhang, and J. Lua, *Branched carbon nanotube reinforcements for improved strength of polyethylene nanocomposites.* Applied Physics Letters, 2012. **101**(16): p. 161907-5.

146. Buehler, M.J., *Multiscale mechanics of biological and biologically inspired materials and structures.* Acta Mechanica Solida Sinica, 2010. **23**(6): p. 471-483.

147. Cranford, S.W., et al., *Nonlinear material behaviour of spider silk yields robust webs.* Nature, 2012. **482**(7383): p. 72-76.

148. Schreiber, H. and O. Steinhauser, *Cutoff size does strongly influence molecular dynamics results on solvated polypeptides.* Biochemistry, 1992. **31**(25): p. 5856-5860.

149. Plimpton, S., *Fast Parallel Algorithms for Short-Range Molecular Dynamics.* Journal of Computational Physics, 1995. **117**(1): p. 1-19.

150. Uhlenbeck, G.E. and L.S. Ornstein, *On the Theory of the Brownian Motion.* Physical Review, 1930. **36**(5): p. 823-841.

151. Boresi, A.P., R. Schmidt, and O. Sidebottom, *Advanced mechanics of materials*. 1993: John Wiley, New York.

152. Li, T., et al., *Molecular investigation of the mechanical properties of single actin filaments based on vibration analyses.* Computer Methods in Biomechanics and Biomedical Engineering, 2012: p. DOI: 10.1080/10255842.2012.706279.

153. Zhan, H. and Y.T. Gu, *A fundamental numerical and theoretical study for the vibrational properties of nanowires.* Journal of Applied Physics, 2012. **111**(12): p. 124303-124303-9.

154. Sato, M., et al., *Mechanical properties of actin.* oo, 1985. **260**(14): p. 8585-8592.

155. Pollard, T.D., *Regulation of Actin Filament Assembly by Arp2/3 Complex and Formins.* Annual Review of Biophysics and Biomolecular Structure, 2007. **36**(1): p. 451-477.

156. Xu, J., Y. Tseng, and D. Wirtz, *Strain Hardening of Actin Filament Networks REGULATION BY THE DYNAMIC CROSS-LINKING PROTEIN α-ACTININ.* Journal of Biological Chemistry, 2000. **275**(46): p. 35886-35892.

157. Guo, B. and W.H. Guilford, *Mechanics of actomyosin bonds in different nucleotide states are tuned to muscle contraction.* Proceedings of the National Academy of Sciences, 2006. **103**(26): p. 9844-9849.

158. de Gennes, P.G., *Soft Matter.* Science, 1992. **256**(5056): p. 495-497.

159. Karplus, M. and J.A. McCammon, *Molecular dynamics simulations of biomolecules.* Nature Structural & Molecular Biology, 2002. **9**(9): p. 646-652.

160. Splettstoesser, T., et al., *Structural modeling and molecular dynamics simulation of the actin filament.* Proteins: Structure, Function, and Bioinformatics, 2011. **79**(7): p. 2033-2043.

161. Gautieri, A., et al., *Coarse-grained model of collagen molecules using an extended MARTINI force field.* Journal of Chemical Theory and Computation, 2010. **6**(4): p. 1210-1218.

162. Rudd, R.E. and J.Q. Broughton, *Coarse-grained molecular dynamics: Nonlinear finite elements and finite temperature.* Physical Review B, 2005. **72**(14): p. 144104.

163. Xu, G.-K., et al., *Theoretical study of the competition between cell-cell and cell-matrix adhesions.* Physical Review E, 2009. **80**(1): p. 011921.

164. Le Goff, L., et al., *Tracer Studies on F-Actin Fluctuations.* Physical Review Letters, 2002. **89**(25): p. 258101.

165. Berendsen, H.J.C., D. van der Spoel, and R. van Drunen, *GROMACS: A message-passing parallel molecular dynamics implementation.* Computer Physics Communications, 1995. **91**(1): p. 43-56.

166. Jorgensen, W.L., D.S. Maxwell, and J. Tirado-Rives, *Development and Testing of the OPLS All-Atom Force Field on Conformational Energetics and Properties of Organic Liquids.* Journal of the American Chemical Society, 1996. **118**(45): p. 11225-11236.

167. Parrinello, M. and A. Rahman, *Polymorphic transitions in single crystals: A new molecular dynamics method.* Journal of Applied Physics, 1981. **52**(12): p. 7182-7190.

168. Berendsen, H., et al., *Interaction models for water in relation to protein hydration.* Intermolecular forces, 1981. **331**: p. 331-338.

169. Humphrey, W., A. Dalke, and K. Schulten, *VMD: visual molecular dynamics.* Journal of Molecular Graphics, 1996. **14**(1): p. 33-38.

170. Sollich, P., et al., *Rheology of Soft Glassy Materials.* Physical Review Letters, 1997. **78**(10): p. 2020-2023.

171. Lieleg, O., et al., *Slow dynamics and internal stress relaxation in bundled cytoskeletal networks.* Nat Mater, 2011. **10**(3): p. 236-242.

172. Ridley, A.J., et al., *Cell Migration: Integrating Signals from Front to Back.* Science, 2003. **302**(5651): p. 1704-1709.

173. Chamaraux, F., et al., *Kinetics of Cell Spreading.* Physical Review Letters, 2005. **94**(15): p. 158102.

174. Li, Y., et al., *A molecular mechanisms-based biophysical model for two-phase cell spreading.* Applied Physics Letters, 2010. **96**(4): p. 043703-3.

175. Ponti, A., et al., *Two Distinct Actin Networks Drive the Protrusion of Migrating Cells.* Science, 2004. **305**(5691): p. 1782-1786.

176. Small, J.V., et al., *The lamellipodium: where motility begins.* Trends in Cell Biology, 2002. **12**(3): p. 112-120.

177. Burridge, K. and K. Wennerberg, *Rho and Rac take center stage.* Cell, 2004. **116**(2): p. 167-180.

178. Lee, K., et al., *Self-Assembly of Filopodia-Like Structures on Supported Lipid Bilayers.* Science, 2010. **329**(5997): p. 1341-1345.

179. Lauffenburger, D.A. and A.F. Horwitz, *Cell Migration: A Physically Integrated Molecular Process.* Cell, 1996. **84**(3): p. 359-369.

180. Stevenson, R.P., D. Veltman, and L.M. Machesky, *Actin-bundling proteins in cancer progression at a glance.* Journal of Cell Science, 2012. **125**(5): p. 1073-1079.

181. Wozniak, M.A., et al., *Focal adhesion regulation of cell behavior.* Biochimica et Biophysica Acta (BBA) - Molecular Cell Research, 2004. **1692**(2–3): p. 103-119.

182. Mattila, P.K. and P. Lappalainen, *Filopodia: molecular architecture and cellular functions.* Nature Reviews. Molecular Cell Biology, 2008. **9**(6): p. 446-454.

183. Claessens, M.M.A.E., et al., *Actin-binding proteins sensitively mediate F-actin bundle stiffness.* Nature Materials, 2006. **5**(9): p. 748-753.

184. Zidovska, A. and E. Sackmann, *On the Mechanical Stabilization of Filopodia.* Biophysical Journal, 2011. **100**(6): p. 1428-1437.

185. Shin, J.H., et al., *Bending Stiffness of a Crystalline Actin Bundle.* Journal of Molecular Biology, 2004. **337**(2): p. 255-261.

186. Lieleg, O., et al., *Mechanics of Bundled Semiflexible Polymer Networks.* Physical Review Letters, 2007. **99**(8): p. 088102.

187. Bathe, M., et al., *Cytoskeletal Bundle Mechanics.* Biophysical Journal, 2008. **94**(8): p. 2955-2964.

188. Mogilner, A. and B. Rubinstein, *The Physics of Filopodial Protrusion.* Biophysical Journal, 2005. **89**(2): p. 782-795.

189. Kroy, K. and E. Frey, *Force-Extension Relation and Plateau Modulus for Wormlike Chains.* Physical Review Letters, 1996. **77**(2): p. 306-309.

190. Pelletier, O., et al., *Structure of Actin Cross-Linked with α-Actinin: A Network of Bundles.* Physical Review Letters, 2003. **91**(14): p. 148102.

191. Plimpton, S., *LAMMPS: Large‐scale Atomic/Molecular Massively Parallel Simulator.* Sandia National Laboratories, 2007.

192. Wilson, C.A., et al., *Myosin II contributes to cell-scale actin network treadmilling through network disassembly.* Nature, 2010. **465**(7296): p. 373-377.

193. Liu, L., G. Cao, and X. Chen, *Mechanisms of Nanoindentation on Multiwalled Carbon Nanotube and Nanotube Cluster.* Journal of Nanomaterials, 2008. **2008**: p. 12.

194. Gardel, M.L., et al., *Mechanical integration of actin and adhesion dynamics in cell migration.* Annual review of cell and developmental biology, 2010. **26**: p. 315-333.

195. Al-Alwan, M., et al., *Fascin Is a Key Regulator of Breast Cancer Invasion That Acts via the Modification of Metastasis-Associated Molecules.* PLoS ONE, 2011. **6**(11): p. e27339.

196. Lieleg, O. and A.R. Bausch, *Cross-Linker Unbinding and Self-Similarity in Bundled Cytoskeletal Networks.* Physical Review Letters, 2007. **99**(15): p. 158105.

197. Fan, J., Marissa G. Saunders, and Gregory A. Voth, *Coarse-Graining Provides Insights on the Essential Nature of Heterogeneity in Actin Filaments.* Biophysical Journal, 2012. **103**(6): p. 1334-1342.

198. Kim, T., W. Hwang, and Roger D. Kamm, *Dynamic Role of Cross-Linking Proteins in Actin Rheology.* Biophysical Journal, 2011. **101**(7): p. 1597-1603.

199. Ferrer, J.M., et al., *Measuring molecular rupture forces between single actin filaments and actin-binding proteins.* Proceedings of the National Academy of Sciences, 2008. **105**(27): p. 9221.

200. Furuike, S., T. Ito, and M. Yamazaki, *Mechanical unfolding of single filamin A (ABP-280) molecules detected by atomic force microscopy.* FEBS Letters, 2001. **498**(1): p. 72-75.

201. Hummer, G. and A. Szabo, *Kinetics from Nonequilibrium Single-Molecule Pulling Experiments.* Biophysical Journal, 2003. **85**(1): p. 5-15.

202. Schmoller, K.M., O. Lieleg, and A.R. Bausch, *Internal stress in kinetically trapped actin bundle networks.* Soft Matter, 2008. **4**(12): p. 2365-2367.

203. Pravincumar, P., D.L. Bader, and M.M. Knight, *Viscoelastic Cell Mechanics and Actin Remodelling Are Dependent on the Rate of Applied Pressure.* PLoS ONE, 2012. **7**(9): p. e43938.

204. Susana, M.-F., et al., *Stress relaxation and creep on living cells with the atomic force microscope: a means to calculate elastic moduli and viscosities of cell components.* Nanotechnology, 2010. **21**(44): p. 445101.

205. Tharmann, R., M. Claessens, and A. Bausch, *Viscoelasticity of isotropically cross-linked actin networks.* Physical Review Letters, 2007. **98**(8): p. 88103.

206. Kumar, S., et al., *Viscoelastic Retraction of Single Living Stress Fibers and Its Impact on Cell Shape, Cytoskeletal Organization, and Extracellular Matrix Mechanics.* Biophysical journal, 2006. **90**(10): p. 3762-3773.

207. Chasiotis, I., et al., *Strain rate effects on the mechanical behavior of nanocrystalline Au films.* Thin Solid Films, 2007. **515**(6): p. 3183-3189.

208. Heussinger, C., *Stress relaxation through crosslink unbinding in cytoskeletal networks.* New Journal of Physics, 2012. **14**(9): p. 095029.

209. Schwaiger, I., et al., *A mechanical unfolding intermediate in an actin-crosslinking protein.* Nat Struct Mol Biol, 2004. **11**(1): p. 81-85.

210. Miyata, H., R. Yasuda, and K. Kinosita Jr, *Strength and lifetime of the bond between actin and skeletal muscle α-actinin studied with an optical trapping technique.* Biochimica et Biophysica Acta (BBA), 1996. **1290**(1): p. 83-88.

211. Kim, T., W. Hwang, and R.D. Kamm, *Computational Analysis of a Cross-linked Actin-like Network.* Experimental Mechanics, 2009. **49**(1): p. 91-104.

212. Dominguez, R. and K.C. Holmes, *Actin structure and function.* Annual Review of Biophysics, 2011. **40**: p. 169.

213. Guck, J., et al., *Optical Deformability as an Inherent Cell Marker for Testing Malignant Transformation and Metastatic Competence.* Biophysical Journal, 2005. **88**(5): p. 3689-3698.

214. Lieleg, O., et al., *Transient Binding and Dissipation in Cross-Linked Actin Networks.* Physical Review Letters, 2008. **101**(10): p. 108101.

215. Li, T., et al., *Physical mechanism of the compressive response of F-actin networks: significance of crosslinker unbinding events.* Theoretical and Applied Mechanics Letters, 2014. **4**(5): p. -.

216. Ju, L., *AtomEye: an efficient atomistic configuration viewer.* Modelling and Simulation in Materials Science and Engineering, 2003. **11**(2): p. 173.

217. Huxley, H.E., *The Mechanism of Muscular Contraction.* Science, 1969. **164**(3886): p. 1356-1366.

218. Gordon, A., A.F. Huxley, and F. Julian, *The variation in isometric tension with sarcomere length in vertebrate muscle fibres.* The Journal of Physiology, 1966. **184**(1): p. 170-192.

219. Bárány, M., *ATPase activity of myosin correlated with speed of muscle shortening.* The Journal of general physiology, 1967. **50**(6): p. 197-218.

220. Nath, D., *Cell biology: Myosin in motion.* Nature, 2010. **468**(7320): p. 43-43.

221. Thorstensson, A., G. Grimby, and J. Karlsson, *Force-velocity relations and fiber composition in human knee extensor muscles.* Journal of Applied Physiology, 1976. **40**(1): p. 12-16.

222. Hynes, T.R., et al., *Movement of myosin fragments in vitro: domains involved in force production.* Cell, 1987. **48**(6): p. 953-963.

223. Oiwa, K., et al., *Steady-state force-velocity relation in the ATP-dependent sliding movement of myosin-coated beads on actin cables in vitro studied with a centrifuge microscope.* Proceedings of the National Academy of Sciences, 1990. **87**(20): p. 7893.

224. Piazzesi, G., et al., *Skeletal muscle performance determined by modulation of number of myosin motors rather than motor force or stroke size.* Cell, 2007. **131**(4): p. 784-795.

225. Kitamura, K., et al., *A single myosin head moves along an actin filament with regular steps of 5.3 nanometres.* Nature, 1999. **397**(6715): p. 129-134.

226. Buehler, M.J., *Nature designs tough collagen: explaining the nanostructure of collagen fibrils.* Proceedings of the National Academy of Sciences, USA, 2006. **103**(33): p. 12285-12290.

227. Huxley, H., *The double array of filaments in cross-striated muscle.* The Journal of biophysical and biochemical cytology, 1957. **3**(5): p. 631-648.

228. Behrmann, E., et al., *Structure of the Rigor Actin-Tropomyosin-Myosin Complex.* Cell, 2012. **150**(2): p. 327-338.

229. Molloy, J., et al., *Movement and force produced by a single myosin head.* Nature, 1995. **378**(6553): p. 209-212.

230. Dobesh, D.P., J.P. Konhilas, and P.P. de Tombe, *Cooperative activation in cardiac muscle: impact of sarcomere length.* American Journal of Physiology-Heart and Circulatory Physiology, 2002. **282**(3): p. H1055-H1062.

231. Fadeel, B. and A.E. Garcia-Bennett, *Better safe than sorry: Understanding the toxicological properties of inorganic nanoparticles manufactured for biomedical applications.* Advanced Drug Delivery Reviews, 2010. **62**(3): p. 362-374.

232. Stankovich, S., et al., *Graphene-based composite materials.* Nature, 2006. **442**(7100): p. 282-286.

233. Loh, K.P., et al., *Graphene oxide as a chemically tunable platform for optical applications.* Nat Chem, 2010. **2**(12): p. 1015-1024.

234. Hu, X. and Q. Zhou, *Health and Ecosystem Risks of Graphene.* Chemical Reviews, 2013. **113**(5): p. 3815-3835.

235. Yang, K., et al., *Graphene in Mice: Ultrahigh In Vivo Tumor Uptake and Efficient Photothermal Therapy.* Nano Letters, 2010. **10**(9): p. 3318-3323.

236. Wang, K., et al., *Biocompatibility of Graphene Oxide.* Nanoscale Res Lett, 2011. **6**(1): p. 8.

237. Matesanz, M.-C., et al., *The effects of graphene oxide nanosheets localized on F-actin filaments on cell-cycle alterations.* Biomaterials, 2013. **34**(5): p. 1562-1569.

238. Zhang, Y.Q., G. Liu, and X. Han, *Transverse vibrations of double-walled carbon nanotubes under compressive axial load.* Physics Letters A, 2005. **340**(1–4): p. 258-266.

239. Zhang, Y.Q., X. Liu, and G.R. Liu, *Thermal effect on transverse vibrations of double-walled carbon nanotubes.* Nanotechnology, 2007. **18**(44): p. 445701.

240. Qin, Z., Q.-H. Qin, and X.-Q. Feng, *Mechanical property of carbon nanotubes with intramolecular junctions: Molecular dynamics simulations.* Physics Letters A, 2008. **372**(44): p. 6661-6666.

241. Zhang, T., et al., *Flaw Insensitive Fracture in Nanocrystalline Graphene.* Nano Letters, 2012. **12**(9): p. 4605-4610.

242. Zhang, Y.Q., G.R. Liu, and J.S. Wang, *Small-scale effects on buckling of multiwalled carbon nanotubes under axial compression.* Physical Review B, 2004. **70**(20): p. 205430.

243. Zhang, Y.Q., G.R. Liu, and X. Han, *Effect of small length scale on elastic buckling of multi-walled carbon nanotubes under radial pressure.* Physics Letters A, 2006. **349**(5): p. 370-376.

244. Qiu, D., et al., *The GB/SA Continuum Model for Solvation. A Fast Analytical Method for the Calculation of Approximate Born Radii.* The Journal of Physical Chemistry A, 1997. **101**(16): p. 3005-3014.

245. Yamazaki, K., et al., *Selective adsorption of protein molecules on phase-separated sapphire surfaces.* Journal of Colloid and Interface Science, 2011. **361**(1): p. 64-70.

246. Vashist, S.K., et al., *Delivery of drugs and biomolecules using carbon nanotubes.* Carbon, 2011. **49**(13): p. 4077-4097.

247. Collins, J.H. and M. Elzinga, *The primary structure of actin from rabbit skeletal muscle. Completion and analysis of the amino acid sequence.* Journal of Biological Chemistry, 1975. **250**(15): p. 5915-5920.

248. Liu, W.W., J.N. Wang, and X.X. Wang, *Charging of unfunctionalized graphene in organic solvents.* Nanoscale, 2012. **4**(2): p. 425-428.

249. Zhang, H., et al., *One-Step Electrophoretic Deposition of Reduced Graphene Oxide and Ni(OH)2 Composite Films for Controlled Syntheses Supercapacitor Electrodes.* The Journal of Physical Chemistry B, 2012. **117**(6): p. 1616-1627.

250. Grimard, R., P. Tancrede, and C. Gicquaud, *Interaction of Actin with Positively Charged Phospholipids: A Monolayer Study.* Biochemical and Biophysical Research Communications, 1993. **190**(3): p. 1017-1022.

251. Svitkina, T.M., *Actin bends over backward for directional branching.* Proceedings of the National Academy of Sciences, 2012. **109**(8): p. 2693-2694.